Volume 24, Number 1, 2024 ISSN 1562-8353

NONLINEAR DYNAMICS AND SYSTEMS THEORY
An International Journal of Research and Surveys

Volume 24 Number 1 2024

CONTENTS

Sequential Initial Value Problems with Delay 1
A. Adoui, A. Guezane-Lakoud and R. Khaldi

A General Kinematic-Based Walking Algorithm of a Hexapod Robot on Irregular Terrain 12
A. Aissaoui, C. Mahfoudi and S. Djeffal

Analysis of Customer Satisfaction Survey on E-Wallets Using Simple Additive Weighting and TOPSIS Methods 28
M. Y. Anshori, I. H. Santoso, T. Herlambang, M. Tafrikan, and M. Adinugroho, K. Oktafianto and A. A. Firdaus

A New Feedback Control for Exponential and Strong Stability of Semi-Linear Systems with General Decay Estimates 41
M. Chqondi, S. Chqondi, K. Tigma and Y. Akdim

Spectral Analysis and Invariant Measure in Studying the Dynamics of a Metabolic Process in the Glycolysis-Gluconeogenesis System 54
V. I. Grytsay and I. V. Musatenko

A New Efficient Step-Size in Karmarkar's Projective Interior Point Method for Optimization Problems 65
F. Leulmi and A. Leulmi

Thermo-Electroelastic Contact Problem with Temperature Dependent Friction Law 80
A. Oultou, O. Baiz and H. Benaissa

Regional Weak and Strong Stabilization of Time Delay Infinite Dimensional Bilinear Systems 99
E. Zerrik, A. Akoubi and A. Ait Aadi

NONLINEAR DYNAMICS & SYSTEMS THEORY

Volume 24, No. 1, 2024

Nonlinear Dynamics and Systems Theory

An International Journal of Research and Surveys

 ISSN 1562-8353 Printed in Ukraine
To receive contents and abstracts by e-mail, visit our Website at: **http://www.e-ndst.kiev.ua**

InforMath Publishing Group
http://www.e-ndst.kiev.ua

Nonlinear Dynamics and Systems Theory
An International Journal of Research and Surveys

INSTRUCTIONS FOR CONTRIBUTORS

(1) General. Nonlinear Dynamics and Systems Theory (ND&ST) is an international journal devoted to publishing peer-refereed, high quality, original papers, brief notes and review articles focusing on nonlinear dynamics and systems theory and their practical applications in engineering, physical and life sciences. Submission of a manuscript is a representation that the submission has been approved by all of the authors and by the institution where the work was carried out. It also represents that the manuscript has not been previously published, has not been copyrighted, is not being submitted for publication elsewhere, and that the authors have agreed that the copyright in the article shall be assigned exclusively to InforMath Publishing Group by signing a transfer of copyright form. Before submission, the authors should visit the website:

http://www.e-ndst.kiev.ua

for information on the preparation of accepted manuscripts. Please download the archive Sample_NDST.zip containing example of article file (you can edit only the file Samplefilename.tex).

(2) Manuscript and Correspondence. Manuscripts should be in English and must meet common standards of usage and grammar. To submit a paper, send by e-mail a file in PDF format directly to

Professor A.A. Martynyuk, Institute of Mechanics,
Nesterov str.3, 03057, Kiev-57, Ukraine
e-mail: journalndst@gmail.com

or to one of the Regional Editors or to a member of the Editorial Board. Final version of the manuscript must typeset using LaTex program which is prepared in accordance with the style file of the Journal. Manuscript texts should contain the title of the article, name(s) of the author(s) and complete affiliations. Each article requires an abstract not exceeding 150 words. Formulas and citations should not be included in the abstract. AMS subject classifications and key words must be included in all accepted papers. Each article requires a running head (abbreviated form of the title) of no more than 30 characters. The sizes for regular papers, survey articles, brief notes, letters to editors and book reviews are: (i) 10-14 pages for regular papers, (ii) up to 24 pages for survey articles, and (iii) 2-3 pages for brief notes, letters to the editor and book reviews.

(3) Tables, Graphs and Illustrations. Each figure must be of a quality suitable for direct reproduction and must include a caption. Drawings should include all relevant details and should be drawn professionally in black ink on plain white drawing paper. In addition to a hard copy of the artwork, it is necessary to attach the electronic file of the artwork (preferably in PCX format).

(4) References. Each entry must be cited in the text by author(s) and number or by number alone. All references should be listed in their alphabetic order. Use please the following style:

Journal: [1] H. Poincare, Title of the article. *Title of the Journal* **volume** (issue) (year) pages. [Language]

Book: [2] A.M. Lyapunov, *Title of the Book.* Name of the Publishers, Town, year.

Proceeding: [3] R. Bellman, Title of the article. In: *Title of the Book.* (Eds.). Name of the Publishers, Town, year, pages. [Language]

(5) Proofs and Sample Copy. Proofs sent to authors should be returned to the Editorial Office with corrections within three days after receipt. The corresponding author will receive a sample copy of the issue of the Journal for which his/her paper is published.

(6) Editorial Policy. Every submission will undergo a stringent peer review process. An editor will be assigned to handle the review process of the paper. He/she will secure at least two reviewers' reports. The decision on acceptance, rejection or acceptance subject to revision will be made based on these reviewers' reports and the editor's own reading of the paper.

NONLINEAR DYNAMICS AND SYSTEMS THEORY
An International Journal of Research and Surveys
Published by InforMath Publishing Group since 2001

Volume 24 Number 1 2024

CONTENTS

Sequential Initial Value Problems with Delay 1
A. Adoui, A. Guezane-Lakoud and R. Khaldi

A General Kinematic-Based Walking Algorithm of a Hexapod Robot on Irregular Terrain 12
A. Aissaoui, C. Mahfoudi and S. Djeffal

Analysis of Customer Satisfaction Survey on E-Wallets Using Simple Additive Weighting and TOPSIS Methods 28
M. Y. Anshori, I. H. Santoso, T. Herlambang, M. Tafrikan, and M. Adinugroho, K. Oktafianto and A. A. Firdaus

A New Feedback Control for Exponential and Strong Stability of Semi-Linear Systems with General Decay Estimates 41
M. Chqondi, S. Chqondi, K. Tigma and Y. Akdim

Spectral Analysis and Invariant Measure in Studying the Dynamics of a Metabolic Process in the Glycolysis-Gluconeogenesis System 54
V. I. Grytsay and I. V. Musatenko

A New Efficient Step-Size in Karmarkar's Projective Interior Point Method for Optimization Problems 65
F. Leulmi and A. Leulmi

Thermo-Electroelastic Contact Problem with Temperature Dependent Friction Law 80
A. Oultou, O. Baiz and H. Benaissa

Regional Weak and Strong Stabilization of Time Delay Infinite Dimensional Bilinear Systems 99
E. Zerrik, A. Akoubi and A. Ait Aadi

Founded by A.A. Martynyuk in 2001.
Registered in Ukraine Number: KB No 5267 / 04.07.2001.

NONLINEAR DYNAMICS AND SYSTEMS THEORY

An International Journal of Research and Surveys

Impact Factor from SCOPUS for 2022: SJR – 0.293, SNIP – 0.784 and CiteScore – 1.5

Nonlinear Dynamics and Systems Theory (ISSN 1562–8353 (Print), ISSN 1813–7385 (Online)) is an international journal published under the auspices of the S.P. Timoshenko Institute of Mechanics of National Academy of Sciences of Ukraine and Curtin University of Technology (Perth, Australia). It aims to publish high quality original scientific papers and surveys in areas of nonlinear dynamics and systems theory and their real world applications.

AIMS AND SCOPE

Nonlinear Dynamics and Systems Theory is a multidisciplinary journal. It publishes papers focusing on proofs of important theorems as well as papers presenting new ideas and new theory, conjectures, numerical algorithms and physical experiments in areas related to nonlinear dynamics and systems theory. Papers that deal with theoretical aspects of nonlinear dynamics and/or systems theory should contain significant mathematical results with an indication of their possible applications. Papers that emphasize applications should contain new mathematical models of real world phenomena and/or description of engineering problems. They should include rigorous analysis of data used and results obtained. Papers that integrate and interrelate ideas and methods of nonlinear dynamics and systems theory will be particularly welcomed.

PUBLICATION AND SUBSCRIPTION INFORMATION

Nonlinear Dynamics and Systems Theory will have 6 issues in 2024, printed in hard copy (ISSN 1562–8353) and available online (ISSN 1813–7385), by InforMath Publishing Group, Nesterov str., 3, Institute of Mechanics, Kiev, MSP 680, Ukraine, 03057. Subscription prices are available upon request from the Publisher, EBSCO Information Services (`mailto:journals@ebsco.com`), or website of the Journal: `http://e-ndst.kiev.ua`. Subscriptions are accepted on a calendar year basis. Issues are sent by airmail to all countries of the world. Claims for missing issues should be made within six months of the date of dispatch.

ABSTRACTING AND INDEXING SERVICES

Papers published in this journal are indexed or abstracted in: Mathematical Reviews / MathSciNet, Zentralblatt MATH / Mathematics Abstracts, PASCAL database (INIST–CNRS) and SCOPUS.

Nonlinear Dynamics and Systems Theory, **24** (1) (2024) 1–11

Sequential Initial Value Problems with Delay

A. Adoui *, A. Guezane-Lakoud and R. Khaldi

Laboratory of Advanced Materials,
Faculty of Sciences, Badji Mokhtar-Annaba University,
P.O. Box 12, 23000 Annaba, Algeria.

Received: May 6, 2023; Revised: January 21, 2024

Abstract: In this paper, we discuss the solvability of a nonlinear Riemann-Liouville sequential initial value problem with infinite delay. We give sufficient conditions for the existence, uniqueness and stability of solutions. Proofs are carried out employing fixed point theory.

Keywords: *sequential fractional derivative; initial value problem; delay; existence of solution; fixed point theorem; stability.*

Mathematics Subject Classification (2010): 26A33, 34A08, 34K37, 93D05.

1 Introduction

In the last few centuries, non-integer order derivatives were widely expanded as a useful theoretical concept and numerous books were devoted to this field, see monographs [21, 24, 26]. Due to their nonlocal nature, fractional derivatives play a significant role in describing physical phenomena with memory effect and hereditary processes. Hence, they give better accuracy when compared to classical derivatives, the evidence of which has been provided for instance in [3] by virtue of numerical simulations. Consequently, more study has been conducted on new classes of fractional differential equations. In particular, fractional differential equations with time delay were capable to attract the attention of many researchers over the last few years, see [1, 4, 6, 7, 9], and the references therein.

Very recently, sequential fractional differential equations have been the subject of many investigations. Sequential fractional derivatives were introduced for the first time by Miller and Ross in their book [24]. As a matter of fact, they appear often in physics, where the substitution of formulas containing derivatives for one another is

* Corresponding author: mailto:ahlem.a.adoui@gmail.com, ahlem.adoui@univ-annaba.org

very common. Many recent works are devoted to sequential boundary value problems of Caputo, Hadamard, mixed, Caputo-Hadamard, and Hilfer type fractional derivatives, see [27], [23], [5, 13, 14, 19, 20], [2] and [25], respectively. In the following interesting papers, the authors established existence results for fractional differential equations, these results are pertinent to the topic of this work.

In [12], the following Riemann-Liouville sequential fractional differential equation is studied:

$$\mathbb{D}^{\upsilon}_{0+}[(t-a)^{r}\mathbb{D}^{\varrho}_{0+}x(t)] = f(t,x),\ t\in(0,b].$$

In [11], the authors studied a general Basset-Boussinesq-Oseen fractional equation and proved the global existence, uniqueness and regularity of solutions in a partially ordered Banach space for the following problem:

$$\begin{aligned}&\mathbb{D}^{\upsilon}_{0+}(\mathbb{D}^{\varrho}_{0+}+A)x(t)+Bx(t)=f(t),\ \ 0<t\leq 1,\ 0<\upsilon,\varrho\leq 1,\\ &x(0)=a,\\ &\mathbb{D}^{\varrho}_{0+}x(0)=b.\end{aligned}$$

Nonetheless, the analysis of fractional sequential initial value problems is still not sufficiently enriched. To the best of our knowledge, sequential fractional differential equations involving the Riemann-Liouville fractional derivatives associated with infinite delay have not been considered yet. The primary focus of this paper is the investigation of sufficient criteria for nonlinearity that ensure the existence and uniqueness of solutions for the following initial value problem:

$$\begin{aligned}&\mathbb{D}^{\varrho}_{0+}\mathbb{D}^{\upsilon}_{0+}y(t)=f(t,y_t),\ t\in(0,b],\\ &y(t)=\chi(t),t\in(-\infty,0],\\ &\mathbb{D}^{\upsilon}_{0+}y(0)=0,\end{aligned}\tag{1}$$

where $0<\upsilon,\varrho<1,\ f:[0,b]\times\mathbb{B}\to\mathbb{R},\ \chi\in\mathbb{B},\ \chi(0)=0,\ x_t(\theta)=x(t+\theta),\ \theta\leq 0.$
The phase space $\mathbb{B}$ is a semi-normed linear space of functions mapping $(-\infty,0]$ into $\mathbb{R}$ and characterized by the following axioms.
If $y:(-\infty,b]\to\mathbb{R}$ and $y_0\in\mathbb{B}$, then for any $t\in[0,b]$,

1. $y_t\in\mathbb{B}$ and we have

$$\|y_t\|_{\mathbb{B}}\leq K(t)\sup_{s\in[0,t]}|y(s)|+M(t)\|y_0\|_{\mathbb{B}},$$

$$|y(t)|\leq H\|y_t\|_{\mathbb{B}},$$

   where $H\geq 0$ is a constant, $K:[0,b]\to[0,\infty[$ is continuous and $M:[0,\infty[\to[0,\infty[$ is locally bounded. H,K,M are independent of $y(.)$.

2. y_t is a $\mathbb{B}-$valued function on $[0,b]$.

3. $\mathbb{B}$ is complete.

For more details on the theory of delay differential equations, we refer the interested reader to [15,17,22]. The main motivation for our paper is to continue the quest of broadening the study of fractional operators for much larger classes of differential equations. We emphasize that our results are novel in the aforementioned context.

The rest of this paper is structured as follows. In Section 2, we recall some preliminary results which are relevant to our work. Section 3 is devoted to the existence and uniqueness results. In Section 4, in order to enhance the physical meaning of our main outcomes, we study the stability of the problem under consideration. We exhibit an example in Section 5 to illustrate the applicability of our results. Finally, a conclusion is given.

2 Preliminaries

In this section, we recall the basic definitions and properties needed in our proofs.

Definition 2.1 [26] If $f \in L^1(a,b)$ and $\upsilon > 0$, then the left-sided Riemann-Liouville fractional integral is defined by

$$\mathbb{I}^{\upsilon}_{a+} f(x) = \frac{1}{\Gamma(\upsilon)} \int_a^x \frac{f(t)}{(x-t)^{1-\upsilon}} dt, \ x > a.$$

Lemma 2.1 [21] *The operator $\mathbb{I}^{\upsilon}_{a+}$ maps continuous functions into continuous functions.*

Definition 2.2 [26] Let $0 < \upsilon < 1$. The left-sided Riemann-Liouville fractional derivative is defined by

$$\mathbb{D}^{\upsilon}_{a+} f(x) = \frac{1}{\Gamma(1-\upsilon)} \frac{d}{dt} \int_a^x \frac{f(t)}{(x-t)^{\upsilon}} dt, \ x > a.$$

Moreover, if $\mathbb{I}^{1-\upsilon} f \in AC[a,b]$, then $\mathbb{D}^{\upsilon}_{a+} f$ exists almost everywhere on $[a,b]$.

The following lemma gives some properties of the composition of the Riemann-Liouville fractional integral and derivative.

Lemma 2.2 [21] *Let $\upsilon, \varrho > 0$ and $f \in L^1(a,b)$, then*

$$\mathbb{I}^{\upsilon}_{a+} \mathbb{I}^{\varrho}_{a+} f = \mathbb{I}^{\upsilon+\varrho}_{a+} f \tag{2}$$

is satisfied at almost every point $x \in [a,b]$.
Let $\upsilon > 0$ and $f \in L^1(a,b)$. Then

$$\mathbb{D}^{\upsilon}_{a+} \mathbb{I}^{\upsilon}_{a+} f(x) = f(x) \tag{3}$$

at almost every $x \in [a,b]$.
Let $0 < \upsilon < 1$, $f \in L^1(a,b)$ and $\mathbb{I}^{1-\upsilon}_{a+} f \in AC[a,b]$. Then

$$\mathbb{I}^{\upsilon}_{a+} \mathbb{D}^{\upsilon}_{a+} f(x) = f(x) - \frac{\mathbb{I}^{1-\upsilon}_{a+} f(a)}{\Gamma(\upsilon)} (x-a)^{\upsilon-1} \tag{4}$$

holds almost everywhere on $[a,b]$.

Let $a = 0$. In the following, we denote $\mathbb{I}^{\upsilon}_{0+}$ by $\mathbb{I}^{\upsilon}$, and $\mathbb{D}^{\upsilon}_{0+}$ by $\mathbb{D}^{\upsilon}$, for simplicity.

Proposition 2.1 *Let $0 < \upsilon < 1$, $F : [0, b] \to \mathbb{R}$ be a continuous function. Then y is a solution of the IVP*

$$\begin{aligned} &\mathbb{D}^{\upsilon} y(t) = F(t),\ t \in (0, b], \\ &y(0) = 0 \end{aligned} \tag{5}$$

if and only if $y \in C[0, b]$ is a solution of the integral equation

$$y(t) = \frac{1}{\Gamma(\upsilon)} \int_0^t (t - s)^{\upsilon - 1} F(s) ds. \tag{6}$$

Proof. Let $y \in C[0, b]$ be such that $\mathbb{D}^{\upsilon} y = F$, i.e., $\mathbb{D}\mathbb{I}^{1-\upsilon} y = F$. Integrating, we get $\mathbb{I}^{1-\upsilon} y(t) = \mathbb{I}^{1-\upsilon} y(0) + \mathbb{I}^1 F$ so that $\mathbb{I}^{1-\upsilon} y$ is absolutely continuous. Apply operator $\mathbb{I}^{\upsilon}$ to the differential equation in (5), then by virtue of (4), we obtain $y(t) = \frac{c}{\Gamma(\upsilon)} t^{\upsilon - 1} + \mathbb{I}^{\upsilon} F(t)$. Employing the initial condition, we find $c = 0$. Hence, (6) holds.

Conversely, if $y = \mathbb{I}^{\upsilon} F$, then, taking into account Lemma 2.1, we see that y is continuous. Moreover, $y(0) = \mathbb{I}^{\upsilon} F(0) = 0$ because F is continuous. Then, applying operator $\mathbb{I}^{1-\upsilon}$ and (2), we obtain $\mathbb{I}^{1-\upsilon} y = \mathbb{I}^1 F$. Deriving, we get $\mathbb{D}^{\upsilon} y = F$.

3 Existence Results

In this section, we give an existence and uniqueness result based upon Banach's fixed point theorem. Moreover, we retrieve an existence result by means of the nonlinear alternative of Leray-Schauder for a larger class of functions $f(t, y_t)$.

The following space will be considered hereafter. Let Ω be the Banach space of all continuous functions $y : (-\infty, b] \to \mathbb{R}$ such that $y_0 \in \mathbb{B}$ and $y_{\big|_{[0,b]}}$ is continuous.

Definition 3.1 A function $y \in \Omega$ is said to be a solution of (1) if y satisfies the fractional differential equation $\mathbb{D}^{\varrho}\mathbb{D}^{\upsilon} y(t) = f(t, y_t)$ on $(0, b]$, the initial condition $\mathbb{D}^{\upsilon} y(0) = 0$, and $y(t) = \chi(t)$ on $(-\infty, 0]$.

Lemma 3.1 *Let $F(t) = f(t, y_t) \in C[0, b]$. Then y is a solution of the IVP*

$$\begin{aligned} &\mathbb{D}^{\varrho}\mathbb{D}^{\upsilon} y(t) = f(t, y_t),\ t \in (0, b], \\ &\mathbb{D}^{\upsilon} y(0) = 0, \\ &y(0) = 0 \end{aligned} \tag{7}$$

if and only if y is a solution of the fractional integral equation

$$y(t) = \frac{1}{\Gamma(\upsilon + \varrho)} \int_0^t (t - s)^{\upsilon + \varrho - 1} f(s, y_s) ds.$$

Proof. Since F is continuous, applying Proposition 2.1, we obtain that

$$\begin{aligned} &\mathbb{D}^{\upsilon} y(t) = \frac{1}{\Gamma(\varrho)} \int_0^t (t - s)^{\varrho - 1} f(s, y_s) ds, \\ &y(0) = 0. \end{aligned}$$

$\mathbb{I}^{\varrho}F$ is continuous. Hence, using Proposition 2.1 again, we get

$$\begin{aligned} y(t) &= \frac{1}{\Gamma(\upsilon+\varrho)}\int_0^t (t-s)^{\upsilon+\varrho-1} f(s,y_s)ds, \\ y(0) &= 0. \end{aligned}$$

Similarly, the converse is easily shown.

Theorem 3.1 *Let $f : [0,b]\times\mathbb{B}\to \mathbb{R}$ be a continuous function. Suppose that there exists $L>0$ such that*

$$|f(t,u)-f(t,v)| \le L\|u-v\|_{\mathbb{B}}, \quad t\in[0,b], \text{ for every } u,v\in\mathbb{B}.$$

Then the IVP (1) has a unique solution on $[0,b]$ provided that $\frac{b^{\upsilon+\varrho}K_bL}{\Gamma(\upsilon+\varrho+1)} < 1$, where $K_b = \sup\limits_{t\in[0,b]}|k(t)|$.

Proof. Using the previous lemma, we show that solving the initial value problem is equivalent to proving that the operator $S:\Omega\to\Omega$ has a unique fixed point, where

$$(Sy)(t) = \begin{cases} \chi(t),\ t\in(-\infty,0], \\ \frac{1}{\Gamma(\upsilon+\varrho)}\int_0^t (t-s)^{\upsilon+\varrho-1}f(s,y_s)ds,\ t\in[0,b]. \end{cases} \tag{8}$$

Consider the following decomposition.
Let $x(.):(-\infty,b]\to\mathbb{R}$ be the function defined by

$$x(t) = \begin{cases} 0,\ t\in[0,b], \\ \chi(t),\ t\in(-\infty,0]. \end{cases} \tag{9}$$

Then take $z(.):(0,b]\to\mathbb{R}$ given by $z = y_{\big|_{[0,b]}}$, denote by $\overline{z}$ the function defined by

$$\overline{z}(t) = \begin{cases} z(t),\ t\in[0,b], \\ 0,\ t\in(-\infty,0]. \end{cases} \tag{10}$$

Thus, $y(t)=\overline{z}(t)+x(t),\ t\in[0,b]$, then $y_t=\overline{z}_t+x_t,\ t\in[0,b]$.
In addition, set $C_0=\{z\in C([0,b]) : z_0=0\}$ equipped with the semi-norm in C_0 defined by $\|z\|_b = \sup\limits_{t\in[0,b]}|z(t)|$. Consider now the operator $\mathbb{T}:C_0\to C_0$ given by

$$(\mathbb{T}z)(t) = \begin{cases} 0,\ \text{if } t\in(-\infty,0], \\ \frac{1}{\Gamma(\upsilon+\varrho)}\int_0^t (t-s)^{\upsilon+\varrho-1}f(\tau,\overline{z}_s+x_s)ds,\ \text{if } t\in[0,b]. \end{cases} \tag{11}$$

Then the operator S has a fixed point is equivalent to $\mathbb{T}$ has a fixed point.
Indeed, $\mathbb{T}$ is a contraction mapping.

Consider $z, z^* \in C_0$. Then we have for every $t \in [0, b]$,

$$\begin{aligned}
&|(\mathbb{T}z)(t) - (\mathbb{T}z^*)(t)| \\
&\quad \leq \frac{1}{\Gamma(\upsilon+\varrho)} \int_0^t (t-s)^{\upsilon+\varrho-1} |f(s, \overline{z}_s + x_s) - f(s, \overline{z_s^*} + x_s)| ds \\
&\quad \leq \frac{1}{\Gamma(\upsilon+\varrho)} \int_0^t (t-s)^{\upsilon+\varrho-1} L \|\overline{z}_s - \overline{z_s^*}\|_{\mathbb{B}} ds \\
&\quad \leq \frac{LK_b}{\Gamma(\upsilon+\varrho)} \int_0^t (t-s)^{\upsilon+\varrho-1} \sup_{\tau\in[0,s]} |z(\tau) - z^*(\tau)| ds \\
&\quad \leq \frac{LK_b \|z - z^*\|_b}{\Gamma(\upsilon+\varrho)} \int_0^t (t-s)^{\upsilon+\varrho-1} ds \leq \frac{LK_b b^{\upsilon+\varrho}}{\Gamma(\upsilon+\varrho+1)} \|z - z^*\|_b.
\end{aligned}$$

Therefore, $\mathbb{T}$ is a contraction mapping. Hence, applying Banach's fixed point theorem, we see that $\mathbb{T}$ has a unique fixed point.

Now, we give an existence result based upon the nonlinear alternative of Leray-Schauder.

Lemma 3.2 [16] *Let $v : [0, b] \to [0, \infty)$ be a real function and $w(.)$ be a nonnegative, locally integrable function on $[0, b]$ and there exist constants $a > 0$ and $0 < \upsilon < 1$ such that*

$$v(t) \leq w(t) + a \int_0^t \frac{v(s)}{(t-s)^{\upsilon}} ds.$$

Then there exists a constant $K = K(\upsilon)$ such that $v(t) \leq w(t) + Ka \int_0^t \frac{w(s)}{(t-s)^{\upsilon}} ds,\ t \in [0, b]$.

Theorem 3.2 *Under the following assumptions:*

1. *f is a continuous function,*
2. *there exists $p, q \in C([0, b], \mathbb{R}_+)$ such that*

$$|f(t, u)| \leq p(t) + q(t)\|u\|_{\mathbb{B}}, \quad t \in [0, b],\ u \in \mathbb{B},$$

the IVP (1) has at least one solution on $[0, b]$.

Proof. Let $\mathbb{T} : C_0 \to C_0$ be defined as in (11). We will show that $\mathbb{T}$ is a continuous and a completely continuous operator.
Step 1: $\mathbb{T}$ is continuous.
Let (z_n) be a sequence in C_0 such that $z_n \to z$ in C_0. Then

$$\begin{aligned}
&|(\mathbb{T}z_n)(t) - (\mathbb{T}z)(t)| \\
&\quad \leq \frac{1}{\Gamma(\upsilon+\varrho)} \int_0^b (t-s)^{\upsilon+\varrho-1} |f(s, \overline{z}_{n_s} + x_s) - f(s, \overline{z}_s + x_s)| ds \\
&\quad \leq \frac{b^{\upsilon+\varrho}}{\Gamma(\upsilon+\varrho+1)} \|f(., \overline{z}_{n_{(.)}} + x_{(.)}) - f(., \overline{z}_{(.)} + x_{(.)})\|_{\infty},
\end{aligned}$$

which tends to 0 as $n \to \infty$.
Step 2: $\mathbb{T}$ maps bounded sets into bounded sets in C_0.
Let $z \in B_\eta := \{z \in C_0 : \|z\|_b \leq \eta\}$, since f is a continuous function, we have for each $t \in [0, b]$,

$$\begin{aligned}|(\mathbb{T}z)(t)| &\leq \frac{1}{\Gamma(\upsilon+\varrho)}\int_0^b (t-s)^{\upsilon+\varrho-1}(p(s)+q(s)\|\overline{z}_s + x_s\|_{\mathbb{B}})ds \\ &\leq \frac{b^{\upsilon+\varrho}}{\Gamma(\upsilon+\varrho+1)}\|p\|_\infty + \frac{b^{\upsilon+\varrho}}{\Gamma(\upsilon+1)\Gamma(\varrho+1)}\|q\|_\infty \eta_* =: l,\end{aligned}$$

where $\|\overline{z}_s + x_s\|_{\mathbb{B}} \leq \|\overline{z}_s\|_{\mathbb{B}} + \|x_s\|_{\mathbb{B}} \leq K_b\eta + M_b\|\chi\|_{\mathbb{B}} := \eta_*$. Hence, $\|\mathbb{T}z\|_\infty \leq l$.
Step 3: $\mathbb{T}$ maps bounded sets into equicontinuous sets of C_0.
Let $t_1, t_2 \in [0, b], t_1 < t_2$ and let B_η be a bounded set of C_0 as in Step 2. Let $z \in B_\eta$.

$$\begin{aligned}&|(\mathbb{T}z)(t_2) - (\mathbb{T}z)(t_1)| \\ &\quad\leq \frac{1}{\Gamma(\upsilon+\varrho)}\Big(\int_0^{t_1} |(t_2-s)^{\upsilon+\varrho-1} - (t_1-s)^{\upsilon+\varrho-1}||f(s,\overline{z}_s + x_s)|ds \\ &\quad+ \int_{t_1}^{t_2} |(t_2-s)^{\upsilon+\varrho-1} f(s,\overline{z}_s + x_s)|ds\Big) \\ &\quad\leq \frac{\|p\|_\infty + \|q\|_\infty\eta_*}{\Gamma(\upsilon+\varrho)}\int_0^{t_1} |(t_2-s)^{\upsilon+\varrho-1} - (t_1-s)^{\upsilon+\varrho-1}|ds \\ &\quad+ \frac{\|p\|_\infty + \|q\|_\infty\eta_*}{\Gamma(\upsilon+\varrho)}\int_{t_1}^{t_2} (t_2-s)^{\upsilon+\varrho-1}ds.\end{aligned}$$

As $t_1 \to t_2$, the right-hand side of the above inequality tends to zero. By virtue of Steps 1-3, along with the Arzelà-Ascoli theorem, we infer that $\mathbb{T} : C_0 \to C_0$ is continuous and completely continuous.
Step 4: A priori bounds.
It is sufficient to show that there exists an open set $U \subseteq C_0$ with $z \neq \lambda\mathbb{T}z$, for $\lambda \in (0, 1)$ and $z \in \partial U$.
Take $z \in C_0$ and $z = \lambda\mathbb{T}(z)$ for some $0 < \lambda < 1$, then for each $t \in [0, b]$,

$$\begin{aligned}|z(t)| &\leq \frac{1}{\Gamma(\upsilon+\varrho)}\int_0^t (t-\tau)^{\upsilon+\varrho-1}(p(\tau)+q(\tau)\|\overline{z}_\tau + x_\tau\|_{\mathbb{B}})d\tau \\ &\leq \frac{b^{\upsilon+\varrho}}{\Gamma(\upsilon+\varrho+1)}\|p\|_\infty + \frac{1}{\Gamma(\upsilon+\varrho)}\int_0^t (t-\tau)^{\upsilon+\varrho-1}q(\tau)\|\overline{z}_\tau + x_\tau\|_{\mathbb{B}}d\tau.\end{aligned}$$

Then $\|\overline{z}_\tau + x_\tau\|_{\mathbb{B}} \leq K_b \sup_{s\in[0,\tau]} |z(s)| + M_b\|\chi\|_B := w(\tau)$, which implies that

$$|z(t)| \leq \frac{1}{\Gamma(\upsilon+\varrho)}\int_0^t (t-\tau)^{\upsilon+\varrho-1}q(\tau)w(\tau)d\tau + \frac{b^{\upsilon+\varrho}}{\Gamma(\upsilon+\varrho+1)}\|p\|_\infty,\ t \in [0, b].$$

By inserting the above in w, we get for each $t \in [0, b]$,

$$w(t) \leq M_b\|\chi\|_{\mathbb{B}} + \frac{K_b b^{\upsilon+\varrho}}{\Gamma(\upsilon+\varrho+1)}\|p\|_\infty + \frac{K_b\|q\|_\infty}{\Gamma(\upsilon+\varrho)}\int_0^t (t-\tau)^{\upsilon-1}(t-\tau)^{\varrho}w(\tau)d\tau.$$

To this end, applying Lemma 3.2 yields that there exists a constant $K = K(\upsilon)$ such that for each $t \in [0, b]$,

$$|w(t)| \leq M_b\|\chi\|_{\mathbb{B}} + \frac{K_b b^{\upsilon+\varrho}}{\Gamma(\upsilon+\varrho+1)}\|p\|_\infty + K(\upsilon)\frac{K_b\|q\|_\infty b^\varrho}{\Gamma(\upsilon+\varrho)}\int_0^t (t-\tau)^{\upsilon-1}R\, d\tau,$$

where

$$R = M_b\|\chi\|_{\mathbb{B}} + \frac{K_b b^{\upsilon+\varrho}}{\Gamma(\upsilon+\varrho+1)}\|p\|_\infty.$$

Hence,

$$\|w\|_\infty \leq R + R\frac{K(\upsilon)K_b b^{\upsilon+\varrho}}{\upsilon\Gamma(\upsilon+\varrho)}\|q\|_\infty := r.$$

Then $\|z\|_\infty \leq r\|\mathbb{I}^{\upsilon+\varrho}q\|_\infty + \frac{b^{\upsilon+\varrho}}{\Gamma(\upsilon+\varrho+1)}\|p\|_\infty := r^*$.
Set $U = \{z \in C_0 : \|z\|_b < r^* + 1\}$. $\mathbb{T} : \overline{U} \to C_0$ is continuous and completely continuous. From the choice of U, there is no $z \in \partial U$ such that $z = \lambda\mathbb{T}(z)$, for $\lambda \in (0, 1)$.
Consequently, the nonlinear alternative of Leray-Schauder is applicable. It follows that $\mathbb{T}$ has a fixed point z in U.

4 Stability

In this section, we provide sufficient conditions that ensure the Hyers-Ulam stability of our problem.

Definition 4.1 Problem (1) is said to be Hyers-Ulam stable if there exists a constant $\lambda > 0$ such that for each $\epsilon > 0$ and for each $u \in \Omega$,

$$\begin{aligned} &|\mathbb{D}^\varrho\mathbb{D}^\upsilon u - f(t, u_t)| \leq \epsilon,\ t \in [0, b], \\ &u(t) = \chi(t),\ t \in (-\infty, 0], \end{aligned} \tag{12}$$

there exists a solution $v \in \Omega$ of (1) such that $|u(t) - v(t)| \leq \lambda\epsilon,\ t \in [0, b]$.

Theorem 4.1 *Let $f : [0, b]\times \to \mathbb{R}$ be continuous and satisfy the Lipschitz condition with respect to the second variable, i.e., there exists $L > 0$ such that*

$$|f(t, u) - f(t, v)| \leq L\|u - v\|_{\mathbb{B}}, \quad t \in [0, b]\ u, v \in \mathbb{B}.$$

Then (1) is Hyers-Ulam stable provided that $\frac{b^{\upsilon+\varrho}K_b L}{\Gamma(\upsilon+\varrho+1)} < 1$.

Proof. Since f satisfies the assumptions of Theorem 3.1 , the solution of (1) can be written as

$$v(t) = \frac{1}{\Gamma(\upsilon+\varrho)}\int_0^t (t-s)^{\upsilon+\varrho-1}f(s, v_s)ds.$$

Now, let u be a solution to (12), then there exists a function γ such that $|\gamma(t)| \leq \epsilon$ and

$$\mathbb{D}^\varrho\mathbb{D}^\upsilon u = f(t, u_t) + \gamma(t).$$

Proceeding as in Section 2, we find

$$u(t) = \frac{1}{\Gamma(\upsilon+\varrho)}\int_0^t (t-s)^{\upsilon+\varrho-1}f(s, u_s)ds + \frac{1}{\Gamma(\upsilon+\varrho)}\int_0^t (t-s)^{\upsilon+\varrho-1}\gamma(s)ds,$$

which gives $|u(t) - \frac{1}{\Gamma(\upsilon+\varrho)}\int_0^t (t-s)^{\upsilon+\varrho-1} f(s,u_s)ds| \leq \frac{\epsilon}{\Gamma(\upsilon+\varrho+1)} b^{\upsilon+\varrho} := \Lambda\epsilon$ so that

$$\begin{aligned}
|u(t) - v(t)| &\leq |u(t) - \frac{1}{\Gamma(\upsilon+\varrho)}\int_0^t (t-s)^{\upsilon+\varrho-1} f(s,u_s)ds| \\
&+ \frac{1}{\Gamma(\upsilon+\varrho)}|\int_0^t (t-s)^{\upsilon+\varrho-1} f(s,u_s) - \frac{1}{\Gamma(\upsilon+\varrho)}\int_0^t (t-s)^{\upsilon+\varrho-1} f(s,v_s)ds| \\
&\leq \Lambda\epsilon + \frac{L}{\Gamma(\upsilon+\varrho)}\int_0^t (t-s)^{\upsilon-1}(t-s)^{\varrho}\|u_s - v_s\|_{\mathbb{B}}ds \\
&\leq \Lambda\epsilon + \frac{Lb^{\varrho}K_b}{\Gamma(\upsilon+\varrho)}\int_0^t (t-s)^{\upsilon-1} \sup_{\tau\in[0,s]}|u(\tau) - v(\tau)|ds.
\end{aligned} \tag{13}$$

Set $\psi(t) = \sup_{\tau\in[0,t]}|u(\tau) - v(\tau)|$, so $\psi(t) \leq \Lambda\epsilon + \frac{Lb^{\varrho}K_b}{\Gamma(\upsilon+\varrho)}\int_0^t (t-s)^{\upsilon-1}\psi(s)ds$. Applying the Gronwall lemma, we find

$$\begin{aligned}
\psi(t) &\leq \Lambda\epsilon + \frac{Lb^{\varrho}K_b}{\Gamma(\upsilon+\varrho)}\int_0^t (t-s)^{\upsilon-1}\Lambda\epsilon ds \\
&\leq \Lambda\epsilon + K\frac{LK_b}{\upsilon}\frac{b^{\upsilon+\varrho}}{\Gamma(\upsilon+\varrho)}\Lambda\epsilon = \Lambda(1 + K\frac{LK_b}{\upsilon}\frac{b^{\upsilon+\varrho}}{\Gamma(\upsilon+\varrho)})\epsilon.
\end{aligned} \tag{14}$$

5 Example

In this section, we provide a numerical example to show the viability of our outcomes. Take $\upsilon = \varrho = \frac{1}{2}, b = 1, \gamma > 0$. The nonlinearity $f : [0,1] \times \mathbb{B}_\gamma \to \mathbb{R}$ is given by

$$f(t,x) = e^{-\gamma t}(\frac{1}{\sqrt{t+4}}\frac{x^2 + 2|x|}{1+|x|} + \sin(t))$$

and $\chi \in \mathbb{B}_\gamma$ which is defined by

$$\mathbb{B}_\gamma = \{\chi : C((-\infty, 0], \mathbb{R}) : \lim_{s\to-\infty} e^{\gamma s}|\chi(s)| \text{exists in } \mathbb{R}\}$$

and endowed with the norm $\|\chi\|_{\mathbb{B}_\gamma} = \sup_{s\in(-\infty,0]} e^{\gamma s}|\chi(s)|$. It is easily verified that $\mathbb{B}_\gamma$ is an admissible phase space, i.e., it is a Banach space and it fulfills the phase space axioms with $K(t) = 1, M(t) = e^{-\gamma t}$ and $H = 1$.
Moreover, for any $t \in [0,1],\ x, y \in \mathbb{B}_\gamma$, we have

$$\begin{aligned}
|f(t,x) - f(t,y)| &= e^{-\gamma t}\frac{1}{\sqrt{t+4}}|\frac{x^2+2|x|}{1+|x|} - \frac{y^2+2|y|}{1+|y|}| \\
&\leq e^{-\gamma t}\frac{1}{\sqrt{t+4}}|\frac{x^2-y^2}{(1+|x|)(1+|y|)}| \\
&\leq e^{-\gamma t}\frac{1}{\sqrt{t+4}}|x-y| \leq \frac{1}{2}\|x-y\|_{\mathbb{B}_\gamma}
\end{aligned}$$

so that f satisfies the Lipschitz condition with $L = \frac{1}{2}$ and $\frac{b^{\upsilon+\varrho}K_b L}{\Gamma(\upsilon+\varrho+1)} = \frac{1}{4} < 1$, so the IVP has exactly one solution by virtue of Theorem 3.1. Also, the hypothesis from Theorem

4.1 is satisfied, and therefore the IVP is shown to be Hyers-Ulam stable.
Furthermore, for any $t \in [0,1]$ and $x \in \mathbb{B}_\gamma$, we have

$$|f(t,x)| \leq \frac{e^{-\gamma t}}{\sqrt{t+4}} \frac{2+|x|}{1+|x|}|x| + e^{-\gamma t}\sin(t) \leq p(t)\|x\|_{\mathbb{B}_\gamma} + q(t),$$

where $p(t) = \frac{2}{\sqrt{t+4}}$ and $q(t) = e^{-\gamma t}\sin(t)$. We see that f satisfies the conditions of Theorem 3.2. Thus, the existence of solutions follows immediately.

6 Conclusion

In this work, we gave sufficient conditions for the existence, uniqueness and stability of solutions of nonlinear sequential IVPs with delay. The novelty of our findings resides in the usefulness of our existence results in proving the controllability of a more generalized system by the aid of semigroup techniques. Namely, when we extend the differential equation to a fractional differential evolution equation with control, i.e., when the nonlinear part takes the form $Ax(t)+Bu(t)+f(t,x_t)$, where x takes values in a Banach space X, A is a generator of a strongly continuous semigroup of bounded linear operators, B is a bounded linear operator and the control function u is given in $L^2([0,b],U)$, where U is a Banach space. This will make the subject of a future publication.

Acknowledgment

The authors would like to thank the referee and editors for their helpful comments.

References

[1] M. Abdo and S. Panchal. Initial value problem for a fractional neutral differential equation with infinite delay. *Int. J. of Nonlinear Anal. Appl.* **12** (1) (2021) 1195–1206.

[2] B. Ahmad and S. Ntouyas. Existence and uniqueness of solutions for Caputo-Hadamard sequential fractional order neutral functional differential equations. *Electron. J. Differ Equ.* **2017** (36) (2017) 1–11.

[3] R. Almeida, N. R. O. Bastos and M. T. T. Teresa. Modeling some real phenomena by fractional differential equations. *Math. Methods Appl. Sci.* **39** (16) (2015) 4846–4855.

[4] M. Benchohra, J. Henderson, S. K. Ntouyas and A. Ouahab. Existence results for fractional order functional differential equations with infinite delay. *J. Math. Anal. Appl.* **338** (2) (2008) 1340–1350.

[5] A. Cabada and R. Khaldi. Lyapunov-type inequality for higher order left and right fractional p-Laplacian problems. *Proyecciones* **40** (4) (2021) 1031–1040.

[6] C. Chen and Q. Dong. Existence and Hyers-Ulam stability for a multi-term fractional differential equation with infinite delay. *Mathematics* **10** (7) (2022).

[7] J. Deng and H. Qu. New uniqueness results of solutions for fractional differential equations with infinite delay. *Comput. Math. Appl.* **60** (8) (2010) 2253–2259.

[8] S. Dhar and J. T. Neugebauer. Lyapunov-Type Inequalities for a Fractional Boundary Value Problem with a Fractional Boundary Condition. *Nonlinear Dyn. Syst. Theory* **22** (2) (2022) 133–143.

[9] Q. Dong, C. Liu and Z. Fan. Weighted fractional differential equations with infinite delay in Banach spaces. *Open Math.* **14** (1) (2016) 370–383.

[10] C. Duque, H. Leiva and A. Tridane. Existence and Uniqueness of Solutions for a Semilinear Functional Dynamic Equation with Infinite Delay and Impulses. *Nonlinear Dyn. Syst. Theory* **22** (2) (2022) 155–168.

[11] H. Fazli, F. Bahrami and J. Nieto. General Basset-Boussinesq-Oseen equation: existence, uniqueness, approximation and regularity of solutions. *Int. J. Comput. Math. Comput. Syst. Theory* **97** (9) (2020) 1792–1805

[12] K. M. Furati. A Cauchy-type problem involving a weighted sequential derivative in the space of integrable functions. *Comput. Math. Appl.* **66** (5) (2013) 883–891.

[13] A. Guezane-Lakoud and R. Rodríguez-López. Positive solutions to mixed fractional p-Laplacian boundary value problems. *J. Appl. Anal.* (2022).

[14] A. Guezane-Lakoud and A. Ashyralyev. Existence of solutions for weighted p(t)-Laplacian mixed Caputo fractional differential equations at resonance. *Filomat* **36** (1) (2022) 231–241.

[15] J. Hale and J. Kato. Phase Space for Retarded Equations with Infinite Delay. *Funkcial. Ekvac.* **21** (1978) 11–44.

[16] D. Henry. *Geometric Theory of Semilinear Parabolic Partial Differential Equations.* Springer-Verlag, Berlin, 1989.

[17] Y. Hino, S. Murakami and T. Naito. *Functional Differential Equations with Infinite Delay.* Springer, Berlin, Heidelberg, 2006.

[18] E. Kenef and A. Guezane-Lakoud. Impulsive mixed fractional differential equations with delay. *Prog. Fract. Differ. Appl.* **7** (3) (2017) 203–215.

[19] R. Khaldi and A. Guezane-Lakoud. On generalized nonlinear Euler-Bernoulli Beam type equations. *Acta Univ. Sapientiae, Math* **10** (1) (2018) 90–100.

[20] R. Khaldi and A. Guezane-Lakoud. Higher order fractional boundary value problem for mixed type derivatives. *J. Nonlinear Funct. Anal.* 2017:Article ID 30 (2017).

[21] A. A. Kilbas, H. Srivastava and J. Trujillo. *Theory and Applications Of Fractional Differential Equations* Elsevier, Amsterdam, 2006.

[22] V. Lakshmikantham, L. Wen and B. Zhang. *Theory of Differential Equations with Unbounded Delay.* Springer, New York, 1994.

[23] N. Mehmood and N. Ahmad. Existence results for fractional order boundary value problem with nonlocal non-separated type multi-point integral boundary conditions. AIMS Mathematics **1** (2019) 385–398.

[24] K. S. Miller and B. Ross. *An Introduction to the Fractional Calculus and Fractional Differential Equations.* Wiley, New York, 1993.

[25] N. Phuangthong, S. Ntouyas, J. Tariboon and K. Nonlaopon. Nonlocal Sequential Boundary Value Problems for Hilfer Type Fractional Integro-Differential Equations and Inclusions. *Mathematics* **9** (6) (2021).

[26] S. G. Samko, A. A. Kilbas and O. I. Marichev. *Fractional Integrals and Derivatives: Theory and Applications.* Gordon and Breach, Yverdon, 1993.

[27] H. Ye and R. Huang. On the nonlinear fractional differential equations with Caputo sequential fractional derivative. *Adv. Math. Phys.* **2015** (2015) 1–9.

Nonlinear Dynamics and Systems Theory, **24** (1) (2024) 12–27

A General Kinematic-Based Walking Algorithm of a Hexapod Robot on Irregular Terrain

A. Aissaoui [1*], C. Mahfoudi [2] and S. Djeffal [2]

[1] *University of Oum El bouaghi, Algeria.*
[2] *University of Oum El bouaghi, CMASMTF laboratory, Algeria.*

Received: March 7, 2023; Revised: December 31, 2023

Abstract: Developing an algorithm for ensuring a feasible gait of Hexapod Walking Robots (HWRs) poses the challenge of enabling smooth locomotion on uneven terrain, utilizing the mobility of its six legs that alternately make contact with the ground. To this end, a kinematic-based approach is applied that individually takes into account the movements of each leg, while maintaining compatibility with the body's motion through a non-symmetrical tripod gait. Accordingly, the forward kinematics of the robot is established using the Denavit-Hartenberg parameterization and its inverse kinematics is derived using Paul's method. Then, the uneven terrain is represented by elevation differences in a 3D curve trajectory. After that, an algorithm is proposed to ensure the adaptability of the robot's legs with respect to the terrain's shape, namely, the algorithm allows each leg to follow its own trajectory independently. To validate the proposed approach, 3D simulations are conducted using MATLAB software, demonstrating the accuracy and reliability of the purely kinematic approach. The results show that the algorithm enables the HWR to adapt its walking to irregular terrain in various general cases.

Keywords: *Hexapod Walking Robots (HWRs); modeling robots; gait locomotion; tripod gait.*

Mathematics Subject Classification (2010): 70K25, 70K42, 70K70, 93-04, 93-10.

* Corresponding author: mailto:aissaoui.abderahmane@univ-oeb.dz

1 Introduction

Hexapod Walking Robots (HWRs) are mechanical vehicles that emulate the locomotion of insects, characterized by their mobility, maneuverability, adaptability, flexibility, and stability in natural terrains. These robots are inspired by the biological features of insects and utilize six legs for walking, enabling them to navigate various terrains with efficiency and versatility [1,2]. In legged locomotion, HWRs are favored by static stability gait due to having three legs in contact with the ground all the time, flexibility where they move, fault tolerant locomotion, possibility to manipulate objects using their legs as arms.

In addition to the advantages mentioned earlier, Hexapod Walking Robots (HWRs) have superior terrain adaptation capabilities compared to wheeled robots. By utilizing discrete contacts with the ground, HWRs can bypass undesirable footholds, avoid obstacles, select optimal terrain contacts, and adapt their walking posture to navigate through confined spaces. This is made possible due to their high degrees of freedom and flexibility, which make them the ideal solution for locomotion on rough and uneven terrains. HWRs have a unique advantage in navigating complex environments and are well-suited for applications that require versatile and agile mobility in challenging terrains [3–5]. HWRs can be used for intervention in hostile environments like humanitarian demining operations, disaster recovery missions, nuclear plant maintenance, operations in volcanic sites, underwater searching and space exploration. Beyond this type of applications, HWRs can also be used in a wide variety of service tasks such as forest harvesting and service robots [6–9].

In current realizations, hexapod robots are very far from the complexity of real insects in terms of the number of degrees of freedom, velocity and dimensions. Researchers are only interested in extracting the essential characteristics of the insects' walking system and implementing them in real robots. A gait can be described as a sequence of leg motions coordinated with a sequence of body motions for transporting the robot's body [10]. The choice of the gait's mode is the first essential step to guarantee stability and efficiency of the hexapod walking robot motion.

Most studies used for hexapod locomotion the common and basic gait called a tripod gait where the body is propelled continuously by the cyclic sequencing of the movements of three legs which were in the air and come to rest on the ground while the other three release the contact there and return after half a period (legs coordination). Each leg performs a walking step in two phases [11]: a support phase during which the foot of the leg remains in contact with the ground, its active joints cause the robot's body to move forward horizontally; and a swing phase where the end of the leg follows a trajectory in the air and then comes back into contact with the ground to start a new step. This tripod gait of the hexapod can achieve fast movement with stability.

In terms of the hexapod robot's gait generation, we note that the legged locomotion of the HWRs is performed according to two major types of approaches: analytical approaches and bio-inspired approaches. Since it does not require complex geometrical calculation, the majority of studies are made according to the bio-inspired approaches to generate symmetrical gaits and reproduce different type of gaits for a hexapod robot. The most common approach for the design of a bio-inspired architecture consists of a Central Pattern Generator (CPG) network with six coupled nonlinear oscillators [12]. By controlling the durations of the ascending and descending phase of the limb trajectory, they control the durations of the swing and stance step phases, respectively. This network produces synchronized rhythms that give the correct pattern for locomotion [13, 14].

As regards the analytical approaches, we note firstly that the existing works regarding gait generation in flat terrain, only deal with a single X direction and describe the kinematic model by using a matrix approach and propose different gaits (tripod gait, quadrangular gait, and pentagonal gait) where the sequences of coordination legs according to different rhythms are converted by the Inverse Kinematics Model (IKM) and preloaded on a computer which sends commands to the servo controller and the hexapod executes corresponding instructions [10, 15–17]. The models mentioned above only work on flat ground and constitute a compulsory phase to begin with, but in reality, it is necessary to take into account, during the modeling, the nature of the real terrain which is uneven and which presents irregularities.

A synthesis of the works quoted above allowed us to notice that the generation of trajectories of HWRs on an uneven ground which presents irregularities in terms of variation of altitude is an extension of walking on flat ground, which is a reduced case of walking. For this, we are motivated by the study of the general case of real walking which can model at the same time and in an exact mathematical way the HWRs with all its 24 degrees of freedom in walking interaction on a rough terrain of arbitrary shape which can be modeled by a 3D curve without any restriction either on the model of the robot or on the terrain. The rest of the paper is structured as follows. Section 2 presents the kinematic modeling of the HWR. The proposed walking algorithm is studied in detail in Section 3. Section 4 illustrates the results obtained using this approach. Finally, conclusions are made in Section 5.

2 HWR Model

A hexapod walking robot consists of a rectangular body to which six identical legs are articulately attached, see Figure 1. Each leg of the robot has three degrees of freedom allowing the robot to move its legs dexterously according to the given position within its workspace.

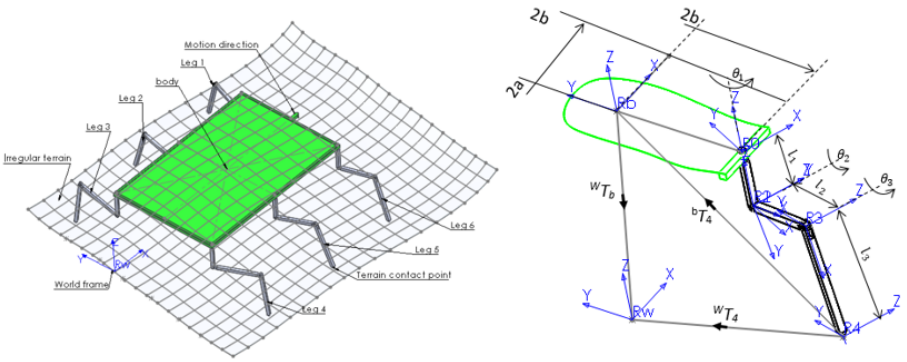

Figure 1: (Left) CAD Model of the HWRs with six legs; (Right) Attachment of the reference frames for the robot's five legs as a model.

2.1 Forward kinematic model of the hexapad robot

The forward kinematic model (FKM) [18–20] for a hexapod robot resides in finding the location of robot body with respect to robot's legs joint variables according to the

coordinate frames established in Figure 1 (right). To model the HWRs having a body of length $2a$ and a width $2b$, the leg number five is chosen as the leg-model [21]. It is made up of three segments of respective lengths l_1, l_2, l_3 and three rotoid articulations of angle θ_1, θ_2 and θ_3. The D-H parameters of the leg-model are shown in equation (6). The FKM of a leg relative to the world frame is calculated by the product of the homogeneous transformation matrices according to equation (1), namely it provides the positions of the contact points of each leg according to the world frame.

$$ {}^{W}T_{4,j} = {}^{W}T_{b}\,{}^{b}T_{0,j}\,{}^{0,j}T_{1,j}\,{}^{1,j}T_{2,j}\,{}^{2,j}T_{3,j}\,{}^{3,j}T_{4,j} \tag{1} $$

with $j = \overline{1,6}$ being the legs' index.

The matrix situation of the robot's base can be expressed as follows:

$$ {}^{W}T_{b} = {}^{W}Trans_{b}\,{}^{W}Rot_{b}(Z_{\psi}, Y_{\theta}, X_{\varphi}) \tag{2} $$

with

$$ {}^{0}Trans_{b} = \begin{bmatrix} 1 & 0 & 0 & x_b \\ 0 & 1 & 0 & y_b \\ 0 & 0 & 1 & z_b \\ 0 & 0 & 0 & 1 \end{bmatrix}. \tag{3} $$

The matrix of articulations points of each leg can be expressed by the following:

$$ {}^{b}T_{0,j} = \begin{bmatrix} 1 & 0 & 0 & x_{0,j} \\ 0 & 1 & 0 & y_{0,j} \\ 0 & 0 & 1 & z_{0,j} \\ 0 & 0 & 0 & 1 \end{bmatrix}, \tag{4} $$

$$ \begin{aligned} x_{0,j} &= \begin{bmatrix} -a & -a & -a & a & a & a \end{bmatrix}, \\ y_{0,j} &= \begin{bmatrix} b & b & b & -b & -b & -b \end{bmatrix}, \\ z_{0,j} &= \begin{bmatrix} 0 & 0 & 0 & 0 & 0 & 0 \end{bmatrix}. \end{aligned} \tag{5} $$

The parameters table of Denavit-Hertberg corresponding to the leg_j is

$$ DH_j = \begin{bmatrix} 0 & 0 & \theta_{1,j} & -l_1 \\ -\pi/2 & 0 & \theta_{2,j} & 0 \\ 0 & l_{2,j} & \theta_{3,j} & 0 \\ 0 & l_{3,j} & 0 & 0 \end{bmatrix}. \tag{6} $$

The homogenous matrix of Denavit-Hertberg can be expressed as follows:

$$ {}^{j-1}T_{j} = \begin{bmatrix} C\theta_j & -S\theta_j & 0 & d_j \\ C\alpha_j S\theta_j & C\alpha_j C\theta_j & -S\alpha_j & -r_j S\alpha_j \\ S\alpha_j S\theta_j & S\alpha_j C\theta_j & C\alpha_j & r_j C\alpha_j \\ 0 & 0 & 0 & 1 \end{bmatrix} \tag{7} $$

$$ with\ C(.) = Cos(.)\ ,\ S(.) = Sin(.). $$

Four matrices of the leg-model are worth, respectively,

$$ {}^{0}T_{1} = \begin{bmatrix} C1 & -S1 & 0 & 0 \\ S1 & C1 & 0 & 0 \\ 0 & 0 & 1 & -l1 \\ 0 & 0 & 0 & 1 \end{bmatrix}, \tag{8} $$

$$ {}^{1}T_2 = \begin{bmatrix} C2 & -S2 & 0 & 0 \\ 0 & 0 & 1 & 0 \\ -S2 & -C2 & 0 & 0 \\ 0 & 0 & 0 & 1 \end{bmatrix}, \tag{9} $$

$$ {}^{2}T_3 = \begin{bmatrix} C3 & -S3 & 0 & l2 \\ S3 & C3 & 0 & 0 \\ 0 & 0 & 1 & 0 \\ 0 & 0 & 0 & 1 \end{bmatrix}, \tag{10} $$

$$ {}^{3}T_4 = \begin{bmatrix} 1 & 0 & 0 & l3 \\ 0 & 1 & 0 & 0 \\ 0 & 0 & 1 & 0 \\ 0 & 0 & 0 & 1 \end{bmatrix}. \tag{11} $$

This yields the FKM of leg model 5 (Figure 2).

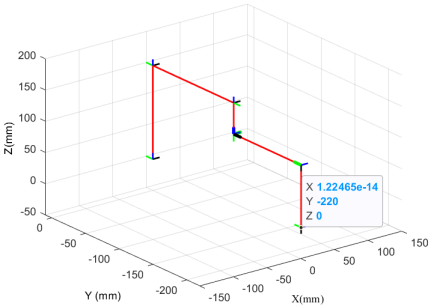

Figure 2: FKM of the leg model 5.

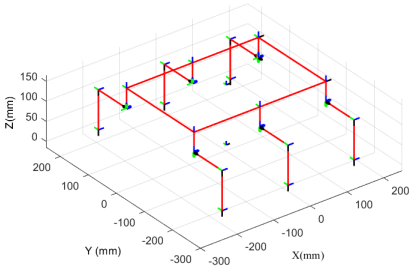

Figure 3: HWR's FKM.

After calculating the FKM of the leg-model, the FKM of the entire robot consists in distributing six legs around its body as it is shown in Figure 3.

2.2 Inverse kinematic model of hexapod robot

The inverse kinematic model (IKM) of the HWR's leg is firstly calculated according to the body frame R_b. As previously mentioned, the FKM of the robot can be expressed by the following equation:

$$ U_0 = \begin{bmatrix} s_x & n_x & a_x & PX \\ s_y & n_y & a_y & PY \\ s_z & n_z & a_z & PZ \\ 0 & 0 & 0 & 1 \end{bmatrix} = {}^{b}T_{0,j}\,{}^{0,j}T_{1,j}\,{}^{1,j}T_{2,j}\,{}^{2,j}T_{3,j}\,{}^{3,j}T_{4,j}. \tag{12} $$

Paul's method consists in multiplying the equation (12) by ${}^{1,j}T_b$ which is the inverse of ${}^{b}T_{1,j}$:

$$ {}^{1,j}T_b U_0 = {}^{1,j}T_{2,j}\,{}^{2,j}T_{3,j}\,{}^{3,j}T_{4,j}, \qquad j = \overline{1,6}. \tag{13} $$

By identifying the elements of the fourth column of the product on the left-hand side of equation (13) with those of the fourth column of the product on the right, we will have

$$ S1 = PY - y_{0,j},\ S1 = PX - x_{0,j}, $$
$$ \theta_1 = ATAN2(S1, C1),\ \theta_1^{'} = \theta_1 + \pi. $$

The second multiplication yields

$$
\begin{aligned}
&X = (PX - x_{0,j})C1 + (PY - y_{0,j})S1 \ , \\
&Y = PZ + l_1 \, , \ \ Z_1 = -l_2 \ , \ Z2 = 0 \ , \ \ W = l_3, \\
&B1 = -2(XZ2 + YZ1) \ , B2 = 2(XZ1 - YZ2), \\
&B3 = W^2 - X^2 - Y^2 - Z1^2 - Z2^2, \\
&S2 = (B1B3 + B2(B1^2 + B2^2 - B3^2)^{0.5})/(B1^2 + B2^2), \\
&C2 = (B2B3 - B1(B1^2 + B2^2 - B3^2)^{0.5})/(B1^2 + B2^2), \\
&\theta_2 = ATAN2\,(S2, C2)\,,
\end{aligned}
$$

$$
\begin{aligned}
S3 &= (-XS2 - YC2 + Z2)/W, \\
C3 &= (XC2 - YS2 + Z1)/W, \\
\theta_3 &= ATAN2(S3, C3)\,.
\end{aligned}
$$

The hexapod robot simulation via MATLAB is executed to verify the efficiency of the derived IKM with different curbs followed by the robot leg points of contact. As it is shown in Figures 4, 5, 6, 7, the robot's leg follows spatial straight line, circle-like shape, cycloid and spiral trajectories, respectively.

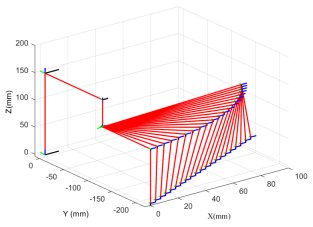

Figure 4: The robot's leg follows spatial linear trajectory.

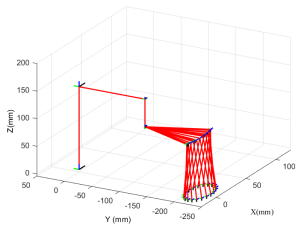

Figure 5: The robot's leg follows circular trajectory.

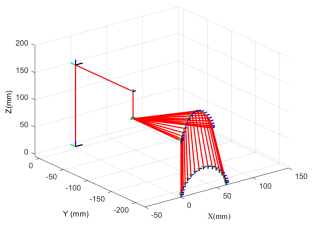

Figure 6: The robot's leg follows cycloid trajectory.

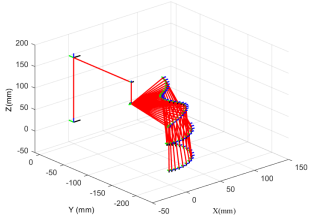

Figure 7: The robot's leg follows spiral trajectory.

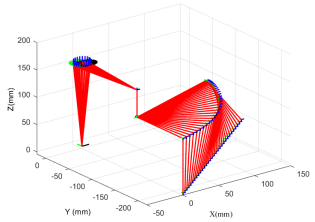

Figure 8: Simultaneous movement of the leg's point of contact (linear) and body of the robot (circular).

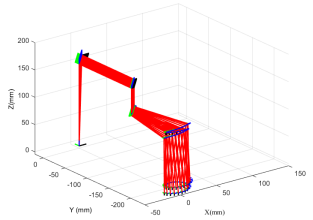

Figure 9: Simultaneous movement of the leg's point of contact (spiral) and body of the robot (linear-spatial).

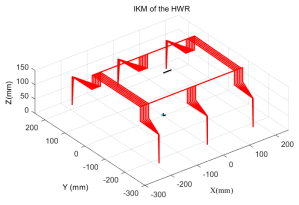

Figure 10: Linear trajectory along X.

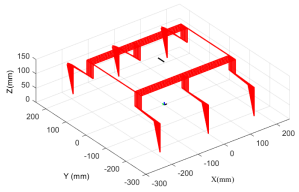

Figure 11: Linear trajectory along Y.

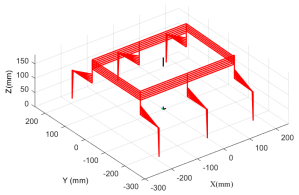

Figure 12: Linear trajectory along Z.

Additionally, the movement of robot's leg point of contact can be performed simultaneously with that of the body as is depicted in Figures 8, 9.

Finally, we validate the established IKM of the whole robot, namely the robot's body can perform six degrees of freedom $(x_b, y_b, z_b, Z_\psi, Y_\theta, X_\varphi)$, meanwhile its legs can further move according to any given trajectory belonging to the robot's workspace as it is graphically represented in Figures 10, 11, 12, 13, 14, 15.

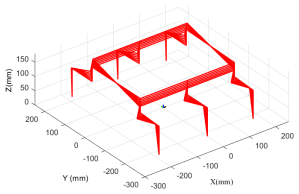

Figure 13: HWR's body rotation ϕ around X

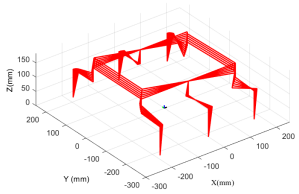

Figure 14: HWR's body rotation θ around Y

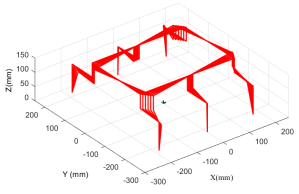

Figure 15: HWR's body rotation ψ around Z

.

In conclusion, for the HWR's IKM, an example is given in Figure 16 which represents the eighteen values of the angles $(\theta_1, \theta_2, \theta_3)$ of the HWR's six legs corresponding to the posture of Figure 16 previously presented.

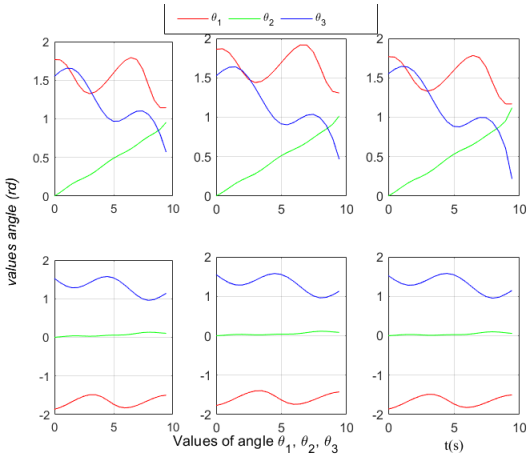

Figure 16: Values of angles $(\theta_1, \theta_2, \theta_3)$ which correspond to the posture of Figure 15.

3 Proposed Walking Algorithm of a HWR on Irregular Terrain

The generation of the walk of an HWR on irregular terrain must take into account, in addition to the modeling of the robot, the irregular shape of the terrain which is manifested by differences in altitudes of the contact points with the ground. These differences express the variation of the Z component of these contact points which is zero for a flat terrain and different from zero for irregular terrain. To achieve this objective of walking on irregular terrain, we propose in this paper a general algorithm that works according to the following flowchart.

- Step 1: input: Geometrical parameters of the HWR (a=180; b=120; l1=50; l2=100; l3=100).
- Step 2: input: Any 3D terrain composed of 6 trajectories, each comprising n_{steps}.
- Step 3: Model of irregular terrain and extraction of its parameters.
  - ✓ for each step k (k=1: n_{steps}) do:
    - ✓ for t=0:n (n refers to the step's period)
    - ∗ *if t≤n/2 do*
  - − for each leg$_j$ ($j = 1 : 6$) do:
- Step 4: Adaptation of the Normal Cycloid$_j$ (NC)$_j$ (leg$_j$: $j = 1, 3, 5$) to its irregular terrain$_j$.
- Step 5: Adaptation of leg$_j$ to follow the Adapted Cycloid$_j$ (AC)$_j$.
- Step 6: Synchronization of the movements of six legs (tripod gait: 135_{swing} and 246_{stanse}).
- Step 7: Adaptation of the movement of the HWR's body to the movements of its six legs.
- Step 8: IKM of leg$_j$.
- Step 9: FKM of leg$_j$.
- Step 10: End for each leg$_j$.
- if t>=n/2: do
- Step 11: Actualization of body position.
- for each leg$_j$ do
- Step 12: Adaptation of the Normal Cycloid$_j$ (NC)$_j$ (leg$_j$: $j = 2, 4, 6$) to its irregular terrain$_j$.
- Step 13: Adaptation of leg$_j$ to follow the Adapted Cycloid$_j$ (AC)$_j$.
- Step 14: Synchronization of the movements of six legs (tripod gait: 246_{swing} and 135_{stanse}).

- Step 15: Adaptation of the movement of the body of the HWR to the movements of its six legs.
- Step 16: IKM of leg_j.
- Step 17: FKM of leg_j.
- End for each leg$_j$.
- End for t=0:n.
- End for each step k.

It is noteworthy to say that the aforementioned algorithm's steps for HWR walking are elaborately detailed in the following sections.

3.1 Model of the irregular terrain and extraction of its parameters

In general, the walking of a hexapod walking robot (HWR) may not be symmetrical, and each leg may follow a different trajectory compared to the others. To account for this, we define the model of the irregular terrain for each leg as a set of contact points belonging to a 3D curve. As a result, the irregular terrain can be represented by six curves, within the reachable domain of the robot, derived from the shape of the reference terrain, which is defined by

$$\begin{cases} x_T, \\ y_T = f_x\left(x_T\right), \\ z_T = f_{xy}\left(x_T, y_T\right), \end{cases} \tag{14}$$

with

- x_T : Evolution of the terrain along the X axis with a step length and a number of n_{step};
- f_x : A function of x_T representing the evolution of the terrain along the Y axis;
- f_{xy} : A function of x_T and y_T denoting the variation in altitude of different points of the terrain.

The position of six legs relative to the reference is given by the matrix T_{R1} as

$$T_{R1} = \begin{bmatrix} x_T + a & y_T + (b + l2) & z_T \\ x_T - pas/2 & y_T + (b + l2) & z_T \\ x_T - a & y_T + (b + l2) & z_T \\ x_T - a - pas/2 & y_T - (b + l2) & z_T \\ x_T & y_T - (b + l2) & z_T \\ x_T + a - pas/2 & y_T - (b + l2) & z_T \end{bmatrix}^T . \tag{15}$$

Then, we distinguish between these six identical trajectories by introducing the following coefficients $k_{i,j}$:

$$T_{Rk} = \begin{bmatrix} k_{11}x_T + a & k_{21}y_T + (b + l2) & k_{31}z_T \\ k_{12}x_T + pas/2 & k_{22}y_T + (b + l2) & k_{32}z_T \\ k_{13}x_T - a & k_{23}y_T + (b + l2) & k_{33}z_T \\ k_{14}x_T - a - pas/2 & k_{24}y_T - (b + l2) & k_{34}z_T \\ k_{15}x_T & k_{25}y_T - (b + l2) & k_{35}z_T \\ k_{16}x_T + a - pas/2 & k_{26}x_T - (b + l2) & k_{36}z_T \end{bmatrix}^T . \tag{16}$$

Remarkably, T_{Rk} can describe any type of irregular terrains that the HWR can track according to the given values of the coefficients k_{ij} :

- $k_{ij} = 1$ for a reference terrain;
- $k_{3j} = 0$ for flat terrain;
- Remaining case for any uneven terrain.

Figure 17 illustrates 6 independent trajectories corresponding to six legs of the HWR:

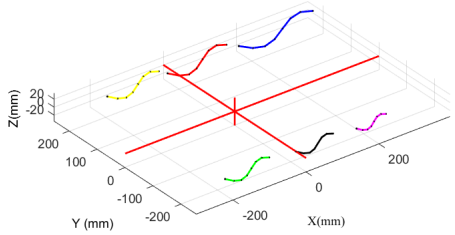

Figure 17: 6 curves representing 6 trajectories to follow.

For each terrain$_j$ composed of n_{steps} that the leg$_j$ must follow, we calculate the geometric parameters of two contact points P_O (x_{T0j}, y_{T0j}, z_{T0j}) of the beginning and P_1 (x_{T1j}, y_{T1j}, z_{T1j}) of the end of a walking step (see Figure 18) according to

$$\Psi_j = -\operatorname{atan2}\left(\left(y_{T1j} - y_{T0j}\right), \left(x_{T1j} - x_{T0j}\right)\right), \tag{17}$$

$$lp_j = \sqrt{\left(x_{T1j} - x_{T0j}\right)^2 + \left(y_{T1j} - y_{T0j}\right)^2}, \tag{18}$$

$$\Theta_j = \operatorname{atan2}\left(\left(z_{T1_j} - z_{T0_j}\right), lp_j\right), \tag{19}$$

$$ls_j = \sqrt{\left(x_{T1_j} - x_{T0j}\right)^2 + \left(y_{T1j} - y_{T0j}\right)^2 + \left(z_{T1j} - z_{T0j}\right)^2}, \tag{20}$$

$$R_j = \frac{ls_j}{2 \times \pi}, \tag{21}$$

Ψ_j : the rotation angle along OZ;
lp_j : the length of the step in the plane XOY;

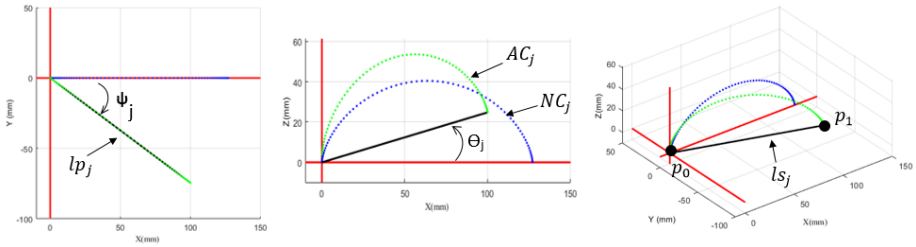

Figure 18: Adaptation of the cycloïd 5 to the irregular terrain at the origin XY.

Θ_j : the rotation angle along OY;
ls_j : the length of the step in the space;
R_j : the cycloid' radius.

3.2 Adaptation of the normal cycloid$_j$ to the irregular terrain$_j$

We define a Normal Cycloid$_j$ trajectory in the XOZ plane (Figure 19)that the leg$_j$ must follow in the swing phase by the following equation:

$$\begin{cases} x_{NCj} = R_j \times (t - \sin(t)), \\ y_{NCj} = 0, \\ z_{NCj} = R_j \times (1 - \cos(t)). \end{cases} \tag{22}$$

We adapt the normal cycloid NC_j so that it matches its terrain$_j$ by the combination of two rotations and a translation (Figure 20) and it is denoted AC_j, thus it is adapted to the terrain$_j$ by the relations

$$AC_j = NC_j \times rot(Y, \Theta_j) \times rot(Z, \Psi_j) + [x_{T0j}; y_{T0j}; z_{T0j}], \tag{23}$$

$rot(Z, \Psi_j)$: Rotation matrix around OZ;
$rot(Y, \Theta_j)$: Rotation matrix around OY.

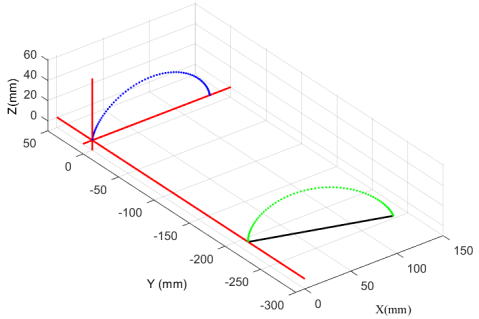

Figure 19: Adaptation of the cycloid$_5$ to the irregular terrain$_5$ for one step.

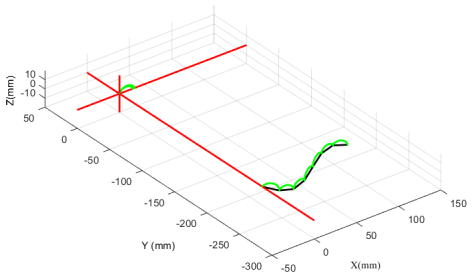

Figure 20: Adaptation of the cycloid to uneven terrain composed of seven steps.

3.3 Adaptation of leg$_j$ to the cycloid of its terrain$_j$

Depending on the desired number of steps, each leg$_j$ follows the cycloids adapted with a fixed body (see Figure 21) using the developed IKM.

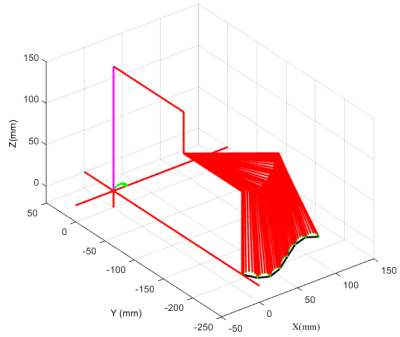

Figure 21: Adaptation of the leg$_j$ to the cycloids of its terrain$_j$.

3.4 Synchronization of the movements of six legs in the tripod mode

Each leg of the HWR performs a walking step in two phases: a support phase and a swing phase (see Figure 22). The most used mode of walking which can ensure speed and stability is the alternating tripod, it is carried out by the sequencing of six legs, three by three during a period T: in the first half-period, the legs 135 are in the swing phase and legs 246 are in the support phase as they alternate in the second half-period for one and seven walking steps, respectively. Furthermore, for instance, the synchronization is given between two consecutive legs number five and six (see Figure 23).

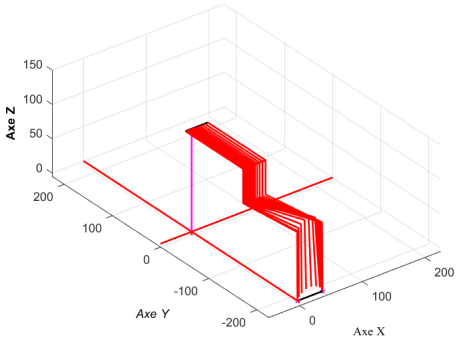

Figure 22: Two phases of a leg$_j$ for one walking step.

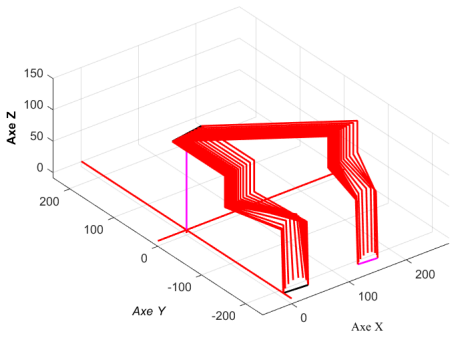

Figure 23: Synchronisation of a walking step for legs 5 and 6.

3.5 Adaptation of body's movement to the movements of its six legs

The spatial displacement of the body of the HWR occurs when the legs in contact with the ground propel it into a given coherent situation (position and orientation). To ensure

the compatibility between the movement of the legs and that of the body, we propose for the body:

- movement in the XOY plane in small straight segments as the average resultant of the movement of six legs along

  ✓ the X axis:

$$\begin{cases} x_{T0} = \sum_{j=1}^{6} \frac{x_{T0j}}{6}, \\ x_{T1} = \sum_{j=1}^{6} \frac{x_{T1j}}{6}, \\ x_b = \frac{x_{T1}-x_{T0}}{2n} t + x_{00}, \end{cases} \tag{24}$$

  where x_{00} refers to the initial position of the robot's body;

  ✓ the Y axis:

$$\begin{cases} y_{T0} = \sum_{j=1}^{6} \frac{y_{T0j}}{6}, \\ y_{T1} = \sum_{j=1}^{6} \frac{y_{T1j}}{6}, \\ y_b = \frac{y_{T1}-y_{T0}}{x_{T1}-x_{T0}} x_b + y_{T0} - \frac{(y_{T1}-y_{T0})}{(x_{T1}-x_{T0})} x_{T0}; \end{cases} \tag{25}$$

- the Z axis, a sinusoidal [22,23] movement (see Figure 25) which describes the case of the real gait of the insect and that at a fixed height (see Figure 24) of its body.

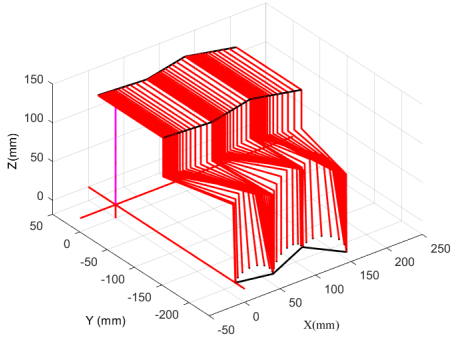

Figure 24: Alternating tripod gait of the HWR on flat terrain at a fixed height of the body.

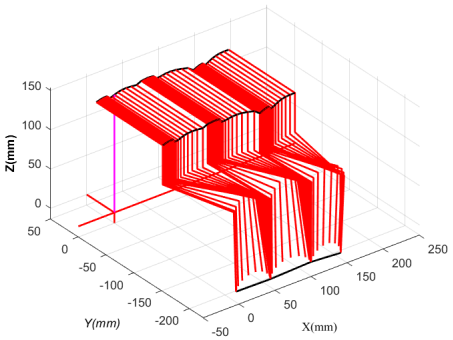

Figure 25: Alternating tripod gait of the HWR on flat terrain with sinusoidal height of the body.

4 Results and Discussion

In this section, the obtained results are mainly based on three types of terrain progressively ordered by the degree of locomotion's difficulty:

- A flat terrain is characterized by its null altitude ($Z = 0$). It is obviously clear from (Figure 26), the HWR executes two steps of alternating tripod walking while its body remains horizontal at a constant height $(l1+l3)$ and it oscillates horizontally (see Figure 27).

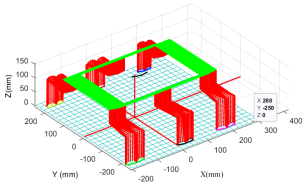

Figure 26: Alternating tripod gait of the HWR on flat terrain at a fixed height of the body.

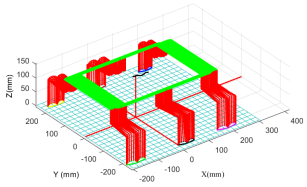

Figure 27: Alternating tripod gait of the HWR on flat terrain with a sinusoidal height of the body.

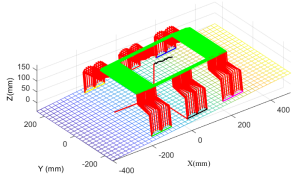

Figure 28: Alternating tripod gait of the HWR on inclined terrain with sinusoidal movement while the body remains parallel to the sloped terrain.

- On slopped terrain, in this simulation, the HWR executes two steps of alternating tripod gait on an inclined plan and it oscillates sinusoidally and remains parallel to terrain (see Figure 28).
- An irregular terrain with a constant and variable height of the body (see Figures 29 and 30).

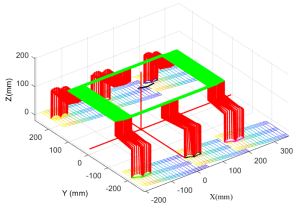

Figure 29: Walking on uneven ground at a fixed body height.

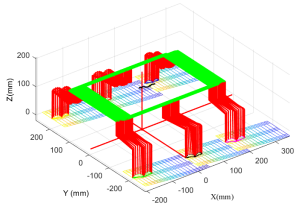

Figure 30: Walking on irregular terrain with sinusoidal height of the body.

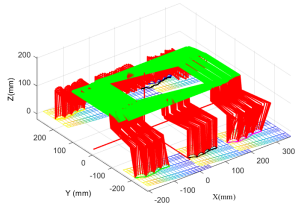

Figure 31: Walking on irregular terrain with sinusoidal height of the body with body's orientation.

- General case: We take credit from the redundancy of the HWR's body, namely we can activate all its degrees of freedom for the sake of providing the HWR with any given orientation during the walking process, which results in avoiding the encountered obstacles, where this orientation is inevitably required as the oriented posture given in Figure 31.

5 Conclusion

The proposed walking algorithm for the HWR on irregular terrain, based on the key elements of modeling the robot and its legs, modeling the terrain, adapting the legs to

the terrain, synchronizing the legs for a tripod gait, and ensuring compatibility with the body's movement, shows promising results. The algorithm is demonstrated to be accurate and reliable in following the shape of irregular terrains, regardless of the terrain type or leg and body trajectories.

One of the major advantages of this algorithm is its applicability to various types of legged robots, including jumpers, bipeds, quadrupeds, and hexapods, due to the utilization of the HWR's redundancy and activation of all degrees of freedom of the robot's body.

Future perspectives for this research could include testing the algorithm on a real robot with data from real terrains to validate its performance in real-world conditions. Additionally, further investigation of the walking stability of the HWR in relation to terrain irregularities could provide valuable insights for enhancing the algorithm's performance.

Overall, this research contributes to the advancement of robot control for complex geometries and irregular terrains, paving the way for improved locomotion capabilities of legged robots in challenging environments.

References

[1] R. D. Quinn, G. M. Nelson, R. J. Bachmann, D. A. Kingsley and R. E. Ritzmann. Insect designs for improved robot mobility. *Proc. 4th Int. Conf. On Climbing and Walking Robots* (2001) 69–76.

[2] K. Lagaza. A Literature Review on Motion Planning of Hexapod Machines Using Different Review Article - Mechanical Engineering A Literature Review on Motion Planning of Hexapod Machines Using Different Soft Computing Methods. *Global Journal of Engineering, Science and Social Science Studies* **3** (1) (2018) 1–10.

[3] X. Ding, Z. Wang, A. Rovetta and J. M. Lagaza. Locomotion Analysis of Hexapod Robot. *Climbing and Walking Robots* (2010) 291–312. https://doi.org/10.5772/8822

[4] D. Wettergreen and B. D. Wettergreen. Robotic walking in natural terrain Gait planning and behavior-based control for statically-stable walking robots. *IEEE International Conference on Intelligent Robots and Systems, December* (1995) 134.

[5] S. S. Nair. Modeling and simulation of a six-legged walking robot power system. *Simulation* **58** (3) (1992) 185–195.

[6] I. Doroftei and Y. Baudoin. A concept of walking robot for humanitarian demining. *Industrial Robot: An International Journal* **39** (5) (2012) 441–449. https://doi.org/10.1108/01439911211249733.

[7] G. Heppner, A. Roennau, J. Oberländer, S. Klemm and R. Dillmann. Laurope-six legged walking robot for planetary exploration participating in the spacebot cup. *WS on Advanced Space Technologies for Robotics and Automation* **2** (13) (2015) 69–76.

[8] F. Tedeschi and G. Carbone. Design Issues for Hexapod Walking Robots. *Robotics* **2014** (3) (2014) 181–206. https://doi.org/10.3390/robotics3020181.

[9] M. Billah, M. Ahmed and S. Farhana. Walking Hexapod Robot in Disaster Recovery : Developing Algorithm for Terrain Negotiation and Navigation. *International Journal of Mechanical and Mechatronics Engineering* **2** (6) (2008) 795–800.

[10] F. Zhang, S. Zhang, Q. Wang, Y. Yang and B. Jin. Straight Gait Research of a Small Electric Hexapod Robot. *Applied science* **11** (8) (2021) 3714.

[11] R. Ramirez, A. Arellano-Delgado, R. M. Lopez-Gutierrez, J. Pliego-Jimenez and C. Cruz-Hernández. Master-Slave Synchronization of a Planar 2-DOF Model of Robotic Leg. *Nonlinear Dynamics and Systems* Theory **21** (4) (2021) 420–433.

[12] J. Coelho, F. Ribeiro, B. Dias, G. Lopes and P. Flores. Trends in the control of hexapod robots: A survey. *Robotics* **10** (3) (2021) 1–22. https://doi.org/10.3390/robotics10030100.

[13] H. Cruse, T. Kindermann, M. D. Schummand and J. Schmitz. Walknet – a biologically inspired network to control six-legged walking. *Neural networks.* **11** (7-8) (1998) 1435–1447.

[14] W. Qidi, L. I. U. Chengju, Z. Jiaqi and C. Qijun. Survey of locomotion control of legged robots inspired by biological concept. *Information Sciences* **52** (10) (2009) 1715–1729.

[15] G. Figliolini and P. Rea. *Mechanics and Simulation of Six-Legged Walking Robots.* INTECH Open Access Publisher, 2007.

[16] K. Priandana and A. Buono. Hexapod Leg Coordination using Simple Geometrical Tripod-Gait and Inverse Kinematics Approach. *In International Conference on Advanced Computer Science and Information Systems (ICACSIS)* (2017) 35–40.

[17] R. Wang. Hybrid Gait Planning of a Hexapod Robot. *Modern Electronic Technology* **4** (2) (2020), 11. https://doi.org/10.26549/met.v4i2.5075.

[18] H. Xia, X. Zhang and H. Zhang. A new foot trajectory planning method for legged robots and its application in hexapod robots. *Applied Sciences (Switzerland)* **11** (19) (2021). https://doi.org/10.3390/app11199217.

[19] S. I. Beaber, A. S. Zaghloul, M. A. Kamel and W. M. Hussein. Dynamic modeling and control of the hexapod robot using matlab simmechanics. *ASME International Mechanical Engineering Congress and Exposition* (2018) 52033.

[20] B. Stanczyk and J. Awrejcewicz. Six-Legged Robot Gait Analysis. *Nonlinear Dynamics and Systems Theory* **15** (1) (2015) 63–72.

[21] C. Mahfoudi, K. Djouani, S. Rechak and M. Bouaziz. Optimal force distribution for the legs of an hexapod robot. *Proceedings of 2003 IEEE Conference on Control Applications, 2003. CCA* 1 (2003) 657–663.

[22] H. M. Schepers, E. H. F. Van Asseldonk, J. H. Buurke and P. H. Veltink. Ambulatory estimation of center of mass displacement during walking. *IEEE Transactions on Biomedical Engineering* **56** (4) (2009) 1189–1195.

[23] T. Wöhrl, L Reinhardt and R. Blickhan. Propulsion in hexapod locomotion: how do desert ants traverse slopes. *Journal of Experimental Biology* **220** (9) (2017) 1618–1625.

Nonlinear Dynamics and Systems Theory, **24** (1) (2024) 28–40

Analysis of Customer Satisfaction Survey on E-Wallets Using Simple Additive Weighting and TOPSIS Methods

M. Y. Anshori [1], I. H. Santoso [2], T. Herlambang [3*], M. Tafrikan [4], M. Adinugroho [1], K. Oktafianto [5] and A. A. Firdaus [6]

[1] *Department of Management, Universitas Nahdlatul Ulama Surabaya, Indonesia.*
[2] *Department of Accounting Magister, University of Wijaya Kusuma, Surabaya, Indonesia.*
[3] *Department of Information System, Universitas Nahdlatul Ulama Surabaya, Indonesia.*
[4] *Department of Mathematics, University of PGRI Ronggolawe, Indonesia.*
[5] *Department of Mathematics, University of Islam Negeri Walisongo, Indonesia.*
[6] *Department of Engineering, Faculty of Vocational, Universitas Airlangga, Indonesia.*

Received: August 3, 2023; Revised: January 19, 2024

Abstract: Understanding customer's behaviors has an important role in business. The customer's behaviors dramatically change in line with technology development. In this modern era, customers buy goods no longer by cash payment but by electronic payment. E-wallet (electronic wallet) is a form of Fintech (Finance Technology) that utilizes internet and is used as an alternative payment method such as Funds, Shopeepay, Gopay, Ovo, Sakuku. In this study, the researchers examined which one had the high rate of the e-wallet customer satisfaction using the SAW and TOPSIS methods. Both methods were able to make more accurate assessments and predetermined preference weights. After the method implementation was done, it was concluded that the customer satisfaction surveys on e-wallet applications by using the SAW and TOPSIS methods showed the same results, that is, the first highest was DANA, the second was Shopeepay, the third was Gopay, the fourth was OVO, and the fith was Sakuku. Based on those results, the SAW and TOPSIS methods were recommended for use because they have relevant results.

Keywords: *e-wallet; customers; SAW, TOPSIS.*

Mathematics Subject Classification (2010): 90B50, 68U35.

* Corresponding author: mailto:aa.firdaus@vokasi.unair.ac.id

1 Introduction

Understanding customer's behaviors has an important role in business. The customer's behaviors dramatically change in line with technology development. In the past era, customers bought goods using cash payments. In this modern era or nowadays, customers buy goods no longer by cash payments. The payments are made electronically. The electronic payment system is an alternative payment system making it easier for consumers to make payments via the internet network [1].

Digital wallets or e-wallets are used for various things, particularly for money transfers. There are various uses of e-wallets, including e-wallets used to transfer funds between banks and between accounts, e-wallets used to pay various bills (for example, electric bills, telephone bills, etc.), e-wallets used to buy pulses or data packages, and those used as a place to save money known as savings. There are various types of e-wallets available in the community, that is, Dana, Shopeepay, Gopay, Ovo, and Sakuku.

The use of the Simple Additive Weighting (SAW) method is due to the fact that this method is able to provide more accurate estimates [2], [3], [4] and forecasts [5], [6], [7] assessment based on predetermined criteria values and preference weights. Besides, the Simple Additive Weighting (SAW) method can also determine the best alternative among several existing alternatives [8], [9], [10]. It does ranking process after determining the weight for each attribute. This study also used the Technique for Order Preference by Similarity to Ideal Solution (TOPSIS) method for its higher accuracy in determining the results.

2 Literature Review

2.1 The simple additive weighting (SAW)

The SAW (Simple Additive Weighting) method is often called the weighted sum method. The basic concept of the SAW method is to find a weighted sum of performance ratings for each alternative on all attributes [11], [12]. The SAW method requires the process of normalizing the decision matrix (x) to a scale that can be compared with all existing alternative ratings.

2.2 The SAW method procedure

1. Determine the criteria to be used as a reference in decision making, namely C_i.
2. Determine the suitability rating of each alternative for each criterion.
3. Make a decision matrix formed from a match table, according to the given preference weights.
4. The final result is obtained from the ranking process, namely the sum of the multiplication of the normalized matrix R with the weight vector so that the largest value is selected as the best alternative (A_i) as a solution.

The formula for doing normalization is as follows:

$$r_{ij} \begin{cases} \frac{x_{ij}}{Max\ x_{ij}} \ if\ j : atribute\ of\ benefit, \\ \frac{Min\ x_{ij}}{x_{ij}} \ if\ j : atribute\ of\ cost, \end{cases} \tag{1}$$

where r_{ij} is the normalized performance rating of A_i alternative on the C_j atrribute, $i = 1, 2, \ldots, m$ and $j = 1, 2, \ldots, n$. The preference value for each alternative (V_i) is given as

$$V_i = \sum_{j=1}^{n} w_j r_{ij}, \tag{2}$$

where V_i is the final value of the alternative, w_j is the predefined weight, r_{ij} is the normalised matrix. The higher value of V_i indicates that the alternative A_i is preferred.

2.3 Technique for order preference by similarity to ideal solution (TOPSIS) method

TOPSIS is based on the concept that the best chosen alternative not only has the shortest distance from the positive ideal solution but also has the longest distance from the negative ideal solution [13]. This concept is widely used in several MADM models to solve practical decision problems [13], [14], [15]. This is because the concept is simple and easy to understand, computation is efficient, and it has the ability to measure the relative performance of alternative decisions in a simple mathematical form.

2.4 The TOPSIS procedure

1. Make a normalized decision matrix.
2. Make the normalized decision matrix.
3. Determine the positive ideal solution matrix and the negative ideal solution matrix.
4. Determine the distance between the values of each alternative with the positive ideal solution matrix and the negative ideal solution one.
5. Determine the preference value for each alternative.

TOPSIS requires a performance rating for each alternative A_i on each normalized C_j criterion, that is,

$$r_{ij} = \frac{x_{ij}}{\sqrt{\sum_{i=1}^{m} x_{ij}^2}}, \tag{3}$$

$i = 1, 2, \ldots, m$ and $j = 1, 2, \ldots, n$.

The positive ideal solution A^+ and the negative ideal solution A^- can be determined based on the normalized weight rating (y_{ij}) as follows:

$$y_{ij} = w_i r_{ij}, \tag{4}$$

$i = 1, 2, \ldots, m$ and $j = 1, 2, \ldots, n$.

$$A^+ = \left(y_1^+, y_2^+, \ldots, y_n^+\right), \tag{5}$$

$$A^- = \left(y_1^-, y_2^-, \ldots, y_n^-\right) \tag{6}$$

with

$$y_j^+ \begin{cases} max\ y_{ij}; if\ j : atribute\ of\ benefit, \\ min\ y_{ij}; if\ j : atribute\ of\ cost, \end{cases}$$

$$y_j^- \begin{cases} max\ y_{ij}; if\ j : atribute\ of\ benefit, \\ min\ y_{ij}; if\ j : atribute\ of\ cost. \end{cases}$$

The distance between the alternative A_i and the positive ideal solution is formulated as follows:

$$D_i^+ = \sqrt{\sum_{j=1}^{n} \left(y_i^+ - y_{ij}\right)^2}; i = 1, 2, \ldots, m. \tag{7}$$

The distance between the alternative A_i and the negative ideal solution is formulated as follows:

$$D_i^- = \sqrt{\sum_{j=1}^{n} \left(y_{ij} - y_i^-\right)^2}; i = 1, 2, \ldots, m. \tag{8}$$

The preference value of each alternative (V_i) is given as

$$V_i = \frac{D_i^-}{D_i^- + D_i^+}; i = 1, 2, \ldots, m. \tag{9}$$

The higher value of V_i indicates that A_i is the preferred value.

2.5 E-wallet (digital wallet)

In Indonesia, an online-based payment system using electronic money (e-money) has been widely used. E-wallet (digital wallet) is a form of Fintech (Finance Technology) utilizing internet media and used as an alternative payment method such as Shopeepay, Funds, OVO, GoPsy, Sakuku. The E-wallet structure is as follows:

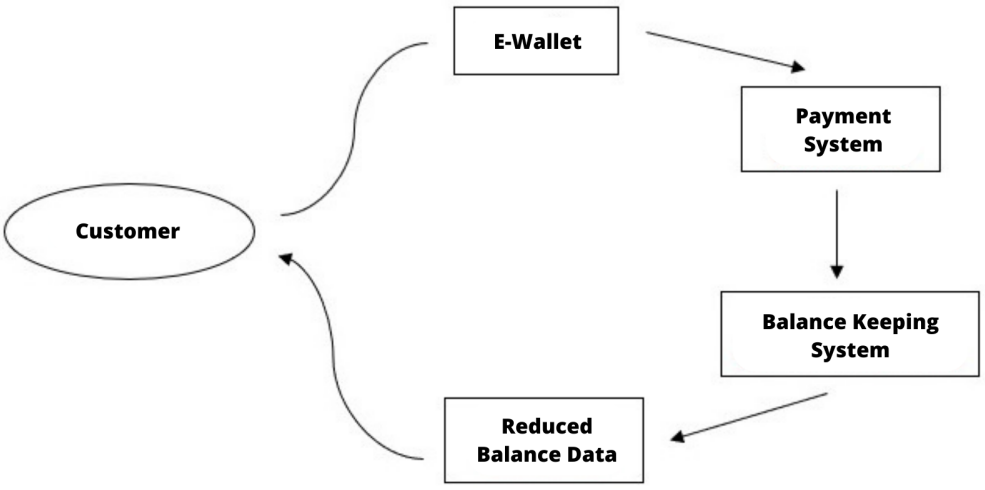

Figure 1: Source: niagahoster.co.id.

Based on the picture above, each customer has an e-wallet (digital wallet). After that, in the e-wallet feature, there is a payment system when a customer buys something. The e-wallet also has a balance storage system feature if the customer wants to save,

and the e-wallet can also view customer reduced balance data. The customer profile information is very meaningful for the company in relation to improving customer service and satisfaction.

3 Research Methodology

In this research, the Fuzzy Multiple Attribute Decision Making (FMADM) method was used by applying the Simple Additive Weighting (SAW) method and the Technique-for-Preference-by- Similarity-to-Ideal-Solution (TOPSIS) method.

In the SAW method, criteria and weights are required to do the calculations so as to obtain the best alternative. Simple Additive Weighting (SAW) is a weighted addition method. The basic concept of SAW is to find the weighted sum of the performance ratings for each alternative and criteria. The SAW method requires the process of normalizing the decision matrix (x) to a scale that can be compared with all existing alternative ratings. The SAW method recognizes the existence of 2 (two) attributes, that is, the criteria for benefits and the criteria for costs. The basic difference between these criteria is in the selection of decision-making criteria.

Meanwhile, the TOPSIS method requires a performance rating for each alternative A_i on each normalized C_j criterion. TOPSIS is based on the concept that the best chosen alternative is not only the shortest distance from the positive ideal solution, but also has the longest distance from the negative ideal solution.

In determining customer satisfaction with the e-wallets under study, criteria and weights are required to do the calculation so as to obtain alternatives. The following are the criteria needed for decision making, based on parameters in determining customer satisfaction with e-wallets.

Criteria	Description
C_1	Admin charge
C_2	Display
C_3	Accessibility
C_4	Topup Ease
C_5	Amount of Ballance Limit
C_6	Number of Payment functions

Table 1: Criteria.

Using these criteria, a level of importance of the criteria is determined based on the weight values that have been determined into fuzzy numbers. Next, the weight of each criterion is converted into a fuzzy number which is shown in Table 2.

Next, the weight of each criterion is converted into a fuzzy number as shown in Table 3.

4 Results and Discussion

The reference for the development of the decision support system (SPK) is based on researches commonly conducted on the e-wallet selection process. And in this study, each e-wallet was assessed based on criteria. This study used the Simple Additive Weighting

Value	Rating Scale
1	Very poor
2	Poor
3	Average
4	Good
5	Excellent

Table 2: Rating Scale.

Criteria	Description	Weight
C_1	Admin charge	$30\% = 0.3$
C_2	Display	$10\% = 0.1$
C_3	Accessibility	$10\% = 0.1$
C_4	Topup Ease	$25\% = 0.25$
C_5	Amount of Ballance Limit	$10\% = 0.1$
C_6	Number of Payment functions	$15\% = 0.15$

Table 3: Weight Criteria .

(SAW) method and the Technique for Preference by Similarity to Ideal Solution (TOPSIS) method, having criteria and weights to do calculations so as to obtain the best alternative.

Case sample:

The e-wallets to be studied were determined by taking those most in demand by the public and using several criteria such as admin charge, display, accessibility, topup ease, amount of balance limits, number of payment functions of the e-wallet.

In processing the research data, the researchers determined the completion steps in accordance with the Simple Additive Weighting (SAW) method, covering four stages, that is, determining the criteria to be used as a reference, determining the match rating of each alternative on each criterion, making a decision matrix, and ranking.

The criteria to be used as reference in decision making, that is, C_i, was determined as described in Chapter 2. There are six variables to be used as reference criteria to assess the customer satisfaction with the e-wallets by using the SAW method, namely admin charge, display, accessibility, topup ease, the amount of ballance limit, and the number of payment functions.

Below is the table listing the initials of the respondents along with the values of the assessment results received from the Google form. The value data for each respondent is then converted to a predetermined fuzzy number in Chapter 3, see Table 2.

4.1 Simple additive weighting (SAW) method

4.1.1 Determining match rating

The next step is to determine the match rating of each alternative for each criterion based on Table 4 contained in Chapter 4, as shown in Table 6.

E-Wallet	No	Average Value					
		C_1	C_2	C_3	C_4	C_5	C_6
Shopeepay	70	3.7142	3.8857	4.0714	3.8714	3.8142	4.0571
Dana	70	3.7142	4.0285	4.0857	4.0571	3.6714	4.0857
Ovo	70	3.4285	3.7142	3.7142	3.7571	3.5285	3.6571
Gopay	70	3.4142	3.7285	3.7714	4	3.5714	3.8857
Sakuku	70	3.3	3.3714	3.3428	3.3857	3.4285	3.3285

Table 4: Average Value.

Criteria	Description	Weight
C_1	Admin charge	$30\% = 0.3$
C_2	Display	$10\% = 0.1$
C_3	Accessibility	$10\% = 0.1$
C_4	Topup Ease	$25\% = 0.25$
C_5	Amount of Ballance Limit	$10\% = 0.1$
C_6	Number of Payment functions	$15\% = 0.15$

Table 5: Weight Criteria.

Alt	Average Value					
	C_1	C_2	C_3	C_4	C_5	C_6
A_1	3.7142	8.8857	4.0714	3.8714	3.8142	4.0571
A_2	3.7142	4.0285	4.0285	4.0571	3.6714	4.0857
A_3	3.4285	3.7142	3.7142	3.7571	3.5285	3.6571
A_4	3.4142	3.7285	3.7714	4	3.5714	3.8857
A_5	3.3	3.3714	3.3428	3.3857	3.4285	3.3285

Table 6: Match Rating.

4.1.2 Determining decision matrix

The following step for the formation of the decision matrix (x) made by referring to the table of the match rating of each alternative on each criterion is as follows:

$$X = \begin{pmatrix} 3.7142 & 8.8857 & 4.0714 & 3.8714 & 3.8142 & 4.0571 \\ 3.7142 & 4.0285 & 4.0285 & 4.0571 & 3.6714 & 4.0857 \\ 3.4285 & 3.7142 & 3.7142 & 3.7571 & 3.5285 & 3.6571 \\ 3.4142 & 3.7285 & 3.7714 & 4 & 3.5714 & 3.8857 \\ 3.3 & 3.3714 & 3.3428 & 3.3857 & 3.4285 & 3.3285 \end{pmatrix}.$$

Then, calculate the normalized value of each alternative with formula (1) as follows:

a. Criteria for Admin Charge (C_1):

$$r_{11} = \frac{3.7142}{3.7142} = 1, r_{21} = \frac{3.7142}{3.7142} = 1, r_{31} = \frac{3.4285}{3.7142} = 0.9230,$$

$$r_{41} = \frac{3.4142}{3.7142} = 0.9192, r_{51} = \frac{3.3}{3.7142} = 0.8884$$

so that the normalized value of the alternative production cost is obtained, then look for the normalized value of other alternatives.

b. Criteria for Display (C_2):

$$r_{12} = \frac{3.8857}{4.0285} = 0.9645, r_{22} = \frac{4.0285}{4.0285} = 1, r_{32} = \frac{3.7142}{4.0285} = 0.9291,$$

$$r_{42} = \frac{3.7285}{4.0285} = 0.9255, r_{52} = \frac{3.3714}{4.0285} = 0.8368$$

so that the normalized value of the alternative display is obtained, then find out the normalized value of another alternative.

c. Criteria for Accessibility (C_3):

$$r_{13} = \frac{4.0714}{4.0857} = 0.9965, r_{23} = \frac{4.0857}{4.0857} = 1, r_{33} = \frac{3.7142}{4.0857} = 0.9090,$$

$$r_{43} = \frac{3.7714}{4.0857} = 0.9263, r_{53} = \frac{3.3428}{4.0857} = 0.8181$$

so that the normalized value of the alternative accessibility is obtained, then find out the normalized value of another alternative.

d. Criteria for Topup Ease (C_4):

$$r_{14} = \frac{3.8714}{4.0571} = 0.9542, r_{24} = \frac{4.0571}{4.0571} = 1, r_{34} = \frac{3.7571}{4.0571} = 0.9260,$$

$$r_{44} = \frac{4}{4.0571} = 0.9859, r_{54} = \frac{3.3857}{4.0571} = 0.8345$$

so that the normalized value of the alternative Topup Ease is obtained, then find out the normalized value of another alternative.

e. Criteria for the Amount of Balance Limit (C_5):

$$r_{15} = \frac{3.8142}{3.8142} = 1, r_{25} = \frac{3.6714}{3.8142} = 0.9625, r_{35} = \frac{3.5285}{3.8142} = 0.9250,$$

$$r_{45} = \frac{3.5714}{3.8142} = 0.9363, r_{55} = \frac{3.4285}{3.8142} = 0.8988$$

so that the normalized value of the alternative amount of balance limit is obtained, then find out the normalized value of the other alternative.

f. Criteria for the Number of Payment Functions (C_6):

$$r_{16} = \frac{4.0571}{4.0857} = 0.9930, r_{26} = \frac{4.0857}{4.0857} = 1, r_{36} = \frac{3.6571}{4.0857} = 0.8950,$$

$$r_{46} = \frac{3.8857}{4.0857} = 0.9510, r_{56} = \frac{3.3285}{4.0857} = 0.8146$$

so that the normalized value of the alternative number of payment functions is obtained.

Then, the normalization results are made into the normalized matrix, while the normalized matrix R in this study is as follows:

$$R = \begin{pmatrix} 1 & 0.9645 & 0.9965 & 0.9542 & 1 & 0.9930 \\ 1 & 1 & 1 & 1 & 0.9625 & 1 \\ 0.9230 & 0.9219 & 0.9090 & 0.9260 & 0.9250 & 0.8950 \\ 0.9192 & 0.9255 & 0.9263 & 0.9859 & 0.9363 & 0.9510 \\ 0.8883 & 0.8368 & 0.8181 & 0.8345 & 0.8988 & 0.8146 \end{pmatrix}.$$

4.1.3 Ranking

The last step is to calculate the final preference value (V_i) obtained from the sum of the multiplication of the normalized matrix row elements (R) with the preference weight (W) while the weights used are as follows:

$$W = \{0.30; 0.1; 0.1; 0.25; 0.1; 0.15\}.$$

For the ranking process, use formula (2). Based on the results of the ranking above, it can be concluded that the results are ranked by the value of V, from the highest and smallest values, so that an alternative customer satisfaction survey for the e-wallets is obtained based on the highest value as shown in the following table:

No.	Alternative	The Final Result	Ranking
1	Shopeepay	0.9836	2
2	Dana	0.9962	1
3	Ovo	0.9183	4
4	Gopay	0.437	3
5	Sakuku	0.8527	5

Table 7: Ranking Results.

4.1.4 Description of research data analysis results

Among V_1, V_2, V_3, V_4, and V_5, the highest value is V_2 so that the alternative chosen and entitled to become an e-wallet with the highest customer satisfaction is $V_2 = 0.9962$. Funds with a resulted value of 0.9962 are based on calculations using the Simple Additive Weighting (SAW) method. It is concluded that Dana is the e-wallet with the highest customer satisfaction based on predetermined criteria. Then the most satisfied criterion or service is C_4 (Ease of Topup) with a higher average value compared to other criteria or services.

4.2 Technique of preference by similarity to ideal solution (TOPSIS) method

Processing the research data requires four stages, that is, determining the criteria to be used as a reference, determining the match rating, making a decision matrix, and ranking. In addition, there are also several steps for completion in accordance with the Topsis method procedure consisting of five steps given bellow.

1. Make the normalized decision matrix;

	Average Value					
	C_1	C_2	C_3	C_4	C_5	C_6
	4.0571	3.8142	3.8714	4.0714	3.8857	3.7142
	4.0857	3.6714	4.0571	4.0857	4.0285	3.7142
	3.6571	3.5285	3.7571	3.7142	3.7142	3.4285
	3.8857	3.5714	4	3.7714	3.7285	3.4142
	3.3285	3.4285	3.3857	3.3428	3.3714	3.3
Total	17.5771	18.7283	18.9855	19.0713	18.0140	19.0141
Average	3.5142	3.7456	3.7971	3.8142	3.6028	3.8028

Table 8: Ranking Results by Criteria or Services.

2. Make the weighted normalized decision matrix;
3. Determine the positive ideal solution matrix and the negative ideal solution matrix;
4. Determine the distance between the values of each alternative with the positive ideal solution matrix and the negative ideal solution matrix;
5. Determine the preference value for each alternative;

4.2.1 Determining match rating

In determining the match rating for the TOPSIS method, the same table is used as in finding out the match rating by the SAW method, that is, Table 6 which is obtained from Table 4 in Chapter 4.

4.2.2 Determining decision matrix

The next step is to form a decision matrix (x) made from the match rating table of each alternative on each criterion as follows:

$$X = \begin{pmatrix} 3.7142 & 3.8857 & 4.0714 & 3.8714 & 3.8142 & 4.0571 \\ 3.7142 & 4.0285 & 4.0857 & 4.0571 & 3.6714 & 4.0857 \\ 3.4285 & 3.7142 & 3.7142 & 3.7571 & 3.5285 & 3.6571 \\ 3.4142 & 3.7285 & 3.7714 & 4 & 3.5714 & 3.8857 \\ 3.3 & 3.3714 & 3.3428 & 3.3857 & 3.4285 & 3.3285 \end{pmatrix}.$$

Next, calculate the normalized value of each alternative:

$$|x_1| = \sqrt{(3.7142)^2 + (3.7142)^2 + (3.4285)^2 + (3.4142)^2 + (3.3)^2} = 7.8671,$$

$$r_{11} = 0.4721, r_{21} = 0.4721, r_{31} = 0.4358, r_{41} = 0.4340, r_{51} = 0.4195,$$

$$|x_2| = \sqrt{(3.8857)^2 + (4.0285)^2 + (3.7142)^2 + (3.7285)^2 + (3.3714)^2} = 8.3899,$$

$$r_{12} = 0.4631, r_{22} = 0.4802, r_{32} = 0.4427, r_{42} = 0.4444, r_{52} = 0.40818,$$

$$|x_3| = \sqrt{(4.0714)^2 + (4.0857)^2 + (3.7142)^2 + (3.7714)^2 + (3.3428)^2} = 8.5125,$$

$$r_{13} = 0.4783, r_{23} = 0.4800, r_{33} = 0.4363, r_{43} = 0.4430, r_{53} = 0.3927,$$

$$|x_4| = \sqrt{(3.8714)^2 + (4.0571)^2 + (3.7571)^2 + (4.000)^2 + (3.3857)^2} = 8.5456,$$

$$r_{14} = 0.4530, r_{24} = 0.4748, r_{34} = 0.4377, r_{44} = 0.4430, r_{54} = 0.4253,$$
$$|x_5| = \sqrt{(3.8142)^2 + (3.6714)^2 + (3.5285)^2 + (3.5714)^2 + (3.4285)^2} = 8.0615,$$
$$r_{15} = 0.4731, r_{25} = 0.4554, r_{35} = 0.4377, r_{45} = 0.4430, r_{55} = 0.4253,$$
$$|x_6| = \sqrt{(4.0571)^2 + (4.0857)^2 + (3.6571)^2 + (3.8857)^2 + (3.3285)^2} = 8.5267,$$
$$r_{16} = 0.4758, r_{26} = 0.4792, r_{36} = 0.4289, r_{46} = 0.4557, r_{56} = 0.3904.$$

Then the weighted normalized matrix or normalized matrix R is obtained, that is,

$$R = \begin{pmatrix} 0.4721 & 0.4631 & 0.4783 & 0.4530 & 0.4731 & 0.4758 \\ 0.4721 & 0.4802 & 0.4800 & 0.4748 & 0.4554 & 0.4792 \\ 0.4358 & 0.4427 & 0.4363 & 0.4397 & 0.4377 & 0.4289 \\ 0.4340 & 0.4444 & 0.4430 & 0.4681 & 0.4430 & 0.4557 \\ 0.4195 & 0.4018 & 0.3927 & 0.3962 & 0.4253 & 0.3904 \end{pmatrix},$$

$$W = \{0.30; 0.10; 0.10; 0.25; 0.10; 0.15\},$$
$$v_{11} = 0.1416, v_{21} = 0.1416, v_{31} = 0.1307, v_{41} = 0.1302, v_{51} = 0.1258,$$
$$v_{12} = 0.0463, v_{22} = 0.0480, v_{32} = 0.0443, v_{42} = 0.0444, v_{52} = 0.0402,$$
$$v_{13} = 0.0478, v_{23} = 0.0480, v_{33} = 0.0436, v_{43} = 0.0443, v_{53} = 0.0393,$$
$$v_{14} = 0.1133, v_{24} = 0.1187, v_{34} = 0.1099, v_{44} = 0.1170, v_{54} = 0.0990,$$
$$v_{15} = 0.0473, v_{25} = 0.0455, v_{35} = 0.0438, v_{45} = 0.0443, v_{55} = 0.0425,$$
$$v_{16} = 0.0714, v_{26} = 0.0719, v_{36} = 0.0643, v_{46} = 0.0684, v_{56} = 0.0586.$$

The matrix Y is

$$Y = \begin{pmatrix} 0.1416 & 0.0463 & 0.0478 & 0.1133 & 0.0473 & 0.0714 \\ 0.1416 & 0.0480 & 0.0480 & 0.1187 & 0.0455 & 0.0719 \\ 0.1307 & 0.0443 & 0.0436 & 0.1099 & 0.0438 & 0.0643 \\ 0.1302 & 0.0444 & 0.0443 & 0.1170 & 0.0443 & 0.0684 \\ 0.1258 & 0.0402 & 0.0393 & 0.0990 & 0.0425 & 0.0586 \end{pmatrix}.$$

The positive ideal solution (A^+) is calculated based on formula (5). So it is obtained as

$$A^+ = \{0.1416; 0.0480; 0.0480; 0.1187; 0.0473; 0.0719\}.$$

The negative ideal solution (A^-) is calculated based on formula (6). So it is obtained as

$$A^- = \{0, .258; 0.0402; 0.0393; 0.0990; 0.0425; 0.0586\}.$$

The distance between the weighted values of each alternative and the positive ideal solution can be found using formula (7). So it is obtained as

$$D^+ = \{0.0057; 0.0018; 0.0173; 0.0135; 0.0312\}.$$

The distance between the weighted values of each alternative and the negative ideal solution can be found using formula (8). So it is obtained as

$$D^- = \{0.0274; 0.0310; 0.0146; 0.0220; 0.0000\}.$$

4.2.3 Ranking

The last step is to calculate the final preference value (V_i) obtained from the previously calculated distance using formula (9).

So the closest ideal alternative solution is obtained as

$$V_1 = \frac{0.0274}{0.0274 + 0.0057} = 0,8272; V_2 = \frac{0.0310}{0.0310 + 0.0018} = 0.9459,$$

$$V_3 = \frac{0.0146}{0.0146 + 0.0173} = 0.4579; V_4 = \frac{0.0220}{0.0220 + 0.0425} = 0.6203,$$

$$V_5 = \frac{0.0000}{0.0000 + 0.0312} = 0.0000.$$

Based on the ranking of the V values of the highest through lowest values, it is obtained that

$$V_1 = 0.8272; V_2 = 0.9459; V_3 = 0.4579; V_4 = 0.6203; V_5 = 0.0000.$$

So, the best alternative in terms of having the highest value in e-wallet user satisfaction is $V_2 = Dana$, equal to 0.9459. So it can be concluded that DANA is the e-wallet with the highest customer satisfaction based on predetermined criteria.

5 Conclusion and Suggestions

5.1 Conclusion

Based on the results of the e-wallet user satisfaction survey research above, it was concluded that the first ranking of e-wallet user satisfaction surveys by the SAW and TOPSIS methods is DANA, the second is Shopeepay, the third is Gopay, the fourth is OVO, and the last is Sakuku.

5.2 Suggestions

Based on the research conducted, there were some problems encountered and it needs improving. In this case, the researchers make the following suggestions:

1. Many people do not use e-wallet, meaning not enough respondents, therefore, it is necessary that the Google form be distributed more widely to ensure having more respondents.
2. The number of the e-wallets used in the research is limited, then it is necessary that more e-wallets be added. In fact, many users use other e-wallets unlisted in this study.

References

[1] S. A. Al-Somali, R. Gholami and B. Clegg. Internet Banking Acceptance on the Context of Developing Countries: an Extension of the Technology Acceptance Model. *Operations and Information Management Group* Aston Business School, Birmingham B47ET, UK, 2008.

[2] F. A. Susanto, M. Y. Anshori, D. Rahmalia, K. Oktafianto, D. Adzkiya, P. Katias and T. Herlambang. Estimation of Closed Hotels and Restaurants in Jakarta as Impact of Corona Virus Disease (Covid-19) Spread Using Backpropagation Neural Network. *Nonlinear Dynamics and Systems Theory* **22** (4) (2022) 457–467.

[3] T. Herlambang, H. Nurhadi, A. Muhith, A. Suryowinoto and K. Oktafianto. Estimation of Forefinger Motion with Multi-DOF Using Advanced Kalman Filter. *Nonlinear Dynamics and Systems Theory* **23** (1) (2023) 24–33.

[4] T. Herlambang, F. A. Susanto, D. Adzkiya, A. Suryowinoto and K. Oktafianto. Design of Navigation and Guidance Control System of Mobile Robot with Position Estimation Using Ensemble Kalman Filter (EnKF) and Square Root Ensemble Kalman Filter (SR-EnKF). *Nonlinear Dynamics and Systems Theory* **22** (4) (2022) 390–399.

[5] M. Y. Anshori, I. H. Santoso, T. Herlambang, D. Rahmalia, K. Oktafianto and P. Katias. Forecasting of Occupied Rooms in the Hotel Using Linear Support Vector Machine. *Nonlinear Dynamics and Systems Theory* **23** (2) (2023) 129–140.

[6] A. Muhith, I. H. Susanto, D. Rahmalia, D. Adzkiya and T. Herlambang. The Analysis of Demand and Supply of Blood in Hospital in Surabaya City Using Panel Data Regression. *Nonlinear Dynamics and Systems Theory* **22** (5) (2022) 550–560.

[7] K. Oktafianto, A. Z. Arifin, E. F. Kurniawati, T. Tafrikan, T. Herlambang and F. Yudianto. Tsunami Wave Simulation in the Presense of a Barrier. *Nonlinear Dynamics and Systems Theory* **23** (1) (2023) 69–78.

[8] P. Eni and M. Tabrani. Analisis Survei Keputusan Pelanggan Terhadap E-Commerce Dengan Metode Simple Additive Weighting. *Jurnal Ilmiah Elektronika dan Komputer* **14** (2) (2021) 286–300.

[9] I. M. Al-Jabri and M. S. Sohail. Mobile Banking Adoption: Application Of Diffusion Of Innovation Theory. *Journal of Electronic Commerce Research* **13** (4) (2012) 379–391.

[10] P. G. W. Keen. *Electronic Commerce Relationships: Trust by Design*. Englewood Cliffs, NJ: Prentince-Hall, 1999.

[11] P. C. Fishburn. Additive Utilities with Incomplete Product Set: Application to Priorities and Assignments. *Research Analysis Corporation* **15** (3) (1967) 537–542.

[12] K. R. MacCrimmon. *Decision Making among Multiple Attribute Alternatives: A Survey and Consolidated Approach*. The Rand Corporation, California, 1968.

[13] C. L. Hwang, and K. Yoon. *Multiple Attribute Decision Making: Methods and Applications*. Springer-Verlag, New York, 1981.

[14] S. Kusumadewi, S. Hartati, et.al. *Fuzzy Multi-Atttribute Decision Making (FUZZY MADM)*. Graha Ilmu, Yogyakarta, 2006.

[15] C. H. Yeh. A Problem-based Selection of Multi-Attribute Decision Making Methods. *International Transactions in Operational Research* **9** (2) (2002) 169–181.

Nonlinear Dynamics and Systems Theory, **24** (1) (2024) 41–53

A New Feedback Control for Exponential and Strong Stability of Semi-Linear Systems with General Decay Estimates

M. Chqondi [1*], S. Chqondi [2], K. Tigma [3] and Y. Akdim [1]

[1] *Laboratory LAMA (Analyse Mathématique et Applications), Department of Mathematics and Informatics, Sidi Mohamed Ben Abdellah University, Faculty of Science, Dhar El Mahraz - FES, Morocco.*
[2] *Laboratory ISTM (Innovation in Sciences, Technologies and Modeling) Department of Physics, Faculty of Science, Chouaïb Doukkali University, El Jadida, Morocco.*
[3] *Higher Institute of Maritime Studies, Casablanca, Morocco.*

Received: August 25, 2023; Revised: January 16, 2024

Abstract: In this paper, to study the stabilization for the inhomogeneous nonlinear Schrödinger equation, we will explore the general form of semilinear control systems in Hilbert state space and apply the obtained results to the particular case of the nonlinear Schrödinger equation. We propose a new output feedback control approach that achieves strong and exponential stabilization if certain approximate observability assumptions are met. We demonstrate the existence and uniqueness of solutions and provide an estimate of convergence speed in the case of strong stabilization.

Keywords: *control systems; stabilization of systems by feedback; semilinear systems; exponential stability.*

Mathematics Subject Classification (2010): 93D15, 93C10, 93D20, 34H15.

* Corresponding author: mailto:chminfo@gmail.com

1 Introduction

The inhomogeneous nonlinear Schrödinger equation is a natural occurrence in nonlinear optics when it comes to the propagation of laser beams. A preliminary laser beam can be sent to create a channel with reduced electron density to achieve stable high-power propagation in plasma. This ultimately reduces the non-linearity within the channel. Gill [1] and Tripathi and Liu [2] provide examples of this approach. In this scenario, the propagation of the beam can be explained by the equation

$$I\partial_t u + \Delta u + K(x)|u|^\alpha u = 0,$$

which represents the inhomogeneous non-linear Schrödinger equation and is a typical example of a semi-linear control system in a Hilbert space $\mathcal{H}$ given by the following evolution equation:

$$\begin{cases} y'(t) = Ay(t) + u(t)Ny(t), \\ y(0) = y_0 \in \mathcal{H}, \end{cases} \tag{1}$$

where A is an unbounded operator with domain $\mathcal{D}(A) \subset \mathcal{H}$ and generates a strongly continuous semigroup of contraction $(S(t))_{t\geq 0}$ on an infinite-dimensional real Hilbert space $\mathcal{H}$ (state space) whose norm and scalar product are denoted, respectively, by $\|.\|$ and $\langle .,. \rangle$, N is a nonlinear operator from $\mathcal{H}$ into $\mathcal{H}$, which is locally Lipschitz and sequentially continuous operator such that $N(0) = 0$, the control function $u(.)$ denotes the scalar control.

When trying to stabilize a control system, one of the main approaches is to look for a feedback control that can guarantee that the system is well-posed and that the solution converges to zero over time. This feedback control is usually represented by $u(y(t))$ and must be carefully chosen to achieve the desired stabilization. By formally computing the time rate of change of the energy $\frac{d}{dt}\|y(t)\|^2$ and using the fact that the semigroup is of contraction so that $\langle Ay, y\rangle \leq 0$ for all $y \in D(A)$, we get

$$\frac{d}{dt}\|y(t)\|^2 \leq 2u(t) < y(t); Ny(t) >; \forall t \in [0, T].$$

To make the energy nonincreasing, we consider the family of controls:

$$\text{for } r \geq 0, \quad u_r\left(y(t)\right) = -\frac{\langle y(t), Ny(t)\rangle \mid \langle y(t), Ny(t)\rangle \mid^r}{\|y(t)\|^r}, \quad \forall t \in [0, T]. \tag{2}$$

By using this control, we can guarantee the dissipation of energy while adhering to the following inequality:

$$\frac{d}{dt}\|y(t)\|^2 \leq -2\frac{|\langle y(t), Ny(t)\rangle|^{r+2}}{\|y(t)\|^r}; \forall t \in [0, T]. \tag{3}$$

In our control family, there is a particular case when $r = 0$, and it is called the quadratic feedback control $u_0(y(t)) = -\langle y(t), By(t)\rangle$. Various works have extensively studied this control to achieve weak or strong stabilizability. In Ball and Slemrod (see [3] and [4], p. 175), it has been shown that if $N = B$ is a compact linear operator and $S(t)$ is a semigroup of contractions such that

$$\langle BS(t)y, S(t)y\rangle = 0 \forall t \geq 0 \Longrightarrow y = 0, \tag{4}$$

then the feedback $u_0(y(t))$ weakly stabilizes the system (1).
In Ouzahra (see [5], p. 511 and [6], p. 814), it has been established that if (4) is replaced by the following:

$$\int_0^T |\langle BS(t)y, S(t)y\rangle| dt \geq \delta \|y\|^2 \forall y \in H$$

(for some $T, \delta > 0$), then the control $u_0(y(t))$ strongly stabilizes the system (1). More precisely, the state satisfies the estimate

$$\|z(t)\|^2 = O\left(\frac{1}{t}\right), \text{ as } t \longrightarrow +\infty.$$

In Berrahmoune (see [7]), a strong stabilization result has been obtained using the control $u_0(t)$, and the following estimate $\|y(t)\| = O\left(\frac{1}{\sqrt{t}}\right)$ has been obtained.

In this paper, we study the strong and exponential stabilizability of the system (1) using the control (2) for all $r \geq 0$. By implementing control (2), we can enhance the estimate provided by $u_0(y(t))$ in [3], [4], [5], [6] and [7]. This document is structured in the following manner. Section 2 demonstrates the existence and uniqueness of the solution in the semilinear case using control (2) for all $t \in [-2; +\infty[$. In Section 3, we explore strong stabilization and decay estimates, while Section 4 focuses on the exponential stabilization problem using the selected control $u_r(y(t))$ for all $t \in [-2; +\infty[$. In the last section, we give examples governed by the nonlinear Schroedinger and heat equations to illustrate our findings.

2 Well-Possedness

With the control (2), system (1) becomes

$$\begin{cases} y'(t) = Ay(t) + F_r(t, y(t)), \\ y(0) = y_0, \end{cases} \tag{5}$$

where

$$F_r(t, y(t)) = -\frac{\langle y(t), Ny(t)\rangle |\langle y(t), Ny(t)\rangle|^r}{\|y(t)\|^r} Ny(t) \text{ if } y \neq 0.$$

In this section, we will discuss the existence and uniqueness of the solution of the system (5).

Firstly, we need to demonstrate that the system's state is decreasing. To do so, integrate the inequality (3) over the interval [s, t], it follows that

$$\|y(t)\|^2 - \|y(s)\|^2 \leq -2 \int_s^t \frac{|\langle y(t), Ny(t)\rangle|^{r+2}}{\|y(t)\|^r}, \quad \forall t \geq s \geq 0,$$

therefore $\|y(t)\| \leq \|y_0\|, \forall t \geq 0$.

Theorem 2.1 *Let A generate a semigroup of contractions $S(t)$, let N be a locally Lipschitz and sequentially continuous operator, then for all $r \in [-2, +\infty[$ and $y_0 \in \mathcal{H}$, the system (5) possesses a unique global mild solution $y(t)$ defined on the infinite interval $[0, +\infty[$, which is given by the following variation of constants formula:*

$$y(t) = S(t)y_0 - \int_0^t F_r(s, y(s)) S(t-s) Ny(s) ds.$$

Proof. We will consider the system (5) and demonstrate that the map $F_r : y \mapsto F_r(t, y(t))$ is locally Lipschitz from $\mathcal{H}$ to $\mathcal{H}$. Let $x \in \mathcal{H}$ and let $R > 0$, $L_N > 0$ such that for all $z, y \in \mathcal{H}$ such that $\|x-y\| \leq R$ and $\|x-z\| \leq R$, we have $\|Nz-Ny\| \leq L_N\|z-y\|$. From the development below, it will be clear that we can suppose that $x = 0$ and $0 < \|y\| \leq \|z\|$.

Let us consider two functions: $f_1(y) = \frac{|\langle y, Ny\rangle|^r}{\|y\|^r}$ and $f_2(y) = \langle y, Ny\rangle Ny$. We can then conclude that

$$\begin{aligned}\|F_r(t,y) - F_r(t,z)\| &= \|f_1(y)f_2(y) - f_1(z)f_2(z)\| \\ &\leq L_N^r\|y\|^r\|f_2(y) - f_2(z)\| + L_N^2\|z\|^3\|f_1(y) - f_1(z)\|.\end{aligned}$$

It is easy to increase the value of $L_N^r\|y\|^r\|f_2(y) - f_2(z)\|$, in fact,

$$\begin{aligned}\|f_2(y) - f_2(z)\| &= \|\langle y, Ny\rangle Ny - \langle z, Nz\rangle Nz\| \\ &\leq (L_N\|y\| + 2L_N\|z\|)\, L_N\|y\|\|y - z\| \\ &\leq 3L_N^2\|y\|^2\|y - z\|.\end{aligned}$$

Therefore

$$L_N^r\|y\|^r\|f_2(y) - f_2(z)\| \leq 3L_N^{r+2}\|y\|^{r+2}\|y - z\|. \tag{6}$$

There are two cases to increase the value of $\|f_1(y) - f_1(z)\|$. This can be achieved by utilizing the real function $t \mapsto t^r$, which satisfies the following conditions.

If $r \geqslant 1$, then $|\|z\|^r - \|y\|^r| \leq r\|z\|^{r-1}|\|z\| - \|y\||$.
If $r < 1$, then $|\|z\|^r - \|y\|^r| \leq |\, r \,|\, \|y\|^{r-1}|\|z\| - \|y\||$.

Case 1 : if $r \geqslant 1$. In this case, we have

$$\|f_1(y) - f_1(z)\| \leq r\left|\frac{|\langle z, Nz\rangle|}{\|z\|}\right|^{r-1}\left|\frac{|\langle y, Ny\rangle|}{\|y\|} - \frac{|\langle z, Nz\rangle|}{\|z\|}\right|$$

and since

$$\begin{aligned}\left|\frac{\langle y, Ny\rangle}{\|y(t)\|} - \frac{\langle z, Nz\rangle}{\|z(t)\|}\right| &= \left|\frac{\|z(t)\|\langle y, Ny\rangle - \|y(t)\|\langle z, Nz\rangle}{\|y(t)\|\|z(t)\|}\right| \\ &\leq \frac{\|y\|(L_N\|y\|)\,|\,\|z\| - \|y\|\,| + \|y(t)\|(L_N\|z\| + L_N\|y\|)\,\|z - y\|}{\|y(t)\|\|z(t)\|} \\ &\leq \frac{L_N\|y\|^2|\,\|z\| - \|y\|\,| + 2L_N\|y(t)\|^2\|z - y\|}{\|y(t)\|\|z(t)\|} \\ &\leq \frac{3L_N\|y\|}{\|z\|}\|z - y\|,\end{aligned}$$

we find

$$\begin{aligned}\|f_1(y) - f_1(z)\| &\leq r\left|\frac{|\langle z, Nz\rangle|}{\|z\|}\right|^{r-1}\frac{3L_N\|y\|}{\|z\|}\|z - y\| \\ &\leq r(L_N\|z\|)^{r-1}\frac{3L_N\|y\|}{\|z\|}\|z - y\| \\ &\leq \frac{3rL_N^r\|y\|^r}{\|z\|}\|z - y\|.\end{aligned}$$

Therefore

$$L_N^2\|z\|^3\|f_1(y)-f_1(z)\|\leq 3rL_N^{2+r}\|y\|^{r+2}\|z-y\|. \tag{7}$$

Based on the inequalities (6) and (7) presented above, we can conclude that

$$\|F_r(t,y)-F_r(t,z)\| \leq 3L_N^{r+2}\,(1+r)\,\|y_0\|^{r+2}\|y-z\|.$$

Case 2 : If $-2\leqslant r\leqslant 1$.

We have $\|f_1(y)-f_1(z)\| \leq \dfrac{3\mid r\mid L_N^r\|y\|^r}{\|z\|}\|z-y\|$, therefore

$$L_N^2\|z\|^3\|f_1(y)-f_1(z)\|\leq 3\mid r\mid L_N^{r+2}\|y\|^{r+2}\|z-y\|. \tag{8}$$

By utilizing the inequalities (6) and (8), we can come to the conclusion that

$$\|F_r(t,y)-F_r(t,z)\|\leq 3L_N^{r+2}(1+\mid r\mid)\|y_0\|^{r+2}\|y-z\|.$$

We have proven that for all $r\geqslant -2$, $F_r(t;y(t))$ satisfies a local Lipschitz condition in y, uniformly in t on bounded intervals. It follows (see [8], p.185) that the system (5) possesses a unique mild solution $y(t)$ defined on a maximal interval $[0,t_{\max}[$, which is given by the following variation of constants formula:

$$y(t)=S(t)y_0-\int_0^t F_r(s,y(s))S(t-s)Ny(s)ds.$$

To show that $t_{\max}=+\infty$, it is sufficient to prove that for each $T>0$, the mild solution $y(t)$ is bounded by a constant independent of T. To do this, we discuss two cases:

- For $y_0\in\mathcal{D}(A)$, the solution $y(t)$ is differentiable (see [8], p.189), and since $S(t)$ is a semigroup of contractions (so that A is dissipative), we can write

  $$\frac{d}{dt}\|y(t)\|^2\leq -2\frac{|\langle y(t),Ny(t)\rangle|^{r+2}}{\|y(t)\|^r};\forall t\in[0,T].$$

  Integrate this last inequality over the interval [s, t], it follows that

  $$\|y(t)\|^2-\|y(s)\|^2\leq -2\int_s^t\frac{|\langle y(t),Ny(t)\rangle|^{r+2}}{\|y(t)\|^r},\forall t\geq s\geq 0.$$

  Therefore,

  $$\|y(t)\|\leq\|y_0\|\,,\forall t\geq 0.$$

- If $y_0\notin D(A)$, we can find a sequence $(y_0^n)_n$ of elements in $D(A)$ converging to y_0 in $\mathcal{H}$ since $\overline{D(A)}=\mathcal{H}$. For all $t\in[0,T]$ and all integer n, we know from the first case that $\|y^n(t)\|\leq\|y_0^n\|$. We conclude that $\|y(t)\|\leq\|y_0\|\,,\quad\forall t\in[0,t_{\max}[$, hence $t_{\max}=+\infty$.

3 Strong Stabilization and Decay Estimate

Proposition 3.1 *Let A generate a semigroup of contractions $S(t)$ and N be locally Lipschitz. Then, for all $r\geqslant 0$, the state of the system (4) satisfies the decay estimate as $t\to+\infty$,*

$$\int_0^T|\langle NS(s)y(t),S(s)y(t)\rangle|\mathrm{d}s=O\left(\|y(\tau)\|^{\frac{r}{r+2}}\left(\int_0^T\frac{|\langle y(s+\tau),Ny(s+\tau)+c\rangle|^{r+2}}{\|y(s+\tau)\|^r}\,\mathrm{d}s\right)^{\frac{1}{r+2}}\right). \tag{9}$$

Proof. Using Proposition 3.1, we deduce that the system (9) admits a unique global mild solution given by the following formula of variation of constants:

$$y(t) = S(t)y_0 - \int_0^t \frac{\langle y(t), Ny(t)\rangle \mid \langle y(t), Ny(t)\rangle \mid^r}{\|y(s)\|^r} S(t-s)Ny(s)\mathrm{d}s,$$

and due to the fact that $S(t)$ is a semigroup of contractions, for all $t \in [0,T]$,

$$\begin{aligned}\|y(t) - S(t)y_0\| &\leqslant \int_0^T \frac{|\langle y(s), Ny(s)\rangle|^{r+1}}{\|y(s)\|^r}(\|Ny(s))\|\mathrm{d}s \\ &\leqslant L_N \int_0^T \frac{|\langle y(s), Ny(s)\rangle|^{r+1}}{\|y(s)\|^r}\|y(s)\|\ \mathrm{d}s.\end{aligned}$$

We can apply the Hölder inequality

$$p = \frac{r+2}{r+1} \quad , q = r+2 \quad \left(\frac{1}{p} + \frac{1}{q} = 1\right), \quad r \in]-1+\infty[$$

$$\begin{aligned}\|y(t) - S(t)y_0\| &\leqslant L_N T^{\frac{1}{r+2}} \left(\int_0^T \left(\frac{|\langle y(s), Ny(s)\rangle|^{r+1}}{\|y(s)\|^r}\|y(s)\|\right)^{\frac{r+2}{r+1}} \mathrm{d}s\right)^{\frac{r+1}{r+2}} \\ &\leqslant L_N T^{\frac{1}{r+2}} \left(\int_0^T \frac{|\langle y(s), Ny(s)\rangle|^{r+2}}{\|y(s)\|^r}\|y(s)\|^{\frac{2}{r+1}}\mathrm{d}s\right)^{\frac{r+1}{r+2}}.\end{aligned}$$

Since $r \geqslant 0$, we have $\frac{2}{r+1} > 0$ and the fact that $\|y(t)\| \leq \|y_0\|$. We get $\|y(t)\|^{\frac{2}{r+1}} \leq \|y_0\|^{\frac{2}{r+1}}$. So

$$\|y(t) - S(t)y_0\| \leqslant L_N T^{\frac{1}{r+2}} \|y_0\|^{\frac{2}{r+2}} \left(\int_0^T \frac{|\langle y(s), Ny(s)+\rangle|^{r+2}}{\|y(s)\|^r}\mathrm{d}s\right)^{\frac{r+1}{r+2}}. \tag{9}$$

From the relation

$$\langle NS(t)y_0, S(t)y_0\rangle = \langle NS(t)y_0, S(t)y_0 - y(t)\rangle + \langle NS(t)y_0 - Ny(t), y(t)\rangle + \langle Ny(t), y(t)\rangle,$$

when using $\|y(t)\| \leq \|y(0)\|, \forall t \in [0, t_{\max}[$, the fact that $S(t)$ is a semigroup of contraction, N is locally Lipschitz, and Schwartz's inequality, it comes

$$|\langle NS(s)y_0, S(s)y_0\rangle| \leq 2L_N \|y_0\| \|y(t)) - S(t)y_0\| + \mid \langle Ny(s), y(s)\rangle \mid. \tag{10}$$

Using (9), we have

$$|\langle NS(s)y_0, S(s)y_0\rangle| \leq 2L_N^2 T^{\frac{1}{r+2}} \|y_0\|^{\frac{r+4}{r+2}} \left(\int_0^T \frac{|\langle y(s), Ny(s)\rangle|^{r+2}}{\|y(s)\|^r}\mathrm{d}s\right)^{\frac{r+1}{r+2}} + \mid \langle Ny(s), y(s)\rangle \mid. \tag{11}$$

Replacing y_0 by $y(\tau)$ in (11), we get

$$\begin{aligned}&|\langle NS(s+\tau)y(\tau), S(s+\tau)y(\tau)\rangle| \\ &\leq 2L_N^2 T^{\frac{1}{r+2}} \|y(\tau)\|^{\frac{r+4}{r+2}} \left(\int_0^T \frac{|\langle y(s+\tau), Ny(s+\tau) + c\rangle|^{r+2}}{\|y(s+\tau)\|^r}\mathrm{d}s\right)^{\frac{r+1}{r+2}} \\ &+ |\langle Ny(s+\tau), y(s+\tau)\rangle|.\end{aligned}$$

Integrate the last inequality over the interval $[0, T]$

$$\begin{aligned}&\int_0^T |\langle NS(s+\tau)y(\tau), S(s+\tau)y(\tau)\rangle| \ \mathrm{d}s \\ &\leq \int_0^T \langle Ny(s+\tau), y(s+\tau)\rangle \\ &\mathrm{d}s + 2L_N^2 T^{\frac{1}{r+2}+1}\|y(\tau)\|^{\frac{r+4}{r+2}} \left(\int_0^T \frac{|\langle y(s+\tau), Ny(s+\tau)\rangle|^{r+2}}{\|y(s+\tau)\|^r}\mathrm{d}s\right)^{\frac{r+1}{r+2}}.\end{aligned} \tag{12}$$

Due to the fact that $\|y(s+\tau)\| \leq \|y(\tau)\| \, \forall t \geq 0$, and Hölder's inequality

$$\int_0^T \langle Ny(s+\tau), y(s+\tau)\rangle \ \mathrm{d}s \leq T^{\frac{r+1}{r+2}}\|y(\tau)\|^{\frac{r}{r+2}} \left(\int_0^T \frac{\langle Ny(s+\tau), y(s+\tau)\rangle^{r+2}}{\|y(s+\tau)\|^r} \ \mathrm{d}s\right)^{\frac{1}{r+2}},$$

(12) becomes

$$\begin{aligned}&\int_0^T |\langle NS(s+\tau)y(\tau), S(s+\tau)y(\tau)\rangle| \ \mathrm{d}s \\ &\leq 2L_N^2 T^{\frac{1}{r+2}+1}\|y(\tau)\|^{\frac{r+4}{r+2}} \left(\int_0^T \frac{|\langle y(s+\tau), Ny(s+\tau)\rangle|^{r+2}}{\|y(s+\tau)\|^r}\mathrm{d}s\right)^{\frac{r+1}{r+2}} \\ &\quad + T^{\frac{r+1}{r+2}}\|y(\tau)\|^{\frac{r}{r+2}} \left(\int_0^T \frac{\langle Ny(s+\tau), y(s+\tau)\rangle^{r+2}}{\|y(s+\tau)\|^r} \ \mathrm{d}s\right)^{\frac{1}{r+2}}.\end{aligned} \tag{13}$$

We have

$$\left(\int_0^T \frac{|\langle y(s+\tau), Ny(s+\tau)\rangle|^{r+2}}{\|y(s+\tau)\|^r} \ \mathrm{d}s\right)^{\frac{r+1}{r+2}} = \left(\int_0^T \frac{|\langle y(s+\tau), Ny(s+\tau)\rangle|^{r+2}}{\|y(s+\tau)\|^r} \ \mathrm{d}s\right)^{\frac{1}{r+2}+\frac{r}{r+2}}.$$

And by Schwartz's inequality, it comes

$$\begin{aligned}&\int_0^T \frac{|\langle y(s+\tau), Ny(s+\tau)\rangle|^{r+2}}{\|y(s+\tau)\|^r} \ \mathrm{d}s \leq TL_N^{r+2}\|y(\tau)\|^{r+4} \\ &\left(\int_0^T \frac{|\langle y(s+\tau), Ny(s+\tau)\rangle|^{r+2}}{\|y(s+\tau)\|^r} \ \mathrm{d}s\right)^{\frac{r+1}{r+2}} \\ &\qquad \leq T^{\frac{r}{r+2}} L_N^{\frac{r}{r+2}} |y(\tau)\|^{\frac{r^2+4r}{r+2}} \left(\int_0^T \frac{|\langle y(s+\tau), Ny(s+\tau)\rangle|^{r+2}}{\|y(s+\tau)\|^r} \ \mathrm{d}s\right)^{\frac{1}{r+2}}.\end{aligned}$$

Finally, using (13), we have

$$\begin{aligned}&\int_0^T |\langle NS(s+\tau)y(\tau), S(s+\tau)y(\tau)\rangle| \mathrm{d}s \\ &\qquad \leq \mathcal{M}_{\|y_0\|}\|y(\tau)\|^{\frac{r}{r+2}} \left(\int_0^T \frac{|\langle y(s+\tau), Ny(s+\tau)\rangle|^{r+2}}{\|y(s+\tau)\|^r} \ \mathrm{d}s\right)^{\frac{1}{r+2}},\end{aligned} \tag{14}$$

where $\mathcal{M}_{\|y_0\|} = T^{\frac{r+1}{r+2}} \left(2L_N^2 T L_N^{\frac{r}{r+2}} \|y(\tau)\|^{r+2}+1\right)$.

Theorem 3.1 *Let A generate a C_0-semigroup $S_u(t)$, and suppose that the following conditions hold:*
1. $S_u(t)$ is a contraction semigroup;
2. there exist $\delta, T > 0$ such that

$$\int_0^T |\langle NSs)y(t), S(s)y(t)\rangle| \, ds \geq \delta \|y(t)\|^2, \quad \forall y \in H. \tag{15}$$

Then the feedback (2) for all $r \geqslant 0$, strongly stabilizes the system (1) with the following decay estimate:

$$\|y(t)\| = O\left(t^{-\frac{r+2}{4}}\right) \text{ as } t \to +\infty.$$

Proof. Let us consider the sequence $s_k = \|y(kT)\|^2$, $k \in IN$.
Integrating the inequality (3) over the interval $[kT, (k+1)T]$, we get

$$\int_{KT}^{(k+1)T} \frac{d}{dt}\|y(t)\|^2 dt \leq -2 \int_{KT}^{(k+1)T)} \frac{(\langle Ny(t), y(t)\rangle)^{r+2}}{\|y(t)\|^r} dt$$

$$\|y((K+1)T)\|^2 - \|y(KT)\|^2 \leq -2 \int_{KT}^{(k+1)T)} \frac{(\langle Ny(t), y(t)\rangle)^{2+r}}{\|y(t)\|^r} dt.$$

Using now the estimate (14), we deduce that

$$\int_0^T |\langle NS(s+\tau)y(\tau) + c, S(s+\tau)y(\tau)\rangle| \, \mathrm{d}s$$

$$\leq \left(\mathcal{M}_{\|y_0\|} \|y(\tau)\|^{\frac{r}{2+r}}\right) \left(\int_\tau^{T+\tau} \frac{|\langle Ny(s) + c, y(s)\rangle|^{2+r}}{\|y(s)\|^r} \, \mathrm{d}s\right)^{\frac{1}{2+r}}$$

$$\|y((K+1)T)\|^2 - \|y(KT)\|^2 \leq \frac{-2}{\mathcal{M}_{\|y_0\|} \|y(\tau)\|^{\frac{r}{2+r}}} \int_0^T |\langle NS(s+\tau)y(\tau), S(s+\tau)y(\tau)\rangle| \, \mathrm{d}s$$

and according to the inequality (15), we have

$$\|y((K+1)T)\|^2 - \|y(KT)\|^2 \leq \frac{-2\rho}{\mathcal{M}_{\|y_0\|}} \|y(KT)\|^{\frac{-r}{2+r}} \|y(KT)\|^2$$

$$\|y((K+1)T)\|^2 - \|y(KT)\|^2 \leq \frac{-2\rho}{\mathcal{M}_{\|y_0\|}} \|y(KT)\|^{1+\frac{2}{2+r}}.$$

Letting $s_k = \|y(kT)\|^2, k \in \mathbb{N}$, the last inequality can be written as

$$s_{k+1} \leq s_k - \frac{2\rho}{\mathcal{M}_{\|y_0\|}} s_k^{1+\frac{2}{2+r}}, \quad \forall k \geq 0.$$

Using the fact that $t \mapsto \|y(t)\|$ is a decreasing function on $[0, +\infty[$, we get

$$s_{k+1} \leq s_k - \frac{2\rho}{\mathcal{M}_{\|y_0\|}} s_{k+1}^{1+\frac{2}{2+r}}, \quad \forall k \geq 0.$$

$$s_{k+1} + \frac{2\rho}{\mathcal{M}_{\|y_0\|}} s_{k+1}^{1+\frac{2}{2+r}} \leq s_k, \quad \forall k \geq 0.$$

The last inequality can be written as follows: $s_{k+1} + C s_{k+1}^{2+\alpha} \leq s_k, \quad \forall k \geq 0,$
where $C = \frac{2\rho}{\mathcal{M}_{\|y_0\|}} > 0$ and $\alpha = \frac{-r}{r+2} > -1 \quad \forall r \in \mathbb{R}/(-1,-2)$.
Now, to obtain the decay rate for the solutions of (1), we recall the following lemma, see [9].

Lemma 3.1 *(Lasiecka and Tataru, 1993) Let $(s_k)_{k\geq 0}$ be a sequence of positive real numbers satisfying the relation $s_{k+1} + C s_{k+1}^{2+\alpha} \leq s_k, \quad \forall k \geq 0$, where $C > 0$ and $\alpha > -1$ are constants. Then there exists a positive constant M_2 (depending on α and C) such that $s_k \leq \frac{M_2}{(k+1)^{\frac{1}{\alpha+1}}}, \quad k \geq 0$.*

So, from the lemma (Lasiecka & Tataru, 1993), we have $s_k \leq \frac{M_2}{(k+1)^{\frac{r+2}{2}}}, \quad k \geq 0.$
For $k = E\left(\frac{t}{T}\right), \left(E\left(\frac{t}{T}\right)\right.$ designed the integer part of $\left.\frac{t}{T}\right)$, we obtain $s_k \leq \frac{M_3}{t}$, $(M_3 > 0)$, which gives $\|y(t)\|^2 \leq \frac{M_3}{t^{\frac{r+2}{2}}}$.
Hence, $\|y(t)\| = \mathbf{O}\left(t^{-\frac{r+2}{4}}\right)$ as $t \to +\infty$.

Remark 3.1 *For $r = 0$, we find the estimate guaranteed by $u_0(t)$ in [5] and [6].*

4 Exponential Stabilization

Theorem 4.1 *Let A generate a C_0-semigroup $S(t)$, and suppose that the following conditions hold:*
1. $S(t)$ is a contraction semigroup;
2. there exist $\delta, T > 0$ such that

$$\int_0^T |\langle NS(s)y(t), S(s)y(t)\rangle| \, ds \geq \delta \|y(t)\|^{2+\frac{r}{r+2}}, \quad \forall y \in \mathcal{H}. \tag{16}$$

Then the feedback (2) for all $r \geqslant 0$, exponentially stabilizes the system (5).
More precisely, there exists $\beta > 0$ such that $\|y(t)\| \leq e^{-\beta} \|y_0\| e^{-\frac{\beta}{T}(t)}, \quad \forall t > 0.$

Proof. From

$$\|y((K+1)T)\|^2 - \|y(KT)\|^2 \leq \frac{-2}{\mathcal{M}_{\|y_0\|} \|y(\tau)\|^{\frac{r}{2+r}}} \int_0^T |\langle NS(s+\tau)y(\tau), S(s+\tau)y(\tau)\rangle| \mathrm{d}s$$

and according to the inequality (16), we have

$$\|y((K+1)T)\|^2 - \|y(KT)\|^2 \leq \frac{-2\rho}{\mathcal{M}_{\|y_0\|}} \|y(KT)\|^{\frac{-r}{2+r}} \|y(KT)\|^{2+\frac{r}{2+r}}$$

$$\|y((K+1)T)\|^2 - \|y(KT)\|^2 \leq \frac{-2\delta}{\mathcal{M}_{\|y_0\|}} \|y(KT)\|^2. \tag{17}$$

Letting $s_k = \|y(kT)\|^2, k \in \mathbb{N}$, the inequality (17) can be written as

$$s_{k+1} - s_k \leq \frac{-2\delta}{\mathcal{M}_{\|y_0\|}} s_k, \quad \forall k \geq 0,$$
$$s_{k+1} \leq C s_k, \quad \forall k \geq 0,$$

where $C = \left(1 - \frac{2\delta}{\mathcal{M}_{\|y_0\|}}\right) < 1$, which gives $s_k \leq e^{-k \ln \frac{1}{C}} s_0$, i.e, $\|y(kT)\|^2 e^{-k \ln \frac{1}{C}} \|y_0\|$.
For $k = E\left(\frac{t}{T}\right), \left(E\left(\frac{t}{T}\right)\right.$ designed the integer part of $\frac{t}{T}$), and using the fact that $E\left(\frac{t}{T}\right) T \leq t$ and $t \mapsto \|y(t)\|$ is a decreasing function on $[0, +\infty[$,
we get $\|y(t)\| \leq e^{-\frac{\ln\left(\frac{1}{C}\right)}{2}} \|y_0\| e^{-\frac{\ln\left(\frac{1}{C}\right)}{2T} t}$ for all $t \geq 0$,
$\|y(t)\| \leq e^{-\beta} \|y_0\| e^{-\frac{\beta}{T} t}$ for all $t \geq 0$, where $\beta = \frac{\ln\left(\frac{1}{C}\right)}{2} > 0$.

5 Applications

Example 5.1 Let $\Omega \subset \mathbb{R}^N, H = L^2(\Omega)$. This example will study the nonlinear Schrödinger equation in $\Omega \subset \mathbb{R}^N$. Let us consider the system defined on an open and bounded domain Ω with $\mathcal{C}^\infty$ boundary $\partial\Omega$ by the equation

$$\begin{cases} i\partial_t \psi = \Delta\psi + K(x)|\psi|^\alpha \psi, & \text{in } \Omega\times]0,\infty[, \quad \alpha > 0, \\ \psi(\cdot,t) = 0, & \text{on } \partial\Omega\times]0,\infty[, \\ \psi(\cdot,0) = \varphi. \end{cases} \tag{18}$$

For $\alpha = 2$, it is the Gross-Pitaevskii equation describing the evolution of a Bose-Einstein condensate.

The equation (18) has garnered much interest recently. Bergé conducted a formal study on the stability condition of soliton solutions in [10]. Towers-Malomed, in [11], discovered that a specific type of time-dependent nonlinear medium generates fully stable beams through variational approximation and direct simulations. Merle in [12] and Raphaël-Szeftel in [13] studied (18) for $k_1 < K(x) < k_2$ with $k_1, k_2 > 0$. Fibich-Wang in [14] investigated (18) with $K(x) := K(\epsilon|x|)$, where $\epsilon > 0$ is small and $K \in C^4\left(\mathbb{R}^d\right) \cap L^\infty\left(\mathbb{R}^d\right)$.

In this example, we will study the stability of (18) by considering $K(x) = u_r(\psi(x,t))$, where

$$u_r(\psi(x,t)) = -\frac{\langle\psi(x,t), N\psi(x,t)\rangle|\langle\psi(x,t), N\psi(x,t)\rangle|^r}{\|\psi(x,t)\|^r}; \quad r \geqslant 0.$$

We are considering the control operator $N\psi(x,t) = |\psi(x,t)|^\alpha \psi(x,t)$ in order to express the system (18) in the following form:

$$\begin{cases} i\frac{\partial\psi(x,t)}{\partial t} = A\psi(x,t) + u_r(\psi(x,t))N\psi(x,t), & \text{in } \Omega\times]0,\infty[, \\ \psi(x,t) = 0, & \text{on } \partial\Omega\times]0,\infty[, \\ \psi(x,0) = \varphi. \end{cases} \tag{19}$$

Here, the state space $H = L^2(\Omega)$ is endowed with its natural complex inner product.

- The operator A is defined by $A\psi(x,t) = -i\Delta\psi(x,t), \forall\psi(x,t) \in \mathcal{D}(A)$, where $\mathcal{D}(A) = H^2(\Omega) \cap H_0^1(\Omega)$.
  It is well known that the operator $A = -i\Delta$ with domain $\mathcal{D}(A)$ generates a semi-group of isometries $\{\mathcal{T}(t)\}_{t\in\mathbb{R}} \in \mathcal{L}\left((D(A))^*\right)$.

- The operator of control is given by $N\psi = |\psi|^\alpha\psi$.
  We pose $N\left(\psi(x,t)\right) = f(t,\psi(x,t)) = \frac{\psi(x,t)}{|\psi(x,t)|} f(t,|\psi(x,t)|) \quad \forall\psi \in \mathcal{D}(A), \psi \neq 0$.
  We deduce that
  $$|\psi_1||\psi_2|(f(t,\psi_1) - f(t,\psi_2)|$$

$$= |\psi_1|\psi_2|[f(t,|\psi_1|) - f(t,|\psi_2|)] + [\psi_1(|\psi_2| - |\psi_1| + |\psi_1|(\psi_1 - \psi_2))]\, f(t,|\psi_2|)|.$$

We have $f(t,|\psi_1|) = |\psi_1|^{\alpha+1}$, so for every $K > 0$ and $0 < \psi_1, \psi 2 \leqslant K$, there exists $L_K < \infty$ such that

$$|f(t,|\psi_1|) - f(t,|\psi_2|)| \leq L_K|\psi_1 - \psi_2|.$$

So

$$\begin{aligned} |\psi_1\|\psi_2\|f(t,\psi_1) - f(t,\psi_2)| &\leq |\psi_1\|\psi_2\|f(t,|\psi_1|) - f(t,|\psi_2|)| + 2|\psi_1||\psi_1 - \psi_2\|f(t,|\psi_2|)| \\ &\leq 3|\psi_1\|\psi_2|L_K|\psi_1 - \psi_2|, \end{aligned}$$

$$\begin{aligned} |f(t,\psi_1) - f(t,\psi_2)| &\leq 3L_K|\psi_1 - \psi_2|, \\ ||\psi_1|^{\alpha}\,\psi_1 - |\psi_2|^{\alpha}\psi_2| &\leq L_K|\psi_1 - \psi_2\,|\,. \end{aligned}$$

Therefore N is a nonlinear and locally Lipschitz operator such that $N(0) = 0$, applying Theorem 2.1, we deduce that the system (18) possesses a unique global mild solution $\psi(x,t))$ defined on the infinite interval $[0, +\infty[$, which is given by the following variation of constants formula:

$$\psi(x,t) = \mathcal{T}(t)\varphi + i\int_0^t \mathcal{T}(t-s)u_r(\psi(x,s))N\psi(x,s)ds, \quad \forall t \geq 0.$$

Let us show that the condition of Theorem 3.1 is verified,

$$\begin{aligned} \langle N\mathcal{T}(t)\psi(x,t), \mathcal{T}(t)\psi(x,t)\rangle_H &= \langle |\mathcal{T}(t)\psi(x,t)|^{\alpha}\mathcal{T}(t)\psi(x,t), \mathcal{T}(t)\psi(x,t)\rangle_H \\ &= |\mathcal{T}(t)\psi(x,t)|^{\alpha}\langle \mathcal{T}(t)\psi(x,t), \mathcal{T}(t)\psi(x,t)\rangle_H \\ &= |\mathcal{T}(t)\psi(x,t)|^{\alpha}|\mathcal{T}(t)\psi(x,t)|^2 \\ &= |\mathcal{T}(t)\psi(x,t)|^{\alpha+2}. \end{aligned}$$

We know that $|\mathcal{T}(t)\psi(x,t)| = |\psi(x,t)|$, therefore,

$$\int_0^T \langle N\mathcal{T}(t)\psi(x,t), \mathcal{T}(t)\psi(x,t)\rangle_H dt = \int_0^T |\psi(x,t)|^{\alpha+2}dt.$$

Applying the Holder inequality, we obtain

$$\begin{aligned} \int_0^T |\psi(x,t)|^2\ \mathrm{d}t &\leq T^{\frac{\alpha}{\alpha+2}}\left(\int_0^T |\psi(x,t)|^{\alpha+2}\ \mathrm{d}t\right)^{\frac{2}{\alpha+2}} \\ &\leq T^{\frac{\alpha}{\alpha+2}}\left(\int_0^T |\psi(x,t)|^{\alpha+2}\ \mathrm{d}t\right)^{\frac{2}{\alpha+2}} \\ \sqrt{\int_0^T |\psi(x,t)|_H^2\ \mathrm{d}t} &\leq T^{\frac{\alpha}{2\alpha+4}}\left(\int_0^T |\psi(x,t)|^{\alpha+2}\ \mathrm{d}t\right)^{\frac{1}{\alpha+2}} \\ T^{\frac{-\alpha}{2}}\|\psi(x,t)\|^{\alpha+2}_{L^2(]0,T[;H)} &\leq \int_0^T |\psi(x,t)|^{\alpha+2}\ \mathrm{d}t \\ \int_0^T \langle N\mathcal{T}(t)\psi(x,t), \mathcal{T}(t)\psi(x,t)\rangle_H\ \mathrm{d}t &\geqslant T^{\frac{-\alpha}{2}}\|\psi(x,t)\|^{\alpha+2}_{L^2(]0,T[;H)}. \end{aligned} \tag{20}$$

- For $\alpha = 0$, the system (18) becomes

$$\begin{cases} i\partial_t \psi = \Delta\psi + K(x)\psi, & \text{in } \Omega\times]0,\infty[, \\ \psi(\cdot,t) = 0, & \text{on } \partial\Omega\times]0,\infty[, \\ \psi(\cdot,0) = \varphi. \end{cases} \tag{21}$$

Using (20), we can deduce that for $\delta = 1$ and $T > 0$, we have the inequality

$$\int_0^T \langle N\mathcal{T}(t)\psi(x,t), \mathcal{T}(t)\psi(x,t)\rangle_H \, \mathrm{d}t \geqslant \delta \|\psi(x,t)\|^2_{L^2(]0,T[;H)}.$$

Based on the verification of condition (15), we can apply Theorem 3.1 to confirm that the feedback $u_r(\psi(x,t))$ stabilizes system (21) for all $r \geqslant 0$ with the following decay estimate. Moreover, we can estimate solution decay using the following formula:

$$\|\psi(x,t)\| = O\left(t^{-\frac{r+2}{4}}\right) \text{ as } t \to +\infty.$$

- For $0 < \alpha < 1$, when we set $r = \frac{2\alpha}{1-\alpha}$, we ensure that $r > 0$. Solving for α using the equation $\alpha = \frac{r}{r+2}$ and for $\delta = \frac{1}{\sqrt{T^\alpha}}$, we can then substitute this value into equation (20) to obtain the modified expression

$$\int_0^T \langle N\mathcal{T}(t)\psi(x,t), \mathcal{T}(t)\psi(x,t)\rangle_H \, \mathrm{d}t \geqslant \delta \|\psi(x,t)\|^{2+\frac{r}{r+2}}.$$

Based on the verification of condition (16), we can apply Theorem 4.1 to confirm that the feedback $u_r(\psi(x,t))$ exponentially stabilizes the system (20) for $0 < \alpha < 1$ and $r = \frac{2\alpha}{1-\alpha}$.

More precisely, there exists $\beta > 0$ such that $\|\psi(x,t)\| \leq e^{-\beta} \|\varphi\| e^{-\frac{\beta}{T}(t)}, \quad \forall t > 0,$

where $\beta = \frac{\ln\left(\frac{1}{C}\right)}{2} > 0$, $C = \left(1 - \frac{2\delta}{M_{|\varphi|}}\right) < 1$,

$\mathcal{M}_{\|\varphi\|} = T^{\frac{\alpha+1}{2}+1}\left(2T(\alpha+1)^{\frac{3+5\alpha}{2}+} \mid \varphi \mid^{\frac{\alpha(3+5\alpha)}{2}+\frac{2}{1-\alpha}} +1\right).$

6 Conclusion

This paper introduces a new type of control to enhance the stability of a semilinear system. The suggested control results in strong and exponential stability of the closed-loop system, particularly the inhomogeneous nonlinear Schrödinger equation. Moreover, an estimate of the decay can be achieved through approximate observation assumptions depending on r. Therefore, implementing the new control results in a significantly faster response time than quadratic control. This research raises questions about applying the same family of controls to stabilize inhomogeneous semi-linear systems in physics, including the non-homogeneous case considered in [15].

References

[1] Tarsem Singh Gill. Optical guiding of the laser beam in nonuniform plasma. *Pramana* **55** (2000) 835–842.

[2] V. K. Tripathi and Liu, C. S. Laser guiding in an axially nonuniform plasma channel. *Physics of plasmas* **1** (9) (1994) 3100–3103.

[3] J. M. Ball and M. Slemrod. Feedback stabilization of distributed semilinear control systems. *Applied Mathematics and Optimization* **5** (1) (1979) 169–179.

[4] J. M. Ball. Strongly continuous semigroups, weak solutions, and the variation of constants formula. *Proceedings of the American Mathematical Society* **63** (2) (1977) 370–373.

[5] Mohamed Ouzahra. Stabilization with decay estimate for a class of distributed bilinear systems. *European journal of control* **5** (13) (2007) 509–515.

[6] M. Ouzahra, Strong stabilization with decay estimate of semilinear systems. *Systems and control letters* **57** (10) (2008) 813–815.

[7] Larbi Berrahmoune. Stabilization and decay estimate for distributed bilinear systems. *Systems and control letters* **36** (3) (1999) 167–171.

[8] A. Pazy. Semigroups of linear operators and applications to partial differential equations. *Springer Science and Business Media*, **44** (2012).

[9] D. Tataru and I. Lasiecka. Uniform boundary stabilization of semilinear wave equations with nonlinear boundary damping. *Differential and integral Equations* **6** (3) (1993) 507–533.

[10] Luc Bergé. Soliton stability versus collapse. *Physical Review* **E 62** (3) (2000) R3071.

[11] Isaac Towers and Boris A. Malomed. Stable (2+1)-dimensional solitons in a layered medium with sign-alternating Kerr nonlinearity. *Journal of the Optical Society of America* **B 19** (3) (2002) 537–543.

[12] Franck Merle. Nonexistence of minimal blow-up solutions of equations $iu_t = -\Delta uk(x)|u|^{4/N}u$ in $\mathbb{R}^N$. *Annales de l'IHP Physique théorique* **64** (1) (1996).

[13] Pierre Raphaël and Jeremie Szeftel. Existence and uniqueness of minimal blow-up solutions to an inhomogeneous mass critical NLS. *Journal of the American Mathematical Society*, **24** (2) (2011) 471–546.

[14] Gadi Fibich and Xiao-Ping Wang. Stability of solitary waves for nonlinear Schrödinger equations with inhomogeneous nonlinearities. *Physica D: Nonlinear Phenomena* **175** (2) (2003) 96–108.

[15] M. Baddi, M. Chqondi and Y. Akdim. Exponential and Strong Stabilization for Inhomogeneous Semilinear Control Systems by Decomposition Method. *Nonlinear Dynamics and Systems Theory* **23** (1) (2023) 1–13.

Nonlinear Dynamics and Systems Theory, **24** (1) (2024) 54–64

Spectral Analysis and Invariant Measure in Studying the Dynamics of a Metabolic Process in the Glycolysis-Gluconeogenesis System

V. I. Grytsay [1*] and I. V. Musatenko [2]

[1] *Bogolyubov Institute for Theoretical Physics, 14b, Metrolohichna Str., Kyiv 03143, Ukraine*

Received: May 13, 2023; Revised: January 16, 2024

Abstract: The paper presents an original general mathematical model of the glycolysis-gluconeogenesis metabolic processes chain. The scenario of the appearance of auto-periodic and chaotic modes for the system is studied with the help of the Fourier series of one of the system variables. The invariant measure of the strange attractor is calculated. The histograms of the invariant measure projections of the system onto the phase space plane are constructed. Conclusions are made about the self-organization and adaptation of the system to changes in the cell and the environment.

Keywords: *self-organization; strange attractor; glycolysis; gluconeogenesis; Fourier series; invariant measure; bifurcation, protobions.*

Mathematics Subject Classification (2010): 92C05, 35B32, 42A16, 37L40.

1 Introduction

An essential task of natural sciences is a search for the general physical laws of self-organization in Nature. The gradual development of nonlinear thermodynamics led to the emergence of a new scientific direction - synergetics. The mechanism of structure formation in open nonlinear systems became clear thanks to synergetics [1]. The science of self-organization and evolution of living organisms suggests an answer about the flow of physical and chemical processes in a cell [2].

One of the general chains of metabolic reactions running in each cell is glycolysis and its inverse process, gluconeogenesis. Cells receive energy from glucose in the form of ATP

* Corresponding author: mailto:vigrytsay@gmail.com

by way of glycolysis. Cells further synthesize glucose from nonhydrocarbon substrates using gluconeogenesis.

Glycolysis and gluconeogenesis are two opposite metabolic processes in a cell, where 7 of 10 metabolic reactions are reversible. Three reactions are irreversible and are performed in gluconeogenesis via detouring thermodynamically favorable reactions.

A number of scientists have studied this chain of metabolic reactions. As a result of experimental studies of glycolysis, the auto oscillations were discovered in [3]. In order to explain the origin of auto oscillations, several mathematical models were developed. These models clarified that the oscillations in glycolysis occur as a result of the activation of phosphofructokinase by its products or due to the allosterism of this enzyme [4, 5].

The study in the present work is based on the mathematical model of glycolysis and gluconeogenesis developed in [6]. The peculiarity of this model is that for the first time, it analized the influence of the adenine nucleotide cycle and gluconeogenesis on the phosphofructokinase complex of this allosteric enzyme. It has been claimed that their effects cause fluctuations in glycolysis.

In works [7, 8], this model was improved. The system of equations of the model was refined by applying the conservation law to the intermediate reactions products. It also accounted for the description of the complete closed chain of metabolic processes of glycolysis-gluconeogenesis encircled by a positive feedback loop. The metabolic processes of glycolysis-gluconeogenesis with a positive feedback loop are the electron transfer chain $NAD \cdot H \Longleftrightarrow NAD^{+}$.

The results obtained in papers [7,8] allowed the authors to construct a general mathematical model of the chain of metabolic glycolysis-gluconeogenesis reactions as a single dissipative system of a cell.

Since gluconeogenesis uses mainly the same reversible reactions as glycolysis, the biochemical evolution of the former occurred together with glycolysis. The symbiosis of the given biochemical processes can be considered as a primary open nonlinear biochemical system in a state far from the equilibrium. As a result of self-organization of this biochemical system, a stable dissipative system emerged. It was independent of the other biochemical processes of the primary broth.

The direction of the running reactions in such a system was determined by the energy-beneficial balance. The organic molecule ATP was formed as a result of glycolysis. It became a main carrier of the energy consumed in all the other biochemical processes. But if some biochemical processes needed glucose, then the direction of biochemical reactions in the given system reversed. This chain of metabolic reactions forced all other metabolic processes in a cell to self-organize. During the subsequent biochemical evolution, the given dissipative system was preserved in all types of cells, which indicates their common prehistory. The analysis of the metabolic process allows us to state that this dissipative system probably arose in protobionts in the primary broth in the oxygen-free atmosphere of the Earth 3.5 billion years ago. This primary cell, in which life originated, was named the LUCA (the last universal common ancestor) [9, 10].

2 Mathematical Model and Method of Investigation

A mathematical model of the metabolic process of glycolysis-gluconeogenesis is constructed according to the general schemes of the metabolic reactions presented in Figure 1 and the general schemes of two active and two inactive forms of the allosteric enzyme phosphofructokinase (Figure 2) [7,8]. The model describes the flow of the metabolic pro-

cess in straightforward direction, that corresponds to glycolysis, and in opposite direction during gluconeogenesis.

The mathematical model is a system of 16 nonlinear differential equations. The equations correspond to the basic sections of the metabolic process. They determine a sequence of the reactions, and they influence the stability of the process of glycolysis-gluconeogenesis. Some sections of the metabolic network that are insignificant for the self-organization are described by the equations in the extended meaning. In Figure 1, we show the sections of the metabolic network from the 1-st to 16-th. Each of them corresponds to the number of the differential equation:

$$\frac{dG}{dt} = \frac{G_0}{S}\frac{m_1}{m_1+F} - l_8V(G)V(T), \tag{1}$$

$$\frac{dF_1}{dt} = l_8V(G)V(T) - l_1V(R_1)V(F_1)V(T) + l_5\frac{1}{1+\gamma A}V(F_2) - m_3\frac{F_1}{S}, \tag{2}$$

$$\frac{dF_2}{dt} = l_1V(R_1)V(F_1)V(T) - l_5\frac{1}{1+\gamma A}V(F_2) - m_5\frac{F_2}{S}, \tag{3}$$

$$\frac{d\psi_1}{dt} = \frac{m_5(F_2/S)}{S_1+m_5(F_2/S)} - l_6V(\psi_1)V(D) + m_7V(M-N)V(P), \tag{4}$$

$$\frac{d\psi_2}{dt} = l_6V(\psi_1)V(D) - m_8\frac{\psi_2}{S}, \tag{5}$$

$$\frac{d\psi_3}{dt} = \frac{\psi_2}{S}\frac{m_2}{m_2+\psi_3} - l_2V(\psi_3)V(D) - m_4\frac{\psi_3}{S}, \tag{6}$$

$$\frac{dP}{dt} = l_2V(\psi_3)V(D) - m_6\frac{P}{S} - l_7V(N)V(P), \tag{7}$$

$$\frac{dL}{dt} = l_7V(N)V(P) - m_9\frac{L}{S}, \tag{8}$$

$$\frac{dT}{dt} = l_2V(\psi_3)V(D) - l_1V(R_1)V(F_1)V(T) + l_3\frac{A}{\delta+A}V(T) - l_4\frac{T^4}{\beta+T^4} + \\ + l_6V(\psi_1)V(D) - l_9V(G)V(T), \tag{9}$$

$$\frac{dD}{dt} = l_1V(R_1)V(F_1)V(T) - l_2V(\psi_3)V(D) + 2l_3\frac{A}{\delta+A}V(T) - l_6V(\psi_1)V(D) + \\ + l_9V(G)V(T), \tag{10}$$

$$\frac{dA}{dt} = l_4\frac{T^4}{\beta+T^4} - l_3\frac{A}{\delta+A}V(T), \tag{11}$$

$$\frac{dR_1}{dt} = k_1T_1V(F_1^2) + k_3R_2V(D^2) - k5R_1\frac{T}{1+T+\alpha A} - k_7R_1V(T^2), \tag{12}$$

$$\frac{dR_2}{dt} = k_5R_1\frac{T}{1+T+\alpha A} - k_3R_2V(D^2) + k_2T_2V(F_1^2) - k_8R_2V(T^2), \tag{13}$$

$$\frac{dT_1}{dt} = k_7 R_1 V(T^2) - k_6 T_1 \frac{T}{1+T+\alpha A} + k_4 T_2 V(D^2) - k_1 T_1 V(F_1^2), \tag{14}$$

$$\frac{dT_2}{dt} = k_6 T_1 \frac{T}{1+T+\alpha A} - k_4 T_2 V(D^2) - k_2 T_2 V(F_1^2) + k_8 R_2 V(T^2), \tag{15}$$

$$\frac{dN}{dt} = -l_7 V(N) V(P) + l_7 V(M-N) V(\psi_1), \tag{16}$$

where $V(X) = X/(1+X)$ is the function that describes the adsorption of an enzyme in the locally connected region. The variables of the system are made unitless.

The parameters of the system are: $l_1 = 0.0535$, $l_2 = 0.046$, $l_3 = 0.0017$, $l_4 = 0.01334$, $l_5 = 0.3$, $l_6 = 0.001$, $l_7 = 0.01$, $l_8 = 0.0535$, $l_9 = 0.001$, $k_1 = 0.07$, $k_2 = 0.01$, $k_3 = 0.0015$, $k_4 = 0.0005$, $k_5 = 0.05$, $k_6 = 0.005$, $k_7 = 0.03$, $k_8 = 0.005$, $m_1 = 0.3$, $m_2 = 0.15$, $m_3 = 1.6$, $m_4 = 0.0005$, $m_5 = 0.007$, $m_6 = 10$, $m_7 = 0.0001$, $m_8 = 0.0000171$, $m_9 = 0.5$, $G_0 = 18.4$, $L = 0.005$, $S = 1000$, $A = 0.6779$, $M = 0.005$, $S_1 = 150$, $\alpha = 184.5$, $\beta = 250$, $\delta = 0.3$, $\gamma = 79.7$.

At the first stage (1), glucose G_0 entering a cell is phosphorylized with the help of the enzyme hexokinase to glucose-6-phosphate. The donor of a phosphoryl group is a molecule $ATP(T)$ (1), (9). This reaction is irreversible. The molecules of glucose-6-phosphate are the allosteric inhibitor of the reaction and cannot leave the cell. If the concentration of glucose-6-phosphate in a cell increases above the normal level, then hexokinase is inhibited by glucose-6-phosphate (1). The speed of glucose-6-phosphate formation corresponds to the speed of its consumption in the subsequent reactions. Further, an inverse isomerization of glucose-6-phosphate to fructose-6-phosphate occurs. However, it does not affect the irreversibility of the process.

Equations (2) and (3) describe the processes of fructose-6-phosphate creation (F_1) and its transformation into fructose-1,6-diphosphate (F_2). The last reaction occurs under the catalytic action of the enzyme phosphofructokinase. This enzyme catalyzes the irreversible transfer of a phosphoryl group from ATP (2), (9) onto fructose-6-phosphate with its transformation into fructose-1,6-diphosphate. The substrate fructose-6-phosphate is an activator, and ATP is an inhibitor of the given process. In addition to such regulation, the enzyme is also regulated by the adenine-nucleotide cycle $ATP - ADP - AMP$ (see below). The latter helps to support the optimum stable stationary state.

The equations (2) and (3) also describe the process of gluconeogenesis. The enzyme fructose-1,6-biphosphatase catalyzes the irreversible reaction $F_2 \longrightarrow F_1$ (parameter l_5) by creating the positive feedback loop. It affects the stability of the process.

The subsequent splitting of fructose-1,6-biphosphate into glyceraldehyde-3-phosphate and dioxyacetone-phosphate occurs in a reversible way.

Equation (4) describes the formation of 1,3-diphosphoglycerate (ψ_1). The enzyme glyceraldehyde-3-phosphate is oxidized and joins phosphoric acid using glyceraldehyde-3-phosphate-dehydrigenase. In this case, the coenzyme NAD^+ is an acceptor of hydrogen. The following enzymatic restoration occurs: $NAD^+ \to NAD \cdot H$ (4), (16).

With the help of equation (5), we described a transfer process of a high-energy phosphoryl group from the carboxyl group of 1,3-diphosphoglycerate by the enzyme phosphoglycerate kinase onto ADP. As a result, ATP (9) and 3-phosphoglycerate ψ_2 (5) are formed.

Equation (6) deals with the formation of 2-phosphoglycerate with the help of the phosphoglycerate mutase enzyme. Then a molecule of water is eliminated with the creation of phosphoenolpyruvate ψ_3 (6).

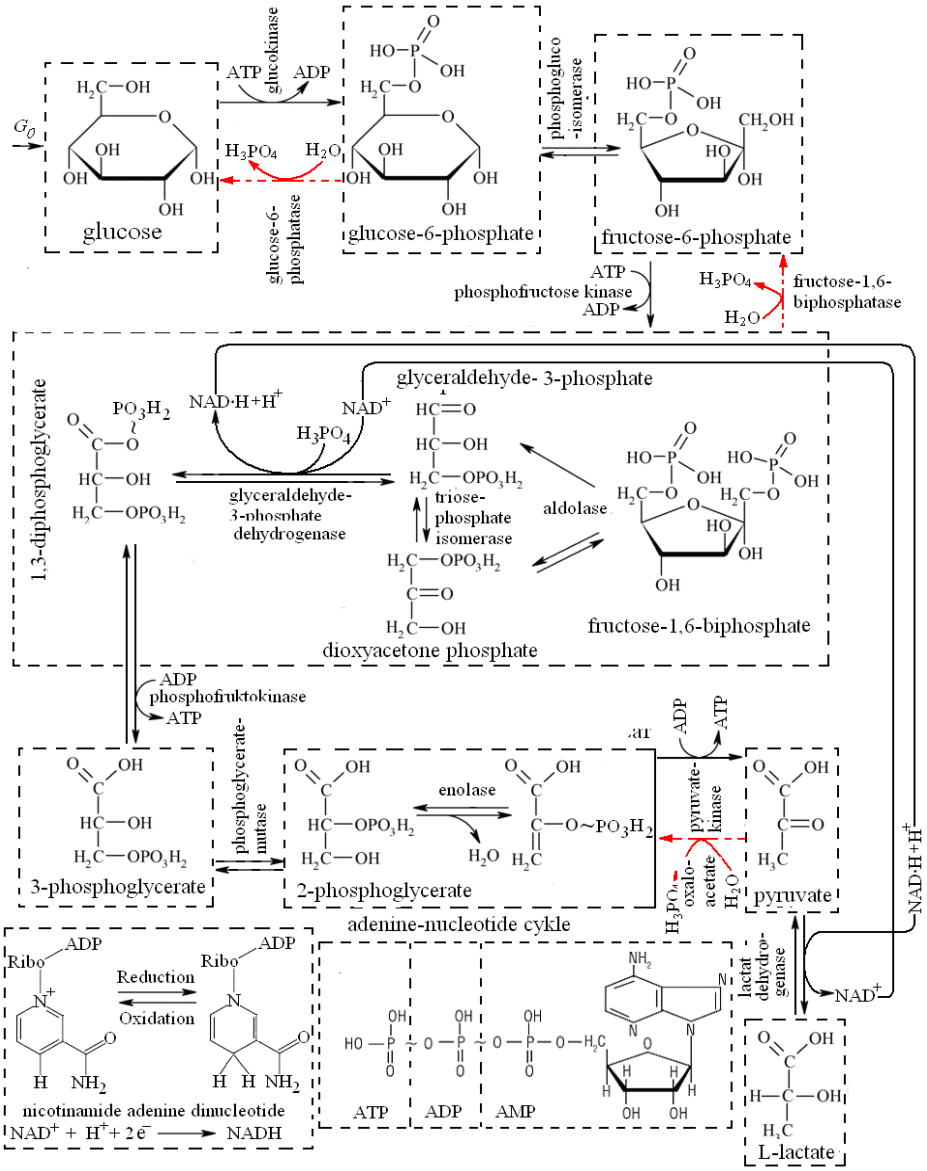

Figure 1: The general scheme of the metabolic process of glycolysis-gluconeogenesis.

The formation of the pyruvate P was considered in (7) under the action of the pyruvate kinase enzyme. So, the phosphorylation of the substrate occurs.

Equation (8) describes the formation of lactate L, which is the second product. With

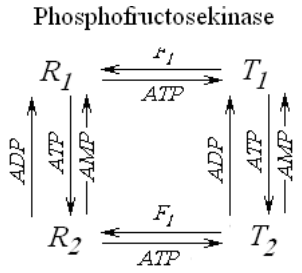

Figure 2: The general scheme of mutual transformations of two active and two nonactive forms of the allosteric enzyme phosphofructokinase.

the help of the lactate dehydrogenase enzyme, the enzymatic oxidation happens: $NAD \cdot H \to NAD^+$. The balance between NAD^+ and $NAD^+ \cdot H$ is preserved, see equation (16).

Equations (9)-(11) are related to the kinetics of the changes in the levels of ATP (9), ADP (10), and AMP (11) according to the metabolic scheme of glycolysis-gluconeogenesis (see above). In general, the adenine-nucleotide cycle arises between given reagents with mutual transitions: $ATP - ADP - AMP$. The adenine-nucleotide cycle helps to conserve the optimum stationary state of the metabolic process.

Equations (12)-(15) demonstrate the kinetics of levels of the allosteric phosphofructokinase enzyme (Figure 2).

We assume that the enzyme has two active forms: R_1 (12) and R_2 (13), and two nonactive: T_1 (14) and T_2 (15). In this case, we can observe the mutual transformation of the forms T_1 and R_1, as well as T_2 and R_2. The equations show the general scheme of regulatory connections. The form R_1 (12) was created from the form T_1 as a result of the saturation of the two allosteric centers by molecules F_1 and the form R_2 with the participation of two molecules D. Inactivation of the form R_1 takes place at the expense of T and with the formation of R_2 (13) and two molecules T (12) with the formation of the form T_1 (14). The invertible inactivation is inhibited by an increase of A according to a high level of T (parameter α) (12). Equations (13)-(15) were constructed in a similar way.

Equation (16) represents the kinetics of changes in the nicotinamide adenine dinucleotide recovered form $NAD \cdot H$ according to its consumption and recovery of the oxidized form NAD^+ (4). The balance between the recovered and oxidized forms is preserved in the glycolytic cycle in invariable form. In this case, the integral of motion is $NAD \cdot H(t) + NAD^+(t) = M$.

The stability dynamics is investigated using the second Liapunov method [12]. The chaotic dynamics of mathematical models can be studied using harmonic analysis [13].

In this paper, we used the Fourier series and invariant measure [14] for system investigation. Let us write down the system (1)-(16) in generalized form

$$\dot{x} = F(x), x \in R^n, \tag{17}$$

where $F(x) = (f_1(x), f_2(x), ..., f_n(x))^T$, the continuous dynamical system $\varphi^t(x)$ is defined by the system of differential equations. Such dynamical system for each τ generates a cascade of

$$x_{k+1} = f(x_k) \equiv \varphi^\tau(x_k). \tag{18}$$

Definition 2.1 The measure μ is an invariant measure of dynamical system (18) if for any measurable set A, the following relation fulfills:

$$\mu(A) = \mu(f^{-1}(A)).$$

Theorem 2.1 *(the Krylov–Bogolyubov theorem on the existence of invariant measures) If a compact set $A \subset P$ is invariant for the dynamic system $\varphi^t(x)$, then there exists at least one probability measure μ (where $\mu(P) = 1$) which is invariant for φ [14].*

Let us divide some phase space region into small enough subsets A_i. The result of solution for the system of differential equations (17) will be trajectories x_k, where $k = \overline{1, N}$, N is a big enough number of points. The measure of each set is estimated as

$$\mu(A_i) = N_i/N, \tag{19}$$

where N_i is the number of points in the subset A_i.

Theorem 2.2 *(The Fourier coefficients) The Fourier series representation of $f(x)$ defined on $[0, 2\pi]$, when it exists, is given by*

$$f(x) = \frac{a_0}{2} + \sum_{n=1}^{\infty} \left(a_n cosnx + b_n sinnx\right), \tag{20}$$

with the Fourier coefficients

$$a_n = \frac{1}{\pi}\int_0^{2\pi} f(x)cosnxdx, \quad b_n = \frac{1}{\pi}\int_0^{2\pi} f(x)sinnxdx, \quad n = 0, 1, 2...$$

3 Result of Studies

The mathematical model is the system of nonlinear differential equations (1)-(16). It describes the open nonlinear biochemical system of glycolysis-gluconeogenesis. Input and output flows for the model are glucose and lactate, respectively. The concentrations of these substances determine the straightforward or inverse directions of the metabolic process dynamics. Both processes are irreversible and are running in the open nonlinear system, far from the equilibrium point. The presence of glycolysis and gluconeogenesis in the system is a cause for autocatalysis in the system. Besides, the whole metabolic process of glycolysis contains the feedback formed by $NAD{\cdot}H$ and the adenine-nucleotide cycle. These factors influence the appearance of instability in the given metabolic system.

Let us investigate the dependence of the dynamics of the metabolic glycolysis-glucogenesis process on the activity of gluconeogenesis, which is regulated by a small parameter l_5. The authors want to show that the fluctuations of fructose-6-phosphate [1,2] can be explained by gluconeogenesis, which occurs under the action of enzyme fructose-1,6-bisphosphatase in the area: fructose-1,6-bisphosphate - fructose-6-phosphate. This is different from the commonly used explanation by phosphofructokinase enzyme allosteric-ity.

In [9], the phasoparametric diagrams of the process dynamics dependence on the parameter l_5 were constructed. Bifurcation points for doubling of the period and the transition to chaos according to Feigenbaum's scenario were found. When the parameter l_5 decreases, the following stable modes are formed:

$$2 \times 2^1(l_5 = 0.268), 2 \times 2^2(l_5 = 0.264), 2 \times 2^4(l_5 = 0.262), 2^x(l_5 = 0.25).$$

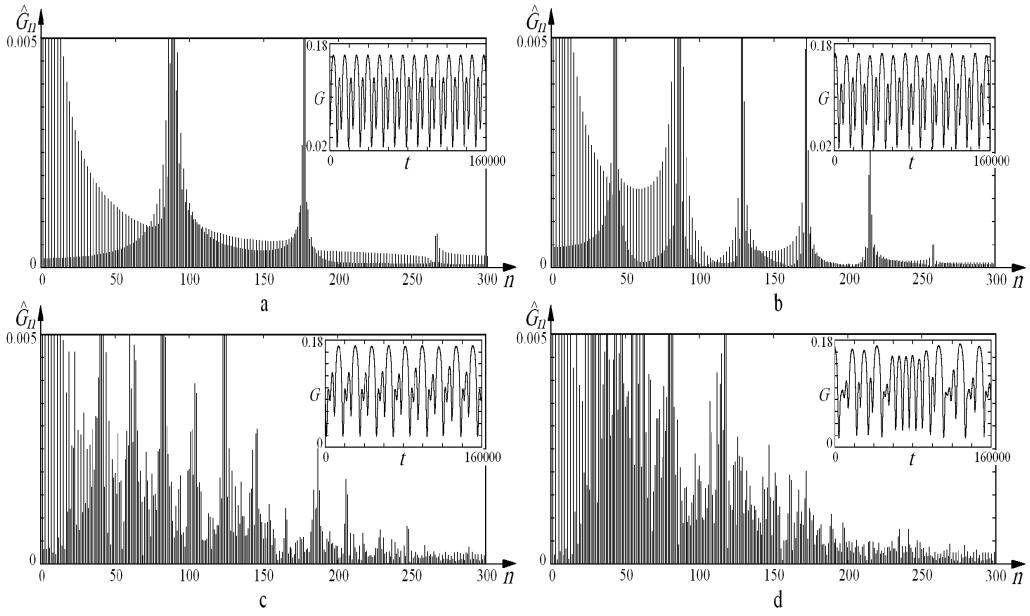

Figure 3: The distribution of the harmonics of the Fourier spectrum for a metabolic process in the system of glycolysis-gluconeogenesis in the modes: a - the autoperiodic process $2 \times 2^1(l_5 = 0.268)$; b – the autoperiodic process $2 \times 2^2(l_5 = 0.264)$; c – the autoperiodic process $2 \times 2^4(l_5 = 0.262)$; d - the chaos mode $2^x(l_5 = 0.25)$.

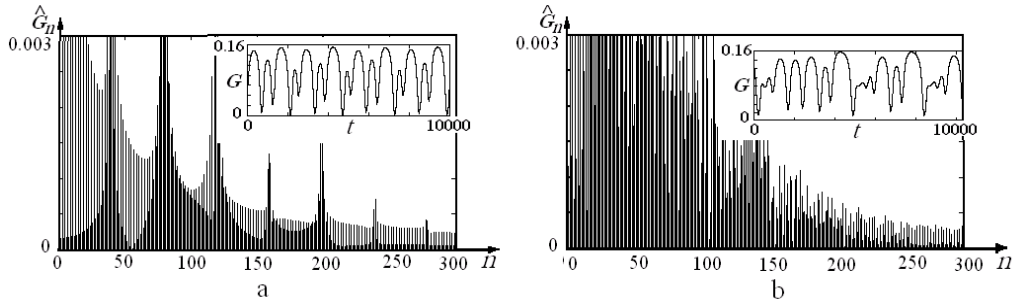

Figure 4: The distribution of the harmonics of the Fourier spectrum for the metabolic process in the system of glycolysis-gluconeogenesis for the parameter $l_5 = 0.3$ in the following modes: a – the quasistable autoperiodic process $2 \times 2^2(G_0 = 17.25)$; b – the chaos mode $2^x(G_0 = 16.8)$.

The spectral plots of the decomposition into a trigonometric Fourier series (20) of the kinetic curve $G(t)$ from equation (1) were constructed for the found self-oscillating modes. $\widehat{G_i}$, $i = \overline{1,n}$, are the harmonics of the Fourier series and they were obtained using equation (20). The kinetic curves for each spectrum are presented in the upper right corner of the corresponding figure. The basis of the decomposition is 1000 harmonics. The decomposition interval is $2l = 8000$, which is equal to the decomposition interval of the kinetics of the strange attractor (Figure 3d). This allowed us to accurately calculate

all the harmonics of the possible oscillating modes of the system, including for the strange attractor.

Doubling of the multiplicity of the periodic regime (see the transition from Figure 3a to Figure 3b and to Figure 3c) leads to the doubling of the number of fundamental harmonics that characterize the multiplicity of periodicity in the laminar phase trajectory of the attractor.

In the transition from Figure 3c to Figure 3d, there was no doubling of the cycle. So there was no increase in the multiplicity of fundamental harmonics. The graph (Figure 3d) shows a significant increase in the turbulence harmonics (compare Figure 3d with the graphs Figure 3a, b, c). The phase trajectory of the system becomes unstable and is characterized as a strange attractor. In this mode, the strict synchronicity of the metabolic processes of the system is violated. The desynchronized chain of glycolysis-gluconeogenesis reactions continues to execute its function, but not strictly periodically, which means the adaptation of cell metabolism to the changes in the cell and to the environment.

Figure 4a and Figure 4b show the distributions of the Fourier spectra of the variable $G(t)$ kinetics, with the increase of the parameter of gluconeogenesis to $l_5 = 0.3$ and with the change of the parameter G_0, for the following two modes: the quasi-stable autoperiodic process - $2 \times 2^2 (G_0 = 17.25)$ (a) and the chaos mode $2^x (G_0 = 16.8)$ (b).

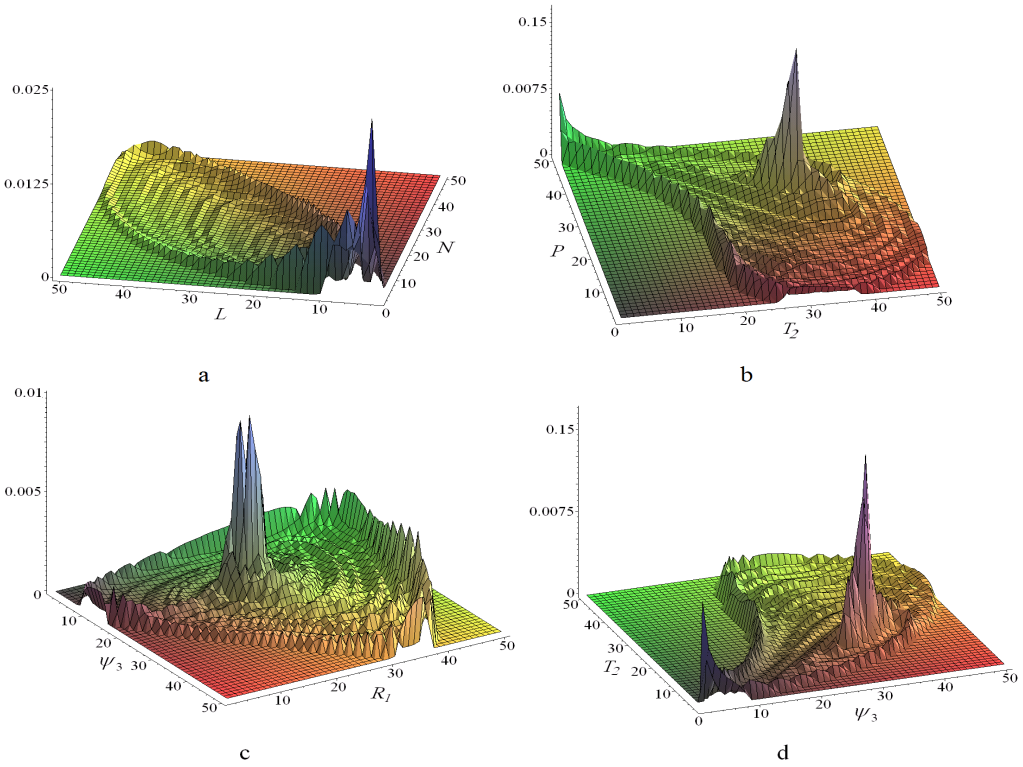

Figure 5: The histograms of the projections of the invariant measure of the strange attractor 2^x, at $l_5 = 0.25$: $t \in [10^6, 10^6 + 8 \cdot 10^5]$: a - onto the plane (L, N); b - onto the plane (T_2, P); c - onto the plane (R_1, ψ_3); d - onto the plane (T_2, ψ_3)

In order to more clearly represent the dynamics of the metabolic process of the glycolysis-gluconeogenesis system, the invariant measure (19) of the strange attractor 2^x was calculated for $l_5 = 0.25$: $t \in [10^6, 10^6 + 8 \cdot 10^5]$.

The histograms of the projections of the invariant measure onto some planes of the phase space of the system (Figure 5) were constructed, using the obtained values. For our results, we took the number of points $N = 50^{10}$ and the time of solving $t \in (10^6, 10^6 + 8 \times 10^5)$.

The histograms of projections of the invariant measure make it possible to generally evaluate the projections of the invariant measure of the corresponding variables of the system and to find its largest value. And this means that the found cell with the maximum of the projection of the invariant measure is also a place of instability in the variables of the system, where bifurcations and the chaotic regime of the strange attractor occur. This makes it possible to determine the sources of instability in the modeled cell biosystem dynamics.

From the presented diagrams, the largest projection of the invariant measure $\mu = 0.01875$ is obtained in Figure 5a, onto the coordinate plane (L, N). These variable models describe the change in lactate levels (8) and $NAD \cdot H$ (16). This means that the instability of these values in the metabolic process of glycolysis-gluconeogenesis most likely leads to the violation of the stability of the biosystem's attractor and the emergence of a strange attractor regime.

So, on the basis of the obtained results, in order to get rid of the chaotic regime and establish the stability of the attractor of the cell biosystem, we recommend to change the level $NAD \cdot H$ (electron carrier) or ψ (kinetic potential of the cell) via the corresponding biochemical action influencing these values.

We calculated the histograms of the invariant measure for other variables. It is also possible to determine their influence on the stability of the biosystem's attractor. In this case, the biochemical effect on the cell will be different.

4 Conclusion

The constructed mathematical model of glycolysis-gluconeogenesis is one of the main constructed models of synergy in biology. Using this model, the authors managed to simulate the structure of protobionts: the LUCA (the last universal common ancestor), from which the life of the primary cell could get its origin and get sustained. Thanks to biological evolution, this process has been reproduced in all living cells.

It was found that the cause of the auto-oscillating process in glycolysis is cell gluconeogenesis.

The results of the paper are as follows.

- The spectrum of the Fourier harmonic decomposition of the kinetics of system attractor formation was calculated. It can be used to determine system modes.

- For the first time, the invariant measures and the histograms of the invariant measures for the chaotic attractors of a dynamic system were calculated using a computer program for the mathematical model of glycolysis-gluconeogenesis.

- The histograms of the invariant measure of the strange attractor of the cell biosystem were constructed.

- Recommendations are made on how to biochemically get rid of the chaotic regime and restore the stability of the cell's life cycle.

Acknowledgment

The present work was partially supported by the Program of Fundamental Research of the Department of Physics and Astronomy of the National Academy of Sciences of Ukraine "Noise-induced dynamics and correlations in non-equilibrium systems" PK No. 0120U101347.

References

[1] H. Hacken. *Synergetics*. Mir, Moscow, 1980, 304–378 (in Russian).

[2] E. Schrödinger. *What is life in terms of physics*. Atomizdat, Moscow, 1972, 70–86 (in Russian).

[3] J. Higgins. A chemical mechanism for oscillation of glycolytic intermediates in yeast cells. *Proc. Nat. Acad. Sci. USA* **51** (1964) 989–994.

[4] E. E. Selkov. Self-oscillations in glycolysis. *Europ. J. Biochem.* **4** (1968) 79–86.

[5] A. Goldbeter, and R. Lefever. Dissipative structures for an allosteric model. Application to glycolytic oscillations. *Biophys J.* **12** (1972) 1302—1315.

[6] V. P. Gachok. *Strange Attractors in Biosystems*. Naukova Dumka, Kiev, 1989, 44–70 (in Russian).

[7] V. I. Grytsay. Self-organization and fractality in the metabolic process of glycolysis. *Ukr. J. Phys.* **60** No.12, (2015) 1253. `https://arxiv.org/abs/1707.05636`

[8] V. I. Grytsay. Self-organization and fractality created by gluconeogenesis in the metabolic process. *Chaotic Modeling and Simulation (CMSIM)* **5** (2016) 113-127. `https://arxiv.org/abs/1707.05678`

[9] A. I. Oparin. *Appeaarnce of a Life on the Earth*. Izd. AN SSSR, Moscow-Leningrad, 1941 (in Russian).

[10] S. L. Miller. A production of amino acids under possible primitive earth conditions. *Science.* **117** (3046) (1953) 528–529. PMID 13056598

[11] N. N. Bogolubov. *Collected Works in 12 Volumes*. Nauka, Moscow, 2005, **vol. 1,** part VI, unit 20, pp. 475–532. (in Russian).

[12] A. Zarour, A. Ouannas, Ch. Latrous, and A. Berkane. Linear Chaos Control of fractional generalized Henon Map *Nonlinear Dynamics and Systems Theory* **21** (2) (2021) 216–224. `http://www.e-ndst.kiev.ua/v21n2/9(77).pdf`

[13] M. W. Ullah, M. A. Uddin and M. S. Rahman. A Modified Harmonic Balance Method for Solving Strongly Generalized Nonlinear Damped Forced Vibration System. *Nonlinear Dynamics and Systems Theory* **21** (5) (2021) 544–552. `http://www.e-ndst.kiev.ua/v21n5/8(80).pdf`

[14] N. Kryloff and N. Bogoliouboff. La Theorie Generale De La Mesure Dans Son Application A L'Etude Des Systemes Dynamiques De la Mecanique Non Lineaire. *Annals of Mathematics* Second Series, **38** (1) (1937) 65–113. (in French).

Nonlinear Dynamics and Systems Theory, **24** (1) (2024) 65–79

A New Efficient Step-Size in Karmarkar's Projective Interior Point Method for Optimization Problems

F. Leulmi [1*] and A. Leulmi [2]

[1] *Brother Mentouri University, Constantine-1, Algeria.*
[2] *Ferhat Abbas University of Setif-1, Algeria*

Received: May 19, 2023; Revised: January 16, 2024

Abstract: In this paper, we are concerned with the optimization problem by using the logarithmic penalty method via new upper bound and lower bound functions in the Karmarkar's algorithm to find the solution. Then, we establish the direction by Newton's method. Also, we propose a new approach based on new upper bound and lower bound functions to determine the step size. To lend further support to our theoretical results, a simulation study is carried out to illustrate the good accuracy of the studied method.

Keywords: *Karmarkar's projective method; logarithmic barrier method; upper and lower bound functions; averaging of perturbations; step size; mathematical modeling; interior point methods.*

Mathematics Subject Classification (2010): 90C05, 70K65, 90C51, 93A30.

1 Introduction

The appearance, rapid evolution and success of interior point methods since their revival by Karmarkar (1984) in the field of linear optimization problems, have prompted researchers around the world to develop a whole arsenal of methods (software) allowing to properly deal with several classes of problems once considered difficult to solve, including nonlinear programming, semi-definite programming, etc.

Linear optimization is a general mathematical framework for modelling and solving some optimization problems and it appears in many areas of applications such as agriculture, finance, economics, geometric problems and optimal control.

Mathematically, the problem is to optimize a linear function under linear constraints on the variables.

* Corresponding author: mailto:faridleulmi233@gmail.com

Historically, linear programming has been developed by George Bernard Danzig since 1947.

Our work concerns the linear optimization (LO) problem which has become a much coveted research topic since the revival of interior point methods from new investigations brought by Karmarkar (1984) and others.

These methods are recognized as formidable competitors of the famous simplex method. Their major drawback (at about 80% of the computational value) is the calculation of the projection which dominates the cost of the iteration.

Our work is devoted to an approach inspired by the interior point logarithmic barrier method, and to avoid the calculation of the projection in Karmarkar's projective method, we propose an original procedure for the calculation of the step size based on the idea of the upper and lower bound functions and we introduce new functions. This study is supported by interesting numerical tests.

To our knowledge, our new upper and lower bound functions have not been studied in the linear optimization literature. These approximate functions have the advantage that they allow computing the step size easily and without consuming much time, contrarily to the line search method, which is time-consuming and expensive to identify the step size. For this, our objective is to optimize a linear problem based on prior efforts, and we propose a straightforward and effective logarithmic barrier method based on new upper and lower bound functions.

The rest of the paper is built as follows. We first present in Section 2 of our paper, a linear optimization problem formulation. We introduce in Section 3, a brief description of the algorithm. In Sections 4 and 5, we establish new upper and lower bound functions and the algorithm. Two lemmas are proved in Section 6 to show the convergence results. A simulation study is carried out to show the good behaviour of our approach in Section 7. Finally, a conclusion is summarized in the last section.

2 Posing of the Problem

We consider the following linear optimization problem:

$$(ka)\begin{cases} \min\langle c, x\rangle = 0, \\ Ax = 0, \\ x \geq 0, \\ x \neq 0, \end{cases}$$

which was applied to the Karmarkar algorithm. Here, $c \in \mathbb{R}^n$ and A is an $m \times n$ matrix of *rank* m.

In all that follows, the following conventions are adopted: the vector $e \in \mathbb{R}^n$ is the vector whose components are all equal to 1, given a vector $x \in \mathbb{R}^n$, X is the diagnonal matrix whose diagonal elements are the components of x (*i.e.*, $X = diag\{x\}$).

The following assumptions are made:

1. $Ax = 0$ and $x \geq 0 \Rightarrow \langle c, x\rangle \geq 0$.
2. We know a point $x > 0$ such that $Ax = 0$ and $\langle c, x\rangle > 0$.
3. We know that the problem (ka) has solutions. We put

$$C = \{x : Ax = 0, x \geq 0, x \neq 0\}.$$

If $\bar{x}$ is a solution of (ka), then $k\bar{x}$ with $k > 0$ is also a solution.

We can thus proceed to a normalization of x and consider, for example, the following linear problem:

$$(pk)\begin{cases} \min c^t x = 0, \\ Ax = 0, \\ \langle e, x\rangle = n, x \geq 0. \end{cases}$$

We note that the set of optimal solutions of this problem is a convex polyhedron contained in the relative boundary of the set of feasible points.

The potential function.

The convergence of the algorithm is based on the following function, called the "multiplicative potential function", defined for all $x \in C, x > 0$, by

$$f(x) = \frac{\langle c, x\rangle^n}{\prod_{i=1}^{n} x_i},$$

which we extend by semi-continuity on C.

One can also consider the function called the "logarithmic potential function" defined by

$$q(x) = \ln f(x) = n \ln(\langle c, x\rangle) - \sum_{i=1}^{n} \ln(x_i).$$

The function f has the following properties:

1) $0 < f(x) < +\infty$ if $x > 0$ and $Ax = 0$.

2) $f(x) = +\infty$ if x belongs to the relative boundary of C without being a solution of (ka).

3) $f(x) = 0$ if x is a solution of (ka) or if $x = 0$.

4) $f(kx) = f(x)$ for all $x \in C$ and all $k > 0$.

Thus, problem (ka) consists of finding the optimal solutions to the problem

$$(km)\begin{cases} \min f\,(x) = 0, \\ Ax = 0, \\ x \geq 0, x \neq 0. \end{cases}$$

3 Description of the Algorithm

Starting from the point $x \in C$ which is known, the Karmarkar algorithm is a descent method which generates, due to the barrier character of the objective function f, a sequence of points all contained in the relative interior of C, hence the name of the method of interior points. We will describe the transition from the initial iterate x to the next iterate $\tilde{x}$.

It is assumed that the iterate $\tilde{x}$ verifies $\tilde{x} > 0$ and $A\tilde{x} = 0$.

3.1 Normalisation

We normalize x by the relation

$$x = \sqrt{\frac{n}{\langle x, x\rangle}}x$$

so that $\langle x, x\rangle = n$.

3.2 Direction of descent

It is easy to see that we have

$$\frac{f(\tilde{x})}{f(x)} = g(z)$$

with

$$z = X^{-1}\tilde{x}, g(z) = \frac{\langle b, z\rangle^n}{\prod_{i=1}^{n} z_i} \text{ and } b = \frac{1}{\langle c, x\rangle} Xc.$$

The conditions $A\tilde{x} = 0,\ \tilde{x} \geq 0$ and $\tilde{x} \neq 0$ transpose to

$$AXz = 0, z \geq 0 \text{ and } z \neq 0.$$

Let $B = AX$. Problem (km) is equivalent to the problem

$$(kmz) \begin{cases} \min g(z) = 0, \\ Bz = 0, \\ z \geq 0, \\ z \neq 0. \end{cases}$$

e is a feasible solution of this problem and we have $g(e) = \langle b, e\rangle = 1$.

Since we have $g(kz) = g(z)$ for all $z \geq 0$ and all $k > 0$, we will work on the following normalized problem:

$$(kz) \begin{cases} \min g(z) = 0, \\ Bz = 0, \\ \langle e, z\rangle = n, \\ z \geq 0. \end{cases}$$

It is easy to see that the matrix (A^t, x) is of rank $m+1$, so is the matrix (B^t, e). The Newtonian descent direction at point e for the problem (kz) is obtained by solving the quadratic problem

$$(PQ) \begin{cases} \min \frac{1}{2} \left\langle \nabla^2 g(e) d, d\right\rangle + \left\langle \nabla g(e), d\right\rangle, \\ Bd = 0, \\ \langle e, d\rangle = 0. \end{cases}$$

To do this, let us introduce the matrix

$$P = I - \left(B^t, e\right) \left[\left(B^t, e\right)^t \left(B^t, e\right)\right]^{-1} \left(B^t, e\right)^t,$$

which corresponds to the projection on the linear subspace:

$$E = \{d : Bd = 0, \langle e, d\rangle = 0\}.$$

We have

$$P^2 = P = P^t, PB^t = 0 \text{ and } Pe = 0.$$

It is easy to see that we have

$$P\nabla g(e) = Pb \text{ and } P\nabla^2 g(e)P = I + n(n-1) Pbb^t P,$$

the quadratic problem is equivalent to

$$\begin{cases} \min \frac{1}{2} \left\langle \nabla^2 g\left(e\right) d, d \right\rangle + \left\langle \nabla g\left(e\right), d \right\rangle, \\ Pd = d, \end{cases}$$

whose optimal solution is collinear with

$$d = -Pb = -P\nabla g\left(e\right).$$

The direction d thus coincides with the direction given by the projected gradient. We are now interested in some properties of d.

First of all, we have

$$\langle d, e \rangle = -\langle Pb, e \rangle = -\langle b, Pe \rangle = 0,$$

we then observe that on the one hand, we have

$$\left\{ \begin{array}{c} z : \langle e, z \rangle = n \\ \|z - e\|^2 \leq \frac{n}{n-1} \end{array} \right\} \subset \left\{ \begin{array}{c} z : \langle e, z \rangle = n \\ z \geq 0 \end{array} \right\} \subset \left\{ \begin{array}{c} z : \langle e, z \rangle = n \\ \|z - e\|^2 \leq n\left(n-1\right) \end{array} \right\}.$$

and on the other hand,

$$\begin{cases} \min \langle b, z - e \rangle = -1, \\ Bz = 0, \\ \langle e, z \rangle = n, \\ z \geq 0, \end{cases}$$

and since $P\left(e - \bar{z}\right) = e - \bar{z}$,

$$\langle b, z - e \rangle = \langle Pb, z - e \rangle,$$

we get

$$\|Pb\| \sqrt{\frac{n}{n-1}} \leq 1 \leq \|Pb\| \sqrt{n\left(n-1\right)}.$$

So, in summary,

$$\langle d, b \rangle = -\|d\|^2 = -\|Pb\|^2, \langle d, e \rangle = 0 \text{ and } \frac{1}{n\left(n-1\right)} \leq \|d\|^2 \leq \frac{n-1}{n}.$$

In the following, we denote by $\bar{d}$ and σ the mean and standard deviations of $\left(d_1, d_2, ..., d_n\right)$. We have

$$\bar{d} = \frac{1}{n} \sum_{i=1}^{n} d_i = 0 \text{ and } \frac{1}{n^2\left(n-1\right)} \leq \sigma^2 = \frac{\|d\|^2}{n} - \bar{d}^2 \leq \frac{n-1}{n^2}. \tag{1}$$

4 Calculation of the Step Size

The calculation of the step size consists in obtaining a value $t > 0$ such that we have $e + td > 0$ and which gives a significant decrease of $\mu_0(t) = g(e + td)$ or, equivalently, of $\omega_0(t) = ln(g(e + td))$.

Since the equation $\omega_0'(t) = 0$ cannot be solved explicitly in a large class of optimization problems, it is normal to think of iterative methods of solution, one can also apply to ω_0

an Armijo-Golstein-Price type method. In both cases, this requires several evaluations of the function ω_0 and its derivative and is therefore expensive. Our approach consists in minimizing an upper bound ω_{MAJ} and lower bound ω_{MIN} of the function ω_0 whose minimum can be obtained explicitly. Recall that we have

$$\omega_0(t) = n \ln\left(1 - t\|d\|^2\right) - \sum_{i=1}^{n} \ln(1 + td_i),$$

it is clear that $\omega_0(0) = 0$.

We need the following theorem to find the upper bound and lower bound functions of $\omega(t)$.

Theorem 4.1 *[1] Suppose that $x_i > 0$ for all $i = 1, 2, \ldots, n$, then*

$$n \ln\left(\bar{x} - \sigma_x\sqrt{n-1}\right) \leq A \leq \sum_{i=1}^{n} \ln(x_i) \leq B \leq n \ln(\bar{x}),$$

with

$$A = (n-1)\ln\left(\bar{x} + \frac{\sigma_x}{\sqrt{n-1}}\right) + \ln\left(\bar{x} - \sigma_x\sqrt{n-1}\right)$$

and

$$B = \ln\left(\bar{x} + \sigma_x\sqrt{n-1}\right) + (n-1)\ln\left(\bar{x} - \frac{\sigma_x}{\sqrt{n-1}}\right),$$

such that $\bar{x}$ and σ_x are, respectively, the mean and standard deviations of a statistical series $\{x_1, x_2, ..., x_n\}$ of n real numbers. These quantities are defined as follows:

$$\bar{x} = \frac{1}{n}\sum_{i=1}^{n} x_i \text{ and } {\sigma^2}_x = \frac{1}{n}\sum_{i=1}^{n} {x^2}_i - \bar{x}^2 = \frac{1}{n}\sum_{i=1}^{n}(x_i - \bar{x}^2).$$

In the following, we take $x_i = 1 + td_i, i = 1, ..., m$, we have $\bar{x} = 1 + td$ and $\sigma_x = t\sigma_d$.

4.1 Upper bound functions

4.1.1 First upper bound function

From the previous theorem, we have

$$A \leq \sum_{i=1}^{n} \ln(x_i),$$

then

$$\begin{aligned}
\sum_{i=1}^{n} \ln(1 + td_i) &\geq (n-1)\ln\left(\bar{x} + \frac{\sigma_x}{\sqrt{n-1}}\right) + \ln(\bar{x} - \sigma_x\sqrt{n-1}), \\
\sum_{i=1}^{n} \ln(1 + td_i) &\geq (n-1)\ln\left(1 + \frac{\sigma t}{\sqrt{n-1}}\right) + \ln\left(1 - \sigma t\sqrt{n-1}\right),
\end{aligned}$$

multiplying by (-1), we find

$$-\sum_{i=1}^{n}\ln(1+td_i)\leq-(n-1)\ln\left(1+\frac{\sigma t}{\sqrt{n-1}}\right)-\ln(1-\sigma t\sqrt{n-1}),$$

and therefore

$$\omega_0\left(t\right)\leq\omega_{MAJ}\left(t\right)=n\ln\left(1-nt\sigma^2\right)-(n-1)\ln\left(1+\frac{\sigma t}{\sqrt{n-1}}\right)-\ln\left(1-\sigma t\sqrt{n-1}\right).$$

From this, we can deduce that the function ω_{MAJ} reaches its minimum at the point

$$\bar{t}_{MAJ}=\frac{n\sqrt{n-1}}{\sqrt{n-1}+n\left(n-2\right)\sigma}.$$

4.1.2 Second upper bound function

Let us consider a function that contains only a logarithm and is simpler than the function ω_{MAJ}. Then, we consider the following function:

$$\omega_{MAJ1}(t)=-2n\left\|d\right\|^2t-\ln\left(1-\sigma t\sqrt{n-1}\right).$$

Lemma 4.1 *$\omega_{MAJ1}(t)$ is strictly convex for all $t\geq0$; and we have*

$$\omega_0(t)\leq\omega_{MAJ1}(t)\leq+\infty.$$

Proof. We have

$$\omega_0\left(t\right)=n\ln\left(1-t\left\|d\right\|^2\right)-\sum_{i=1}^{n}\ln\left(1+td_i\right).$$

We pose

$$g(t)=\omega_{MAJ1}(t)-\omega_0(t),$$

we have $g(0)=0$ and

$$g''(t)=\frac{\sigma^2(n-1)}{(1-\sigma t\sqrt{n-1})^2}+\frac{n\left\|d\right\|^2}{(1-t\left\|d\right\|^2)^2}+\sum_{i=1}^{n}\frac{d_i^2}{(1+td_i^2)^2}\geq0$$

for all $t\geq0$. This gives $g(t)\geq0,\forall t\geq0$.
Then

$$\omega_0(t)\leq\omega_{MAJ1}(t).$$

From this, we can deduce that the function ω_{MAJ1} reaches its minimum at the point

$$\tilde{t}=\frac{1}{\sigma\sqrt{n-1}}-\frac{1}{2n^2\sigma^2}.$$

The new iterate is

$$\tilde{x}=X\left(e+\bar{t}d\right)=x+\bar{t}Xd.$$

By construction, we have $\tilde{x}>0$ and $A\tilde{x}=0$.

4.1.3 The decrease

Replacing $\tilde{t}$ with its value gives

$$\begin{aligned}\omega_{MAJ1}(\tilde{t}) &= -2n^2\sigma^2\tilde{t} - \ln(1-\sigma\tilde{t}\sqrt{n-1}) \\ &= 1 - \frac{2n^2\sigma}{\sqrt{n-1}} - \ln\left(1 - \frac{2n^2\sigma - \sqrt{n-1}}{2n^2\sigma}\right) \\ &= 1 - \frac{2n^2\sigma}{\sqrt{n-1}} - \ln\left(\frac{\sqrt{n-1}}{2n^2\sigma}\right).\end{aligned}$$

The quantity $\omega_{MAJ1}(\tilde{t}) - \omega_{MAJ1}(0) = \omega_{MAJ1}(\tilde{t})$ depends on σ.
Since we have

$$\frac{1}{n\sqrt{n-1}} \leq \sigma \leq \frac{\sqrt{n-1}}{n},$$

we obtain

$$1 \leq \sigma n\sqrt{n-1} \leq n-1.$$

It is useful to put $u = n\sigma\sqrt{n-1}$, then we get $1 \leq u \leq n-1$ and

$$\begin{aligned}\omega_{MAJ1}(\tilde{t}) &= 1 - \frac{2n^2\sigma}{\sqrt{n-1}} - \ln\left(\frac{\sqrt{n-1}}{2n^2\sigma}\right) \\ &= 1 - \frac{2nu}{n-1} - \ln\left(\frac{n-1}{2nu}\right) \\ &= 1 - \frac{2nu}{n-1} - \ln(n-1) + \ln(2nu) \\ &= \xi(u).\end{aligned}$$

The function ξ is concave (a sum of two concave functions) and therefore

$$\omega_{MAJ1}(\tilde{t}) = \xi(u) < \xi(1) + (u-1)\xi'(1).$$

This leads to

$$\omega_{MAJ1}(\tilde{t}) = \xi(u) < \ln\left(\frac{2ne}{(n-1)e^{\frac{2n}{n-1}}}\right) - (u-1)\left(\frac{2n}{n-1} - 1\right).$$

We deduce that in the worst case (where $u = 1$), we have

$$\omega_{MAJ1}(\tilde{t}) = \xi(u) < \ln\left(\frac{2ne}{(n-1)e^{\frac{2n}{n-1}}}\right) \leq 0,$$

then we obtain

$$f(\tilde{x}) \leq \left(\frac{2ne}{(n-1)e^{\frac{2n}{n-1}}}\right) f(x_0).$$

4.2 Lower bound function

4.2.1 First lower bound function

From the previous theorem, we have

$$\sum_{i=1}^{n} \ln(x_i) \leq B,$$

then

$$\begin{aligned}
\sum_{i=1}^{n} \ln(1+td_i) &\leq (n-1)\ln\left(\bar{x} - \frac{\sigma_x}{\sqrt{n-1}}\right) + \ln(\bar{x} + \sigma_x\sqrt{n-1}), \\
\sum_{i=1}^{n} \ln(1+td_i) &\leq (n-1)\ln\left(1 - \frac{\sigma t}{\sqrt{n-1}}\right) + \ln(1 + \sigma t\sqrt{n-1}).
\end{aligned}$$

Multiplying by (-1), we find

$$-\sum_{i=1}^{n} \ln(1+td_i) \geq -(n-1)\ln(1 - \frac{\sigma t}{\sqrt{n-1}}) - \ln(1 + \sigma t\sqrt{n-1}),$$

and therefore

$$\omega_0(t) \geq \omega_{MIN}(t) = n\ln(1-n\sigma^2 t) - (n-1)\ln\left(1 - \frac{\sigma t}{\sqrt{n-1}}\right) - \ln(1+\sigma t\sqrt{n-1}).$$

From this we can deduce that the function ω_{MIN} reaches its minimum at the point

$$\bar{t}_{MIN} = \frac{n\sqrt{n-1}}{\sqrt{n-1} - n\,(n-2)\,\sigma}.$$

4.2.2 Second lower bound function

We can consider a function that contains only a logarithm and is simpler than the function ω_{MIN}. Then let us consider the following function:

$$\omega_{MIN1}(t) = -2n\left\|d\right\|^2 t - (n-1)\ln\left(1 - \frac{\sigma t}{\sqrt{n-1}}\right).$$

Lemma 4.2 *$\omega_{MIN1}(t)$ is strictly convex for all $t \geq 0$; and we have*

$$-\infty \leq \omega_{MIN1}(t) \leq \omega_{MIN}(t).$$

Proof. We have

$$\omega_{MIN}(t) = n\ln(1-n\sigma^2 t) - (n-1)\ln\left(1 - \frac{\sigma t}{\sqrt{n-1}}\right) - \ln(1+\sigma t\sqrt{n-1}).$$

We put

$$g(t) = \omega_{MIN1}(t) - \omega_{MIN}(t).$$

We obtain $g(0) = 0$ and

$$g''(t) = -\frac{\sigma^2(n-1)}{(1+\sigma t\sqrt{n-1})^2} \leq 0$$

for all $t \geq 0$. This gives $g(t) \leq 0, \forall t \geq 0$, then

$$\omega_{MIN}(t) \geq \omega_{MIN1}(t).$$

We deduce that the function ω_{MIN1} reaches its minimum at the point

$$\tilde{t} = \frac{2n^2\sigma\sqrt{n-1} - (n-1)}{2n^2\sigma^2}.$$

4.2.3 The decrease

Replacing $\tilde{t}$ with its value gives

$$\begin{aligned}\omega_{MIN1}(\tilde{t}) &= -2n^2\sigma^2\tilde{t} - (n-1)\ln\left(1 - \frac{\sigma}{\sqrt{n-1}}\tilde{t}\right) \\ &= (n-1) - 2n^2\sigma\sqrt{n-1} - (n-1)\ln\left(\frac{n-1}{2n^2\sigma\sqrt{n-1}}\right).\end{aligned}$$

The quantity $\omega_{MIN1}(\tilde{t}) - \omega_{MIN1}(0) = \omega_{MIN1}(\tilde{t})$ depends on σ.
Since we have

$$\frac{1}{n\sqrt{n-1}} \leq \sigma \leq \frac{\sqrt{n-1}}{n},$$

we get

$$1 \leq \sigma n\sqrt{n-1} \leq n-1,$$

it is useful to set $u = n\sigma\sqrt{n-1}$, then we obtain $1 \leq u \leq n-1$ and

$$\begin{aligned}\omega_{MIN1}(\tilde{t}) &= (n-1) - 2n^2\sigma\sqrt{n-1} - (n-1)\ln\left(\frac{n-1}{2n^2\sigma\sqrt{n-1}}\right) \\ &= (n-1) - 2nu - (n-1)\ln\left(\frac{n-1}{2nu}\right) \\ &= \xi(u).\end{aligned}$$

The function ξ is concave (a sum of two concave functions) and therefore

$$\omega_{MIN1}(\tilde{t}) = \xi(u) < \xi(1) + (u-1)\xi'(1).$$

We can deduce

$$\omega_{MIN1}(\tilde{t}) = \xi(u) < \ln\left(\left(\frac{2ne}{n-1}\right)^{n-1} \times \frac{1}{e^{2n}}\right) - (u-1)(n+1).$$

We deduce that in the worst case (where $u = 1$), we have

$$\omega_{MIN1}(\tilde{t}) = \xi(u) < \ln\left(\left(\frac{2ne}{n-1}\right)^{n-1} \times \frac{1}{e^{2n}}\right) \leq 0,$$

so, we obtain

$$f(\tilde{x}) \leq \left(\left(\frac{2ne}{n-1}\right)^{n-1} \times \frac{1}{e^{2n}}\right) f(x_0).$$

5 The Algorithm

Karmarkar's algorithm via the upper bound and lower bound functions.

Initialization: We start from $x > 0$ such that $Ax = 0$, ϵ is a given precision.
Result: x^*.
Iteration:
While $c^t x > \epsilon$ *do:*
1- Normalization:

$$x = \sqrt{\frac{n}{\langle x, x\rangle}}x.$$

2- Descent direction: We take b and B as follows:

$$b = \frac{1}{\langle c, x\rangle}Xc,\ B = AX.$$

We determine d projection of b onto the linear subspace:

$$\{d : B_k d = 0, \langle e, d\rangle = 0\}.$$

Finally, the descent direction is:

$$\delta = Xd.$$

3- The step size: We calculate:

$$\sigma = \frac{\|d\|}{\sqrt{n}}.$$

Case 1: upper bound function:

$$\bar{t}_{MAJ} = \frac{2n^2\sigma - \sqrt{n-1}}{2n^2\sigma\sqrt{n-1}}.$$

Case 2: lower bound function:

$$\bar{t}_{MIN} = \frac{2n^2\sigma\sqrt{n-1} - (n-1)}{2n^2\sigma^2}.$$

4- The new iterate: is $\tilde{x} = x + t\delta$.
5- Taking $k = k + 1$ and returning to (1).
End While.
$x^* = \tilde{x}$.
End Algorithm.

6 The Convergence

Upper bound function.

Lemma 6.1 *At the* k^{th} *iteration, we have*

$$f(x_k) < \left(\frac{2ne}{(n-1)e^{\frac{2n}{n-1}}}\right)^k f(x_0).$$

Therefore $f(x_k)$ *converges linearly to* 0. *We deduce that any membership value of the sequence* $\{x_k\}$ *is an optimal solution of problem* (ka).

Lower bound function.

Lemma 6.2 *At the k^{th} iteration, we have*

$$f(x_k) < \left(\left(\frac{2ne}{n-1} \right)^{n-1} \times \frac{1}{e^{2n}} \right)^k f(x_0).$$

Therefore $f(x_k)$ converges linearly to 0. We deduce that any membership value of the sequence $\{x_k\}$ is an optimal solution of problem (ka).

7 Numerical Tests

To evaluate our algorithm's efficiency based on our upper and lower bound functions, we conducted comparative numerical tests between our two new approximate functions (the upper bound function (**TUF**)and the lower bound function (**TLF**) and Wolfe's line search method (**LSW**)). The algorithm is described in our work using Matlab10 software. The examples tested are taken from the literature, see for example [4, 5].

We have taken ϵ between (10^{-4} et 10^{-6}). We denote by

TUF: The upper bound function technique.

TLF: The technique of the lower bound function.

LSW: Wolfe's line search method.

iter: The number of iterations required to obtain an optimal solution.

time (s): The calculation time in seconds.

7.1 Examples

Example 1:

$$A = \begin{bmatrix} 0 & 1 & 2 \\ 0 & 3 & 0 \end{bmatrix},\ b = \begin{bmatrix} 2 \\ 1 \end{bmatrix} \text{ and } c = \begin{bmatrix} 2 & 1 & 0 \end{bmatrix}^t.$$

The optimal value is $z^* = \frac{1}{3}$.

The exact optimal solution is $x^* = \begin{bmatrix} 0 & \frac{1}{3} & \frac{5}{6} \end{bmatrix}^t$.

Comparative table:

Method	**iter**	**time (s)**
TUF1	03	0:0:0:1
TLF1	04	0:0:0:19
LSW	11	0:0:01:31

Example 2:

$$A = \begin{bmatrix} 2 & 3 & 1 & 2 \\ 3 & 0 & -2 & 1 \end{bmatrix},\ b = \begin{bmatrix} 2 \\ 0 \end{bmatrix} \text{ and } c = \begin{bmatrix} 4 & 1 & 2 & 0 \end{bmatrix}^t.$$

The optimal value is $z^* = 0.67$.

The exact optimal solution is $x^* = \begin{bmatrix} 0 & 0.67 & 0 & 0 \end{bmatrix}^t$.

Comparative table:

Method	**iter**	**time (s)**
TUF1	06	0:0:0:1
TLF1	09	0:0:0:26
LSW	13	0:0:10:01

Example 3:

$$A=\begin{bmatrix} 2 & 3 & 1 & 0 & 3 \\ 1 & 2 & 5 & 0 & 1 \\ 5 & -1 & 2 & 3 & 0 \end{bmatrix},\quad b=\begin{bmatrix} 1 \\ 2 \\ 3 \end{bmatrix} \text{ and } c=\begin{bmatrix} 1 & 2 & 3 & 5 & 4 \end{bmatrix}^t.$$

The optimal value is $z^*=\frac{22}{9}$.
The exact optimal solution is $x^*=\begin{bmatrix} \frac{1}{3} & 0 & \frac{1}{3} & \frac{2}{9} & 0 \end{bmatrix}^t$.
Comparative table:

Method	**iter**	**time (s)**
TUF	09	0:0:0:01
TLF	11	0:0:0:02
LSW	32	0:0:11:09

Example 4:

$$A=\begin{bmatrix} 2 & 1 & 0 & -1 & 0 & 0 \\ 0 & 0 & 1 & 0 & 1 & -1 \\ 1 & 1 & 1 & 1 & 1 & 1 \end{bmatrix},\quad b=\begin{bmatrix} 0 \\ 0 \\ 1 \end{bmatrix} \text{ and } c=\begin{bmatrix} 3 & -1 & 1 & 0 & 0 & 0 \end{bmatrix}^t.$$

The optimal value is $z^*=-0.5$.
The exact optimal solution is $x^*=\begin{bmatrix} 0 & 0.5 & 0 & 0.5 & 0 & 0 \end{bmatrix}^t$.
Comparative table:

Method	**iter**	**time (s)**
TUF1	10	0:0:0:01
TLF1	13	0:0:0:01
LSW	33	0:0:12:08

Example 5:

$$A=\begin{bmatrix} 1 & 0 & -4 & 3 & 1 & 1 & 1 & 0 & 0 & 0 & 0 & 0 \\ 5 & 3 & 1 & 0 & -1 & 3 & 0 & 1 & 0 & 0 & 0 & 0 \\ 4 & 5 & -3 & 3 & -4 & 1 & 0 & 0 & 1 & 0 & 0 & 0 \\ 0 & -1 & 0 & 2 & 1 & -5 & 0 & 0 & 0 & 1 & 0 & 0 \\ -2 & 1 & 1 & 1 & 2 & 2 & 0 & 0 & 0 & 0 & 1 & 0 \\ 2 & -3 & 2 & -1 & 4 & 5 & 0 & 0 & 0 & 0 & 0 & 1 \end{bmatrix},\quad b=\begin{bmatrix} 1 \\ 4 \\ 4 \\ 5 \\ 7 \\ 5 \end{bmatrix}$$

$$\text{and } c=\begin{bmatrix} -4 & -5 & -1 & -3 & 5 & -8 & 0 & 0 & 0 & 0 & 0 & 0 \end{bmatrix}^t.$$

The optimal value is $z^*=-17$.
The exact optimal solution is $x^*=\begin{bmatrix} 0 & 0 & 2.5 & 3.5 & 0 & 0.5 & 0 & 0 & 0.5 & 0.5 & 0 & 1 \end{bmatrix}^t$.
Comparative table:

Method	**iter**	**time (s)**
TUF1	09	0:0:0:01
TLF1	07	0:0:0:01
LSW	20	0:0:17:12

Example 6: The matrix A is

$$\begin{bmatrix}
1 & 1 & 0 & 0 & 0 & 0 & 0 & 0 & 0 & 0 & 0 & 0 & 0 & 0 & 1 & 0 & 0 & 0 & 0 & 0 & 0 & 0 & 0 & 0 \\
0 & 2 & 1 & 0 & 0 & 0 & 0 & 0 & 0 & 0 & 0 & 0 & 0 & 0 & 0 & 1 & 0 & 0 & 0 & 0 & 0 & 0 & 0 & 0 \\
0 & 0 & 3 & -1 & 0 & 0 & 0 & 0 & 0 & 0 & 0 & 0 & 0 & 0 & 0 & 0 & 1 & 0 & 0 & 0 & 0 & 0 & 0 & 0 \\
0 & 0 & 0 & 2 & 4 & 0 & 0 & 0 & 0 & 0 & 0 & 0 & 0 & 0 & 0 & 0 & 0 & 1 & 0 & 0 & 0 & 0 & 0 & 0 \\
0 & 0 & 0 & 0 & 6 & 2 & 0 & 0 & 0 & 0 & 0 & 0 & 0 & 0 & 0 & 0 & 0 & 0 & 1 & 0 & 0 & 0 & 0 & 0 \\
0 & 0 & 0 & 0 & 0 & -1 & 2 & 0 & 0 & 0 & 0 & 0 & 0 & 0 & 0 & 0 & 0 & 0 & 0 & 1 & 0 & 0 & 0 & 0 \\
0 & 0 & 0 & 0 & 0 & 0 & 4 & -1 & 0 & 0 & 0 & 0 & 0 & 0 & 0 & 0 & 0 & 0 & 0 & 0 & 1 & 0 & 0 & 0 \\
0 & 0 & 0 & 0 & 0 & 0 & 0 & 0 & 3 & 1 & 0 & 0 & 0 & 0 & 0 & 0 & 0 & 0 & 0 & 0 & 0 & 1 & 0 & 0 \\
0 & 0 & 0 & 0 & 0 & 0 & 0 & 0 & 3 & -1 & 1 & 0 & 0 & 0 & 0 & 0 & 0 & 0 & 0 & 0 & 0 & 1 & 0 & 0 \\
0 & 0 & 0 & 0 & 0 & 0 & 0 & 0 & 0 & 1 & 1 & 2 & 0 & 0 & 0 & 0 & 0 & 0 & 0 & 0 & 0 & 0 & 1 & 0 \\
0 & 0 & 0 & 0 & 0 & 0 & 0 & 0 & 0 & 0 & 0 & 1 & 2 & 1 & 0 & 0 & 0 & 0 & 0 & 0 & 0 & 0 & 0 & 1
\end{bmatrix}$$

The vectors c and b are

$$\begin{aligned}
c &= \begin{bmatrix} 2 & -1 & -3 & 5 & -2 & 0 & 4 & 1 & 2 & -1 & 1 & -1 & 0 & 2 \\ & 0 & 0 & 0 & 0 & 0 & 0 & 0 & 0 & 0 & 0 & 0 & & \end{bmatrix}^t, \\
b &= \begin{bmatrix} 8 & 4 & 6 & 2 & 5 & 1 & 2 & 6 & 3 & 9 & 4 \end{bmatrix}^t.
\end{aligned}$$

The optimal value is $z^* = -13.25$.
The exact optimal solution is

$$x^* = \begin{bmatrix} 0 & 1 & 2 & 0 & 0.5 & 1.33 & 0 & 0 & 0 & 1.5 & 0 & 3.48 & 0 \\ 0 & 7 & 0 & 0 & 0 & 1 & 2.33 & 2 & 0.18 & 4.5 & 0 & 0.15 & \end{bmatrix}^t.$$

Comparative table:

Method	**iter**	**time (s)**
TUF1	05	0:0:0:01
TLF1	06	0:0:0:01
LSW	22	0:0:57:09

Example 7: (with a variable size)
We consider the following linear problem of variable size:

$$\zeta = \min[c^T x : x \geq 0,\ Ax = b],$$

where A is the $m \times 2m$ matrix defined by

$$\begin{aligned}
A[i,j] &= \begin{cases} 1 & \text{if } i = j \quad \text{or } j = i + m, \\ 0 & \text{if not.} \end{cases} \\
c[i] &= -1,\ c[i+m] = 0 \text{ and } b[i] = 2,\ \forall i = 1, ...m,
\end{aligned}$$

where the vectors $c \in \mathbb{R}^{2m}$ and $b \in \mathbb{R}^{2m}$.
The optimal value is $z^* = -2m$. The exact optimal solution is

$$x_i^* = \begin{cases} 2 & \text{if } \ i = 1, ..., m, \\ 0 & \text{if } \ i = m+1, ..., n. \end{cases}$$

Comparative table:

size	Method	iter	time (s)
5×10	**TUF**	4	0:0:0:01
	TLF	6	0:0:0:01
	LSW	90	0:02:40:12
25×50	**TUF**	9	0:0:0:09
	TLF	14	0:0:0:15
	LSW	89	0:02:00:07
50×100	**TUF**	8	0:0:0:26
	TLF	10	0:0:0:33
	LSW	89	0:02:33:40

Comments: The numerical tests carried out show that our approach of upper bound and lower bound functions that we have proposed leads to a very significant reduction in the cost of calculation and an improvement in the result. The number of iterations and the computing time are considerably reduced in the upper bound and lower bound functions in comparison with the line search method.

8 Conclusion

Despite the mathematical development in the field of linear programming, many problems remain to be developed.

For this, in this study, we used a logarithmic barrier method for solving this problem. We proposed a new upper and lower bound functions to compute the displacement step, and we showed that our new technique is efficient in reducing the computational cost in Karmarkar's projective algorithm. This method has made it possible to significantly reduce the number of iterations and the time of their calculation. Numerical simulations confirm the efficiency of our approach.

Our future exciting work is to further improve the computational time of the logarithmic barrier algorithm by proposing more efficient upper and lower bound functions. But extensions would be envisaged to the nonlinear, not necessarily to the linear programming problem.

References

[1] R. T. Rockafellar and R. J. B. Wets. *Variational Analysis*. Springer, Berlin, New York, 1997.

[2] F. R. Gantmacher. *Theory of matrices*. Moscow, Nauka, 1988. [Russian]

[3] M. F. Hassan and E. K. Boukas. Constrained linear quadratic regulator: continuous-time case. *Nonlinear Dynamics and Systems Theory* **8** (1) (2008) 35–42.

[4] R. D. Hill. Inertia theory for simultaneously triangulable complex matrices. *Linear Algebra & Appl.* **2** (1969) 131–142.

[5] M. H. Wright. The interior-point revolution in constrained optimization. In: *High-Performance Algorithms and Software in Nonlinear Optimization* (Eds.: R. DeLeone, A. Murli, P. M. Pardalos and G. Toraldo). Kluwer Academic Publishers, Dordrecht, 1998, 359–381.

[6] V. Nevistic and M. Morari. Constrained control of feedback-linearizable systems. In: *Proc. European Control Conf.* Rome, Italy, 1995, 1726–1731.

Nonlinear Dynamics and Systems Theory, **24** (1) (2024) 80–98

Thermo-Electroelastic Contact Problem with Temperature Dependent Friction Law

A. Oultou [1], O. Baiz [2*] and H. Benaissa [1]

[1] *Sultan Moulay Slimane University, FP of Khouribga.*
[2] *Ibnou Zohr University, FP of Ouarzazate.*

Received: August 12, 2023; Revised: January 28, 2023

Abstract: In this work, we consider a dynamical unilateral contact problem with Coulomb's friction and thermo-electroelastic effects. We focus here on the dynamical effects such as frictional heating and thermal softening at the contact interface. The thermo-electro-elastic constitutive law is assumed to be linear and the foundation is thermally and electrically conductive. We derive a variational formulation of the problem and establish the existence of a weak solution. The proof is based on a suitable combination of the penalty method, standard arguments of variational equations and fixed point theorem.

Keywords: *thermo-electro-elastic materials; dynamic contact problem; frictional heating; variational analysis.*

Mathematics Subject Classification (2010): 47J20, 49Sxx, 70K20, 74F05, 74F15, 74G30, 74M10, 74M15, 93Axx.

1 Introduction

A piezoelectric material is a substance that generates electrical charges when mechanical pressure is applied and mechanically deforms when an electric field is applied. As a result, the piezoelectric material performs the function of a transducer, converting electrical energy into mechanical energy and vice versa. These so-called smart materials, among other things, are used as switches in radio-logic, electric-acoustic, and measuring devices. Piezoelectric materials have been extensively studied, and one natural extension of these coupled electro-mechanical models is to include temperature as an additional state variable to account for thermal effects as well as piezoelectric effects.

* Corresponding author: mailto:othman.baiz@gmail.com

General mathematical models on piezoelectricity were studied in [3,9,13]. Results on static frictional contact problems for piezoelectric materials under the assumption that the foundation is insulated can be found in [5, 11, 16], and these results were extended in [7, 8, 12] in the case of an electrically conductive foundation. In the quasi-static case, we refer to [6,10] and references therein. Moreover, the theory of thermo-piezoelectricity was first proposed by [14], the physical laws and the governing equations for thermo-piezoelectric materials have been explored in [7, 14, 15, 17] and for some recent results on the thermo-piezoelectric contact problem, we refer to [1, 4].

Here, we seek to apply the static/quasi-static instances of our previous studies to a dynamical contact problem with temperature-dependent friction. Heat is produced as a result of the body and foundation sliding against one another through friction. This fact serves as the inspiration for our expansion of the dynamic thermo-electroelastic contact issue, which takes into consideration the effects of thermal softening and frictional heating at the contact surface.

The remainder of the paper is organized as follows. The model of the dynamical frictional contact process between a thermo-electro-viscoelastic body and a conductive deformable foundation is described in Section 2. Section 3 introduces some notations, lists the data assumptions, and derives the variational formulation of the model. The main existence and uniqueness result of the model's weak solution is stated in Theorem 4.1. This theorem is proved in several steps in Section 4, the proof is based on the arguments of compactness, time discretization, and the Banach fixed point theorem.

2 Preliminaries

In this section, we recall some useful definitions and lemmas which will be used in the sequel. Let X be a reflexive Banach space and $\langle\cdot,\cdot\rangle$ denote the duality of X and X^*, we have the following interesting results (see e.g., [2]).

Definition 2.1 A single-valued operator $A : X \to X^*$ is pseudomonotone if

1. A is a bounded, i.e., it maps the bounded sets in X into the bounded sets in X^*,

2. for every sequence $\{x_n\} \subset X$ converging weakly to x of X such that $\limsup_{n\infty}\langle Ax_n, x_n - x\rangle \leq 0$, we have $\langle Ax, x - y\rangle \leq \liminf_{n\infty}\langle Ax_n, x_n - y\rangle$ for all $y \in X$.

Definition 2.2 A multi-valued operator $T : X \to 2^{X^*}$ is pseudo-monotone if

1. for every $v \in V$, the set $Tv \subset X^*$ is nonempty, closed and convex,

2. the operator T is upper semi-continuous from each finite-dimensional subspace of X to X^* endowed with weak topology,

3. for any sequences $\{u_n\} \subset X$ and $\{u_n^*\} \subset X^*$ such that $u_n \to u$ weakly in X, $u_n^* \in Tu_n$ for all n, and $\limsup_{n\infty}\langle u_n^*, u_n - u\rangle \leq 0$, we have that for every $v \in X$, there exists $u^*(v) \in Tu$ such that $\langle u^*(v), u - v\rangle \leq \liminf_{n\infty}\langle u_n^*, u_n - v\rangle$.

Let $(F, \|\cdot\|_F) \subset (G, \|\cdot\|_G)$ be the reflexive Banach spaces such that $\|\cdot\|_F \geq \|\cdot\|_G$ and $\overline{F} = G$, thus, we may write $F \subset G \equiv G' \subset F'$. Suppose that $\mathcal{B}$ is a linear, bounded,

positive and symmetric operator from G to G'. Let $\mathbb{F} = L^2([a,b],F)$, $\mathbb{G} = L^2([a,b],G)$ and define $\mathbb{X} = \{w \in \mathbb{F} : (\mathcal{B}w)' \in \mathbb{F}'\}$ which is a reflexive Banach space for the norm

$$\|w\|_{\mathbb{X}} = \|w\|_F + \|(\mathcal{B}w)'\|_{F'}.$$

Moreover, let $\mathcal{A}(t,\cdot)$ be an operator from F to F', and denote by $\mathcal{A} : \mathbb{F} \to \mathbb{F}'$ its natural extension, given by $\mathcal{A}w(t) = A(t,w(t))$. Assume that

$$\begin{aligned} &\mathcal{A} : \mathbb{X} \to \mathbb{X}' \text{ is pseudo-monotone,} \\ &\mathcal{A} : \mathbb{F} \to \mathbb{F}' \text{ is a bounded operator,} \end{aligned} \tag{1}$$

and for some $\lambda \in \mathbb{R}$, one has

$$\lim_{\|w\|_{\mathbb{F}} + \infty} \frac{\lambda \langle \mathcal{B}w, w\rangle_{\mathbb{G}'\times\mathbb{G}} + \langle \mathcal{A}w, w\rangle_{\mathbb{F}'\times\mathbb{F}}}{\|w\|_{\mathbb{F}}} = \infty. \tag{2}$$

Then the following existence theorem holds, see [18, Theorem 3.1].

Theorem 2.1 *Let $\mathcal{A}$ and $\mathcal{B}$ be defined above. Then, for each $w_0 \in G$ and $\ell \in \mathbb{F}'$, there exists a $w \in \mathbb{X}$ such that*

$$\begin{cases} (\mathcal{B}w)' + \mathcal{A}w = \ell \quad in \quad \mathbb{F}', \\ \mathcal{B}w(0) = \mathcal{B}w_0 \quad in \quad G'. \end{cases}$$

3 Problem Statement and Variational Formulation

We consider an elastic body in the reference configuration $\Omega \subset \mathbb{R}^d$ with the dimension $d = 2, 3$. We are interested in the displacement field $u(x;t)$, the electrical potential $\varphi(x,t)$ and the temperature $\theta(x;t)$ for $(x;t) \in \Omega \times (0;T)$, where $(0;T)$ is the given time interval. For the sake of simplicity, we will omit the dependence of various functions on the spatial variable $x \in \bar{\Omega}$. Hence, the local momentum of balance for stress, electric displacement and heat conduction are given as follows:

$$\begin{aligned} &\ddot{u} - \operatorname{Div}\sigma = f_0 && \text{in } \ \Omega \times (0,T), \\ &\operatorname{div} D = \phi_0 && \text{in } \ \Omega \times (0,T), \\ &\dot{\theta} + \operatorname{div} q = -\mathcal{M}\,\varepsilon(\dot{u}) - \mathcal{P}\,E(\varphi) + q_0 && \text{in } \ \Omega \times (0,T). \end{aligned}$$

Here, the quantities f_0, ϕ_0 and q_0 describe the given body forces, volume electric charge and heat source term, acting on Ω. In the case of linear thermo-visco-piezoelectricity, the stress tensor is given by

$$\sigma = \mathcal{A}\,\varepsilon(\dot{u}) + \mathfrak{F}\,\varepsilon(u) - \mathcal{E}^* E(\varphi) - \mathcal{M}\,\theta \ \text{ in } \ \Omega \times (0,T),$$

where $\mathcal{A}$ is the linear viscosity operator, $\mathfrak{F} = (f_{ijkl})$ is the linear elasticity operator, $\varepsilon(u)$ is the linearized strain tensor, $E(\varphi) = -\nabla\varphi$ is the electric field, $\mathcal{E} = (e_{ijk})$ is the third-order piezoelectric tensor and $\mathcal{E}^* = (e_{kij})$ is its transpose, $\mathcal{M} = (m_{ij})$ is the thermal expansion tensor. Moreover, the electric displacement and the heat flux are defined by

$$\begin{aligned} &D = \mathcal{E}\,\varepsilon(u) + \beta\,E(\varphi) + \mathcal{P}^*\,\theta && \text{in } \ \Omega \times (0,T), \\ &q = -\mathcal{K}\,\nabla\theta && \text{in } \ \Omega \times (0,T), \end{aligned}$$

where $\beta = (\beta_{ij})$ is the electric permittivity tensor, $\mathcal{P} = (p_i)$ and $\mathcal{K} = (k_{ij})$ are the thermal expansion and thermal conductivity tensors.

Recall that $\mathbb{S}^d$ is the space of second order symmetric tensors on $\mathbb{R}^d$. The canonical inner products and associated norms on $\mathbb{R}^d$ and $\mathbb{S}^d$ are given by

$$\begin{aligned} &\forall\, u,\, v \in \mathbb{R}^d, \quad u \cdot v = u_i\, v_i \qquad ; \quad \forall\, \sigma,\, \tau \in \mathbb{S}^d, \quad \sigma \cdot \tau = \sigma_{ij}\, \tau_{ij}, \\ &\forall\, u,\, v \in \mathbb{R}^d, \quad \|v\| = (v \cdot v)^{\frac{1}{2}} \quad ; \quad \forall\, \sigma,\, \tau \in \mathbb{S}^d, \quad \|\tau\| = (\tau \cdot \tau)^{\frac{1}{2}}. \end{aligned}$$

If ν is the outward unit normal vector on the boundary $\Gamma = \partial\Omega$, then the normal and tangential components of the displacement vector v and the stress field σ on Γ are

$$v_\nu = v \cdot \nu\ ,\ v_\tau = v - v_\nu\, \nu \quad \text{and} \quad \sigma_\nu = \sigma\, \nu \cdot \nu\ ,\ \sigma_\tau = \sigma\, \nu - \sigma_\nu\, \nu.$$

In order to formulate the boundary conditions and the initial boundary values, we divide the boundary Γ into three disjoint open subsets Γ_D, Γ_N and Γ_C such that $\overline{\Gamma}_D \cup \overline{\Gamma}_N \cup \overline{\Gamma}_C = \overline{\Gamma}$. We also assume that $\Gamma_D \cup \Gamma_N$ is partitioned into two disjoint open parts Γ_a and Γ_b of nonzero measure such that $\overline{\Gamma}_D \cup \overline{\Gamma}_N = \overline{\Gamma}_a \cup \overline{\Gamma}_b$. We assume that the body is clamped on $\Gamma_D \times (0,T)$, the surface traction of density f_N acts on $\Gamma_N \times (0,T)$, the electrical potential vanishes on $\Gamma_a \times (0,T)$, the surface electric charge of density ϕ_b acts on $\Gamma_b \times (0,T)$ and the temperature is assumed to be zero on $\Gamma_D \cup \Gamma_N \times (0,T)$. Therefore, we have

$$\begin{aligned} &u = 0 && \text{on } \ \Gamma_D \times (0,T), \\ &\sigma\, \nu = f_N && \text{on } \ \Gamma_N \times (0,T), \\ &\varphi = 0 && \text{on } \ \Gamma_a \times (0,T), \\ &D \cdot \nu = \phi_b && \text{on } \ \Gamma_b \times (0,T), \\ &\theta = 0 && \text{on } \ \Gamma_D \cup \Gamma_N \times (0,T). \end{aligned}$$

On the contact surface Γ_C, the body is supposed to be in unilateral contact with a rigid foundation by Coulomb's friction law

$$\sigma_\nu(u,\varphi,\theta) \le 0\,,\ (u_\nu - g) \le 0\,,\ \sigma_\nu(u,\varphi,\theta)\,(u_\nu - g) = 0 \quad \text{on } \ \Gamma_C \times (0,T),$$

$$\begin{cases} \|\sigma_\tau\| \le \mu(\theta)\,|R\sigma_\nu| & \\ \|\sigma_\tau\| < \mu(\theta)\,|R\sigma_\nu| \implies [\dot{u}]_\tau = 0 & \text{on } \ \Gamma_C \times (0,T), \\ \|\sigma_\tau\| = \mu(\theta)\,|R\sigma_\nu| \implies \exists\, \lambda \in \mathbb{R},\ \sigma_\tau = -\lambda^2\, \dot{u}_\tau, & \end{cases}$$

where for the temperature dependent coefficient of friction $\mu(\theta) \ge 0$, we use

$$\mu(\theta) = \mu_0\, \frac{[\theta - \theta_d]^2}{[\theta_d - \theta_f]^2},$$

where μ_0 is the static coefficient of friction at the given reference temperature θ_f and θ_d is a damage temperature on the interface. Temperature θ_d is related to the temperature at which frictional stress is no longer due to the solid shearing effects, but is generated by the viscous shear of a molten film on the contact interface. It can be taken as the lowest melting temperature of the body and the foundation in contact. Since $\theta < \theta_d$, we have $\mu'(\theta_d) \le 0$ and $\lim\limits_{\theta_d} \mu(\theta) = 0$. Therefore this equation shows a thermal softening effect. Moreover, the thermal and electrical flow conditions on the contact zone are given by

$$|D \cdot \nu| \le k\,, \quad |D \cdot \nu| = k\frac{\varphi}{|\varphi|} \ \text{ if } \ \varphi \ne 0 \quad \text{on } \ \Gamma_C \times (0,T).$$

This condition represents the electric condition on the contact surface and we assume them by analogy with Tresca's friction law, where k is a given positive function, the electric conductivity coefficient

$$q \cdot \nu = k_c(u_\nu - g)\,\phi_L(\theta - \theta_F) \quad \text{on} \quad \Gamma_C \times (0,T),$$

describes the heat balance on the contact interface, where ϕ_L is the truncation function, k_c represents the thermal conductance function that is supposed such that

$$\phi_L(s) = \begin{cases} -L & \text{if } s < -L \\ s & \text{if } -L \le s \le L \\ L & \text{if } s > L \end{cases}, \quad k_c(r) = \begin{cases} k_c(r) = 0 & \text{if } r < 0, \\ \\ k_c(r) > 0 & \text{if } r \ge 0, \end{cases}$$

where $L > 0$ is a sufficiently large constant. Finally, we denote by u_0, v_0, φ_0 and θ_0 the initial displacement, initial velocity, initial potential and initial temperature, respectively. We collect the above relations to obtain the following mathematical model.

Problem (P) : *Find a displacement* $u : \Omega \times [0,T] \to \mathbb{R}^d$, *an electric potential* $\varphi : \Omega \times [0,T] \to \mathbb{R}$ *and a temperature* $\theta : \Omega \times [0,T] \to \mathbb{R}$ *such that*

$$\sigma = \mathcal{A}\,\varepsilon(\dot u) + \mathcal{F}\,\varepsilon(u) - \mathcal{E}^* E(\varphi) - \mathcal{M}\,\theta \quad \text{in } \Omega \times (0,T), \tag{3}$$

$$D = \mathcal{E}\,\varepsilon(u) + \beta\,E(\varphi) + \mathcal{P}\,\theta \quad \text{in } \Omega \times (0,T), \tag{4}$$

$$q = -\mathcal{K}\,\nabla\theta \quad \text{in } \Omega \times (0,T), \tag{5}$$

$$\ddot u - \operatorname{Div}\sigma = f_0 \quad \text{in } \Omega \times (0,T), \tag{6}$$

$$\operatorname{div} D = \phi_0 \quad \text{in } \Omega \times (0,T), \tag{7}$$

$$\dot\theta + \operatorname{div} q = -\mathcal{M}^*\,\varepsilon(\dot u) - \mathcal{N}\,E(\varphi) + q_0 \quad \text{in } \Omega \times (0,T), \tag{8}$$

$$u = 0 \quad \text{on } \Gamma_D \times (0,T), \tag{9}$$

$$\sigma\nu = f_2 \quad \text{on } \Gamma_N \times (0,T), \tag{10}$$

$$\sigma_\nu(u,\varphi,\theta) \le 0\ ,\ (u_\nu - g) \le 0\ ,\ \sigma_\nu(u,\varphi,\theta)\,(u_\nu - g) = 0 \quad \text{on } \Gamma_C \times (0,T), \tag{11}$$

$$\begin{cases} \|\sigma_\tau\| \le \mu(\theta)\,|R\sigma_\nu| \\ \|\sigma_\tau\| < \mu(\theta)\,|R\sigma_\nu| \implies [\dot u]_\tau = 0 \\ \|\sigma_\tau\| = \mu(\theta)\,|R\sigma_\nu| \implies \exists\,\lambda \in \mathbb{R},\ \sigma_\tau = -\lambda^2\,[\dot u]_\tau \end{cases} \quad \text{on } \Gamma_C \times (0,T), \tag{12}$$

$$\varphi = 0 \quad \text{on } \Gamma_a \times (0,T), \tag{13}$$

$$D \cdot \nu = q_2 \quad \text{on } \Gamma_b \times (0,T), \tag{14}$$

$$|D \cdot \nu| \le k\ ,\ \ |D \cdot \nu| = k\frac{\varphi}{|\varphi|} \ \text{ if } \ \varphi \ne 0 \quad \text{on } \Gamma_C \times (0,T), \tag{15}$$

$$\theta = 0 \quad \text{on } \Gamma_D \cup \Gamma_N \times (0,T), \tag{16}$$

$$q \cdot \nu = k_c(u_\nu - g)\,\phi_L(\theta - \theta_F) \quad \text{on } \Gamma_C \times (0,T), \tag{17}$$

$$u(\cdot,0) = u_0\ ,\ \ \dot u(\cdot,0) = v_0\ ,\ \ \theta(\cdot,0) = \theta_0 \quad \text{in } \Omega. \tag{18}$$

To derive the weak formulation of Problem P, we introduce the following spaces:

$$H = L^2(\Omega)^d\,,\ \ \mathcal{H} = \{\tau = (\tau_{ij})\,,\ \tau_{ij} = \tau_{ji} \in L^2(\Omega)\},$$
$$H_1 = H^1(\Omega)^d\,,\ \ \mathcal{H}_1 = \{\sigma \in \mathcal{H}\,,\ \operatorname{Div}\sigma \in H\},$$

which are the real Hilbert spaces for the associated Euclidean norms to the inner products

$$(u,v)_H = \int_\Omega u_i v_i \, dx \ , \quad (u,v)_{H_1} = (u,v)_H + (\varepsilon(u),\varepsilon(v))_{\mathcal{H}},$$
$$(\sigma,\tau)_{\mathcal{H}} = \int_\Omega \sigma_{ij}\tau_{ij} \, dx \ , \quad (\sigma,\tau)_{\mathcal{H}_1} = (\sigma,\tau)_{\mathcal{H}} + (\mathrm{Div}\,\sigma,\mathrm{Div}\,\tau)_{\mathcal{H}}.$$

Keeping in mind (9), (13) and (16), we define the following variational subspaces:

$$V = \{v \in H_1 \ , \ v = 0 \ \text{ on } \ \Gamma_D\},$$
$$W = \{\psi \in H^1(\Omega) \ , \ \psi = 0 \ \text{ on } \ \Gamma_a\},$$
$$Q = \{\eta \in H^1(\Omega), \ \eta = 0 \ \text{ on } \ \Gamma_D \cup \Gamma_N\}.$$

Over spaces V, Q and W, we use the following inner products and norms given by

$$(u,v)_V = (\varepsilon(u),\varepsilon(v))_{\mathcal{H}} \, , \quad \|u\|_V = (u,u)_V^{1/2}, \quad \forall\, u,\, v \in V, \tag{19}$$
$$(\varphi,\psi)_W = (\nabla\varphi,\nabla\psi)_H \, , \quad \|\varphi\|_W = (\varphi,\varphi)_W^{1/2}, \quad \forall\, \varphi,\, \psi \in W, \tag{20}$$
$$(\theta,\eta)_Q = (\nabla\theta,\nabla\eta)_H \, , \quad \|\theta\|_Q = (\theta,\theta)_Q^{1/2}, \quad \forall\, \theta,\, \eta \in Q. \tag{21}$$

Since V is a closed subspace of the Hilbert space H_1, and $meas(\Gamma_1) > 0$, Korn's inequality holds, then there exists a constant $c_k > 0$ depending only on Ω and Γ_1 such that

$$\|\varepsilon(v)\|_{\mathcal{H}} \geq \, c_k \, \|v\|_{H_1}, \quad \forall\, v \in V. \tag{22}$$

Then the norms $\|\cdot\|_{H_1}$ and $\|\cdot\|_V$ are equivalent on V and therefore $(V, \|\cdot\|_V)$ is a real Hilbert space. Moreover, by the Sobolev trace theorem, there exists a constant $c_0 > 0$ depending only on Ω, Γ_C and Γ_D such that

$$\|v\|_{L^2(\Gamma)^d} \leq c_0 \, \|v\|_V, \quad \forall\, v \in V. \tag{23}$$

Since $meas(\Gamma_a) > 0$, the Friedrichs-Poincaré inequality holds and thus

$$\|\nabla\psi\|_H \geq c_F \|\psi\|_{H^1(\Omega)}, \quad \forall\, \psi \in W, \tag{24}$$

where $c_F > 0$ is a constant which depends only on Ω and Γ_a. It follows from (20) and (24) that $\|\cdot\|_W$ and $\|\cdot\|_{H^1(\Omega)}$ are equivalent norms on W and then $(W, \|\cdot\|_W)$ is a real Hilbert space. The Sobolev trace theorem implies that there exists $c_1 > 0$ depending on Ω, Γ_a and Γ_C such that

$$\|\xi\|_{L^2(\Gamma_C)} \leq c_1 \, \|\xi\|_W, \quad \forall\, \xi \in W. \tag{25}$$

In an analogous way, we can get that $\|\cdot\|_Q$ and $\|\cdot\|_{H^1(\Omega)}$ are equivalent norms on Q and then $(Q, \|\cdot\|_Q)$ is a real Hilbert space. Using the Sobolev trace theorem, we obtain that there exists a constant $c_2 > 0$ depending only on Ω, Γ_D, Γ_N and Γ_C such that

$$\|\eta\|_{L^2(\Gamma)} \leq c_2 \, \|\eta\|_Q, \quad \forall\, \eta \in Q. \tag{26}$$

For a real Banach space $(X, \|\cdot\|_X)$, we denote by X' the dual space of X and by $\langle\cdot,\cdot\rangle_{X'\times X}$ the duality pairing between X' and X. We consider the following standard Bochner-Lebesgue function spaces:

$$\mathbb{H} = L^2([0,T],H) \, , \ \mathbb{V} = L^2([0,T],V) \, , \ \mathbb{W} = L^2([0,T],W) \, , \ \mathbb{Q} = L^2([0,T],Q). \tag{27}$$

The notations $\|.\|_{\mathbb{H}}$, $\|.\|_{\mathbb{V}}$, $\|.\|_{\mathbb{W}}$ and $\|.\|_{\mathbb{Q}}$ stand for the norms of $\mathbb{H}$, $\mathbb{V}$, $\mathbb{Q}$ and $\mathbb{W}$, respectively. We also denote by $\langle .,. \rangle$ the duality pairing between V' and V or W' and W or Q' and Q , as the meaning is evident from the context.

To solve the mechanical problem (3)-(18), we need the following assumptions.

$\underline{A_1}$: (a) The elasticity and the viscosity tensors $\mathfrak{F}, \mathcal{A} : \Omega \times \mathbb{S}^d \to \mathbb{S}^d$, the electric permittivity and the thermal conductivity tensors $\beta, \mathcal{K} : \Omega \times \mathbb{R}^d \to \mathbb{R}^d$ satisfy

$$\mathfrak{F}_{ijkl} = \mathfrak{F}_{klij} = \mathfrak{F}_{jikl} \in L^\infty(\Omega)\ , \quad \beta_{ij} = \beta_{ji} \in L^\infty(\Omega),$$
$$\mathcal{A}_{ijkl} = \mathcal{A}_{jikl} = \mathcal{A}_{lkij} \in L^\infty(\Omega)\ , \quad \mathcal{K}_{ij} = \mathcal{K}_{ji} \in L^\infty(\Omega),$$

(b) There exist positive constants $m_{\mathcal{F}}$, $m_{\mathcal{A}}$, m_β and $m_{\mathcal{K}}$ such that

$$\mathcal{F}_{ijkl}(x)\,\xi_{ij}\xi_{kl} \geq m_{\mathcal{F}}\,\|\xi\|^2\ , \quad \mathcal{A}_{ijkl}(x)\,\xi_{ij}\xi_{kl} \geq m_{\mathcal{A}}\,\|\xi\|^2, \quad \forall\, \xi = (\xi_{ij}) \in \mathbb{S}^d,$$
$$\beta_{ij}(x)\,\zeta_i\zeta_j \geq m_\beta\,\|\zeta\|^2\ , \quad \mathcal{K}_{ij}(x)\,\zeta_i\zeta_j \geq m_{\mathcal{K}}\,\|\zeta\|^2, \quad \forall\, \zeta = (\zeta_i) \in \mathbb{R}^d.$$

Under the previous assumptions, the following constants are well-defined:

$$M_{\mathfrak{F}} = \sup_{ijkl} \|\mathfrak{F}_{ijkl}\|_{L^\infty(\Omega)}\ , \quad M_\beta = \sup_{ij} \|\beta_{ij}\|_{L^\infty(\Omega)},$$
$$M_{\mathcal{A}} = \sup_{ijkl} \|\mathcal{A}_{ijkl}\|_{L^\infty(\Omega)}\ , \quad M_{\mathcal{K}} = \sup_{ij} \|\mathcal{K}_{ij}\|_{L^\infty(\Omega)}.$$

$\underline{A_2}$: The piezoelectric tensor $\mathcal{E} : \Omega \times \mathbb{S}^d \to \mathbb{R}^d$, the pyroelectric tensor $\mathcal{P} : \Omega \times \mathbb{R} \to \mathbb{R}^d$, the thermal expansion tensor $\mathcal{M} : \Omega \times \mathbb{R} \to \mathbb{R}^d$ and the tensors $\mathcal{N} : \Omega \times \mathbb{R}^d \to \mathbb{R}$ satisfy the following properties:

$$\mathcal{E}_{ijk} = \mathcal{E}_{ikj} \in L^\infty(\Omega)\,,\ \mathcal{M}_{ij} = \mathcal{M}_{ji} \in L^\infty(\Omega)\,,\ \mathcal{P}_i \in L^\infty(\Omega)\,,\ \mathcal{N}_i \in L^\infty(\Omega).$$

Under the previous assumptions, the following constants are well-defined:

$$M_{\mathcal{E}} = \sup_{ijk} \|\mathcal{E}_{ijk}\|_{L^\infty(\Omega)}\ , \quad M_{\mathcal{M}} = \sup_{ij} \|\mathcal{M}_{ij}\|_{L^\infty(\Omega)},$$
$$M_{\mathcal{P}} = \sup_{i} \|\mathcal{P}_i\|_{L^\infty(\Omega)}\ , \quad M_{\mathcal{N}} = \sup_{i} \|\mathcal{N}_i\|_{L^\infty(\Omega)}.$$

$\underline{A_3}$: The friction coefficient $\mu : \Gamma_C \times \mathbb{R} \to \mathbb{R}^+$ satisfies

(a) $\exists\, \mu^* > 0$ such that $|\mu(x,u)| \leq \mu^*,\ \forall\, u \in \mathbb{R},$ a.e. $x \in \Gamma_C$,

(b) $\exists\, L_\mu > 0$ such that, for all $u, v \in \mathbb{R}$, one has

$$|\mu(x,u) - \mu(x,v)| \leq L_\mu |u - v|,\ \text{ a.e. } x \in \Gamma_C,$$

(c) $x \mapsto \mu(x,u)$ is measurable on Γ_C for all $u \in \mathbb{R}$.

$\underline{A_4}$: The function $k_c : \Gamma_C \times \mathbb{R} \to \mathbb{R}_+$ satisfies

(a) $\exists\, M_{k_c} > 0$ such that $|k_c(x,u)| \leq M_{k_c},\ \forall\, u \in \mathbb{R},$ a.e. $x \in \Gamma_C$,

(b) $\exists\, L_{k_c} > 0$ such that, for all u, $v \in \mathbb{R}$, one has

$$|k_c(x,u) - k_c(x,v)| \leq L_{k_c} |u - v|,\ \text{ a.e. } x \in \Gamma_C,$$

(c) $\mapsto k_c(x,u)$ is measurable on Γ_C for all $u \in \mathbb{R}$.

$\underline{A_5}$: The truncation function $\varphi_L : \Gamma_C \times \mathbb{R} \to \mathbb{R}$ satisfies

(a) $(\varphi_L(s_1) - \varphi_L(s_2))(s_1 - s_2) \geq 0$ for all $s_1, s_2 \in \mathbb{R}$ a.e. $x \in \Gamma_C$,

(b) $\exists\, L_\varphi > 0$ such that, for all $s_1, s_2 \in \mathbb{R}$, one has

$$|\varphi_L(x,s_1) - \varphi_L(x,s_2)| \leq L_\varphi\, |s_1 - s_2| \text{ a.e. } x \in \Gamma_C,$$

(c) $\exists\, M_\varphi > 0$ such that $|\varphi_L(x,s)| \leq M_\varphi,\ \forall\, s \in \mathbb{R}$ a.e. $x \in \Gamma_C$

(d) $x \mapsto \varphi_L(x,s)$ is measurable on Γ_C for all $s \in \mathbb{R}$.

$\underline{A_6}$: The function $R : H^{-\frac{1}{2}}(\Gamma_C) \to L^\infty(\Gamma_C)$ is bounded and Lipschitz continuous, i.e.,

(a) $\exists\, L_R > 0$ such that for all $s_1,\ s_2 \in H^{-\frac{1}{2}}(\Gamma_C)$, we have

$$\|Rs_1 - Rs_2\|_{L^\infty(\Gamma_C)} \leq L_R\, \|s_1 - s_2\|_{H^{\frac{1}{2}}(\Gamma_C)},$$

(b) $\exists\, M_R > 0$ such that for all $s \in H^{-\frac{1}{2}}(\Gamma_C)$, we have $\|Rs\|_{L^\infty(\Gamma_C)} \leq M_R$.

$\underline{A_7}$: The given forces, charge densities and heat sources satisfy the below regularity

(a) $f_0 \in L^2([0,T], L^2(\Omega)^d)$, $f_2 \in L^2([0,T]; L^2(\Gamma_N)^d)$, $g \in L^2(\Gamma_C)$,

(b) $\phi_0 \in L^2([0,T]; L^2(\Omega))$, $q_2 \in L^2([0,T]; L^2(\Gamma_b))$, $\varphi_f \in L^2([0,T], L^2(\Gamma_C))$.

$\underline{A_8}$: The initial data satisfy $u_0 \in V$, $v_0 \in V$, $\varphi_0 \in W$ and $\theta_0 \in Q$.

We move now to deriving the weak formulation of the problem (3)-(18). To this end, we assume that $(u, \sigma, \varphi, \theta)$ are smooth functions which solve (3)-(18), by invoking standard Green's formula, we obtain the following weak formulation of Problem (P).

Problem (PV) : *Find a displacement $u \in \mathbb{V}$, an electric potential $\varphi \in \mathbb{W}$, and a temperature $\theta \in \mathbb{Q}$ such that*

$$\begin{aligned}
&\langle \ddot{u}, v - \dot{u}\rangle_H + \langle \mathcal{A}\varepsilon(\dot{u}), \varepsilon(v - \dot{u})\rangle_{\mathcal{H}} + \langle \mathcal{F}\varepsilon(u), \varepsilon(v - \dot{u})\rangle_{\mathcal{H}} \\
&- \langle \mathcal{E}^* E(\varphi), \varepsilon(v - \dot{u})\rangle_H - \langle \mathcal{M}\theta, \varepsilon(v - \dot{u})\rangle_H + \int_{\Gamma_C} \mu(\theta)|R\sigma_\nu| \cdot (|v_\tau| - |\dot{u}_\tau|)\, da \\
&\geq \langle f_0, v - \dot{u}\rangle_H + \langle f_N, v - \dot{u}\rangle_{L^2(\Gamma_N)}, \quad \forall\, v \in \mathbb{V},
\end{aligned} \tag{28}$$

$$\begin{aligned}
&\langle \beta\nabla\varphi, \nabla\varphi - \nabla\psi\rangle_H - \langle \mathcal{E}\varepsilon(u), \nabla\varphi - \nabla\psi\rangle_H - \langle \mathcal{P}\theta, \nabla\varphi - \nabla\psi\rangle_H \\
&+ \int_{\Gamma_C} k \cdot (|\varphi| - |\psi|)\, da \geq \langle \phi_0, \varphi - \psi\rangle_H + \langle q_2, \varphi - \psi\rangle_{L^2(\Gamma_N)}, \quad \forall \psi \in \mathbb{W},
\end{aligned} \tag{29}$$

$$\begin{aligned}
&\langle \dot{\theta}, \theta - \eta\rangle_H + \langle \mathcal{K}\nabla\theta, \nabla\theta - \nabla\eta\rangle_H + \langle \mathcal{N}\varphi, \nabla\theta - \nabla\eta\rangle_H - \langle \mathcal{M}^*\varepsilon(\dot{u}), \nabla\theta - \nabla\eta\rangle_H \\
&+ \int_{\Gamma_C} k_c(u_\nu - g)\varphi_L(\theta - \theta_f) \cdot (\eta - \theta)\, da = \langle q_0, \eta - \theta\rangle_H, \quad \forall \eta \in \mathbb{Q}.
\end{aligned} \tag{30}$$

4 Existence and Uniqueness Result

In this section, we will prove the existence and uniqueness of the solution of the previous contact problem, by using the penalty method and intermediate problem. We first rewrite the variational formulation in abstract form. For this purpose, we consider the operators $A,\ F \in \mathcal{L}(\mathbb{V},\mathbb{V}^*)$, $B \in \mathcal{L}(\mathbb{W},\mathbb{W}^*)$, $K \in \mathcal{L}(\mathbb{Q},\mathbb{Q}^*)$, $E_1 \in \mathcal{L}(\mathbb{W},\mathbb{V}^*)$, $M_1 \in \mathcal{L}(\mathbb{Q},\mathbb{V}^*)$, $M_2 \in \mathcal{L}(\mathbb{V},\mathbb{Q}^*)$, $N \in \mathcal{L}(\mathbb{W},\mathbb{Q}^*)$, $E_2 \in \mathcal{L}(\mathbb{V},\mathbb{W}^*)$ and $P \in \mathcal{L}(\mathbb{Q},\mathbb{W}^*)$ defined as follows:

$$\begin{aligned}
&\langle Au,v\rangle = (\mathcal{A}\,\varepsilon(u),\varepsilon(v))_{\mathcal{H}}\,,\ \langle Fu,v\rangle = (\mathfrak{F}\varepsilon(u),\varepsilon(v))_{\mathcal{H}}\,,\ \langle E_1\varphi,v\rangle = (\mathcal{E}^*\nabla\varphi,\varepsilon(v))_H,\\
&\langle M_1\theta,v\rangle = (\mathcal{M}\theta,\varepsilon(v))_H\,,\ \langle B\varphi,\xi\rangle = (\beta\nabla\varphi,\nabla\xi)_H\,,\ \langle E_2u,\xi\rangle = (\mathcal{E}\varepsilon(u),\nabla\xi)_H,\\
&\langle P\theta,\xi\rangle = (\mathcal{P}\theta,\nabla\xi)_H\,,\ \langle K\theta,\eta\rangle = (\mathcal{K}\nabla\theta,\nabla\eta)_H\,,\ \langle M_2u,\eta\rangle = (\mathcal{M}^*\varepsilon(u),\eta)_H,\\
&\langle N\varphi,\eta\rangle = (\mathcal{N}\nabla\varphi,\eta)_H.
\end{aligned} \tag{31}$$

We next introduce the friction functional $j_1 : Q \times H^{-1/2} \times V \to \mathbb{R}$, the thermal and electrical transfer functional $j_2 : W \to \mathbb{R}$ and $h_c : V \times Q \to Q'$, respectively defined by

$$j_1(\theta,s,v) = \int_0^T \int_{\Gamma_C} \mu(\theta)\,|Rs|\cdot|v_\tau|\,da\,dt, \quad \forall v \in V, \tag{32}$$

$$j_2(\varphi) = \int_0^T \int_{\Gamma_C} k\ |\varphi|\,da\,dt, \quad \forall \eta \in W, \tag{33}$$

$$\langle h_c(u,\theta),\eta\rangle = \int_{\Gamma_C} k_c(u_\nu - g)\,\varphi_L(\theta-\theta_f)\cdot\eta\ da, \quad \forall \eta \in Q. \tag{34}$$

By Riesz's representation theorem, there exist $f \in \mathbb{V}'$, $q_e \in \mathbb{W}'$ and $\Theta \in \mathbb{Q}'$ such that

$$\langle f,v\rangle_{\mathbb{V}'\times V} = \int_0^T \int_\Omega f_0(t)\cdot v\,dx\,dt + \int_0^T \int_{\Gamma_N} f_2(t)\cdot v\,da\,dt, \quad \forall\, v \in V, \tag{35}$$

$$\langle q_e,\xi\rangle_{\mathbb{W}'\times W} = \int_0^T \int_\Omega \phi_0(t)\cdot\xi\,dx\,dt - \int_0^T \int_{\Gamma_b} q_2(t)\cdot\xi\,da\,dt, \quad \forall\,\xi \in W, \tag{36}$$

$$\langle \Theta,\eta\rangle_{\mathbb{Q}'\times Q} = \int_0^T \int_\Omega q_0(t)\cdot\eta\,dx\,dt, \quad \forall\,\eta \in Q. \tag{37}$$

Then, Problem $(\mathcal{PV})$ can be formulated in the following abstract form.

Problem $(\mathcal{PV}^1)$**:** Find $u \in \mathbb{V}$, $\varphi \in \mathbb{W}$, and $\theta \in \mathbb{Q}$ such that

$$\ddot{u} \in \mathbb{V}^*,\ \dot{u} \in \mathbb{V}\,,\ \dot{\theta} \in \mathbb{Q}, \tag{38}$$

$$f \in \ddot{u} + A\dot{u} + Fu + E_1\varphi - M_1\theta + \partial_3 j_1(\theta,\sigma_\nu,\dot{u}) \ \text{ in } \ \mathbb{V}^*, \tag{39}$$

$$q_e \in B\varphi - E_2u - P\theta + \partial j_2(\varphi) \ \text{ in } \ \mathbb{W}^*, \tag{40}$$

$$\dot{\theta} + K\theta + N\varphi - M_2\dot{u} + h_c(u,\theta) = \Theta \qquad \text{in } \mathbb{Q}^*, \tag{41}$$

$$u(\cdot,0) = u_0\,,\ \dot{u}(\cdot,0) = v_0\,,\ \theta(\cdot,0) = \theta_0 \ \text{ in } \ \Omega, \tag{42}$$

where $\partial_3 j_1(\theta,s,v)$ denotes the partial sub-differential with respect to v of $j_1(\theta,s,v)$, and $\partial j_2(\varphi)$ for the partial sub-differential with respect to φ of $j_2(\varphi)$.

We are now able to state the following existence and uniqueness result.

Theorem 4.1 *Suppose assumptions* (A_1)-(A_8) *hold. Then Problem* $(\mathcal{PV}^1)$ *has at least one solution* $(u, \varphi, \theta) \in \mathbb{V} \times \mathbb{W} \times \mathbb{Q}$.

Proof. The proof is based on the arguments from the theory of multi-valued pseudo-monotone operators and the fixed point theorem. It consists of two steps. First, let $\zeta = (\zeta_1, \zeta_2) \in L^2(0,T; L^2(\Gamma_3) \times V)$ be a given function, we consider the mappings

$$j^1_\zeta(v) := \int_0^T \int_{\Gamma_C} \zeta_1(t)\, |v_\tau|\, da\, dt, \quad \forall v \in V, \tag{43}$$

$$\langle h_c(\theta_\zeta), \eta \rangle := \int_{\Gamma_C} \zeta_2(s) \varphi_L (\theta_\zeta - \theta_f) \cdot \eta\, da, \quad \forall \eta \in Q. \tag{44}$$

Then, for any given $\xi \in L^2(0,T; L^2(\Gamma_C) \times V)$, we consider the intermediate problem.

Problem $(\mathcal{PV}^1_\zeta)$**:** Find $u_\zeta \in \mathbb{V}$, $\varphi_\zeta \in \mathbb{W}$ and $\theta_\zeta \in \mathbb{Q}$ such that

$$\ddot{u}_\zeta \in \mathbb{V}',\ \dot{u}_\zeta \in \mathbb{V},\ \dot{\theta}_\zeta \in \mathbb{Q}', \tag{45}$$

$$f \in \ddot{u}_\zeta + A\,\dot{u}_\zeta + F u_\zeta + E_1 \varphi_\zeta - M_1 \theta_\zeta + \partial j^1_\zeta(\dot{u}_\zeta) \quad \text{in} \quad \mathbb{V}', \tag{46}$$

$$q_e \in B\varphi_\zeta - E_2 u_\zeta - P\theta_\zeta + \partial j_2(\varphi_\zeta) \qquad \text{in} \quad \mathbb{W}', \tag{47}$$

$$\dot{\theta}_\zeta + K\theta_\zeta + N\varphi_\zeta - M_2 \dot{u}_\zeta + h_c(\theta_\zeta) = \Theta \qquad \text{in} \quad \mathbb{Q}', \tag{48}$$

$$u_\zeta(\cdot, 0) = u_0,\ \dot{u}_\zeta(\cdot, 0) = v_0,\ \theta_\zeta(\cdot, 0) = \theta_0 \qquad \text{in} \quad \Omega. \tag{49}$$

Lemma 4.1 *Assume* (A_1)-(A_2), (A_4)-(A_5) *and* (A_7)-(A_8) *hold. Then, for any given* $\zeta = (\zeta_1, \zeta_2) \in L^2(0,T; L^2(\Gamma_C) \times V)$, *Problem* $(\mathcal{PV}^1_\zeta)$ *admits a unique solution* $(u_\zeta, \varphi_\zeta, \theta_\zeta)$.

Proof. The proof of Lemma 4.1 will be carried out by considering a sequence of regularized approximations to problem (PV_ζ), and the solution of this problem is the limit of the regularized problem. To this end, let $\{\psi^h\}_{h>0}$ be a sequence of positive convex functions of $C^1(\mathbb{R}^d)$ which approximate the inner product $|\cdot|_{\mathbb{R}^d}$, and satisfy for any $h > 0$, the following conditions:

$$|\nabla \psi^h(s)| \le 2\ ,\ 0 \le \langle \nabla \psi^h(s), s \rangle\ ,\ \big|\nabla \psi^h(s) - |s|\,\big| \le s, \quad \forall\, s \in \mathbb{R}^d. \tag{50}$$

We next consider the operator $J^h_\zeta : V \to V$ defined as follows:

$$(J^h_{\zeta(t)} v, w)_V := \int_{\Gamma_C} \zeta_1(t) \nabla \psi^h(v_\tau) \cdot w_\tau\, da, \quad \forall\, v \in V. \tag{51}$$

We then approximate the functional j_2 by a family of regularized functions $J^h_2 : V \to R$, depending on $h > 0$, given for all $v \in V$, by

$$J^h_2(\varphi) = \int_{\Gamma_C} \sqrt{|\varphi|^2 + h}\, da. \tag{52}$$

The functional J^h_2 is Gateaux-differentiable and its derivative J^h_2 is defined as follows:

$$\langle J^h_2 \varphi, \xi \rangle = \int_{\Gamma_3} \frac{\varphi\, \xi}{\sqrt{|\varphi|^2 + h}}\, da, \quad \forall\, v \in V. \tag{53}$$

Let $R_e : V \to V'$ be a Riesz isomorphism, i.e., $u \mapsto \ell_u$, where $\ell_u(v) = \langle u, x\rangle$. Next, for each $h > 0$, we consider the following regularized problem.

Problem $(\mathcal{PV}_\zeta^{1h})$**:** Find $\omega_\zeta^h \in \mathbb{V}$, $u_\zeta^h \in \mathbb{V}$, $\varphi_\zeta^h \in \mathbb{W}$ and $\theta_\zeta^h \in \mathbb{Q}$ such that

$$\dot{\omega}_\zeta^h \in \mathbb{V}', \quad \dot{\theta}_\zeta^h \in \mathbb{Q}', \tag{54}$$

$$\dot{\omega}_\zeta^h + A\,\omega_\zeta^h + F u_\zeta^h + E_1\varphi_\zeta^h - M_1\theta_\zeta^h + J_\zeta^h\omega_\zeta^h = f \ \text{ in } \ \mathbb{V}', \tag{55}$$

$$B\varphi_\zeta^h - E_2 u_\zeta^h - P\theta_\zeta^h + J_2^h\varphi_\zeta^h = q_e \ \text{ in } \ \mathbb{W}', \tag{56}$$

$$\dot{\theta}_\zeta^h + K\theta_\zeta^h + N\varphi_\zeta^h - M_2\omega_\zeta^h + h_c(\theta_\zeta^h) = \Theta \ \text{ in } \ \mathbb{Q}', \tag{57}$$

$$R_e\dot{u}_\zeta^h - R_e\omega_\zeta^h = 0 \ \text{ in } \ \mathbb{V}', \tag{58}$$

$$u_\zeta^h(\cdot,0) = u_0\,, \quad \omega_\zeta^h(\cdot,0) = v_0\,, \quad \theta_\zeta^h(\cdot,0) = \theta_0 \ \text{ in } \ \Omega. \tag{59}$$

Lemma 4.2 *For every $h > 0$ and $\zeta \in L^2(0,T;L^2(\Gamma_C)\times V)$, Problem $(\mathcal{PV}_\zeta^{1h})$ has a unique solution $(w_\zeta^h, u_\zeta^h, \varphi_\zeta^h, \theta_\zeta^h)$. Moreover, under the assumptions of Theorem 4.1, the solution $(w_\zeta^h, u_\zeta^h, \varphi_\zeta^h, \theta_\zeta^h)$ of Problem $(\mathcal{PV}_\zeta^{1h})$ has the following estimation:*

$$\begin{aligned}&\|\omega_\zeta^h(t)\|^2_{L^2(\Omega)^d} + \|u_\zeta^h(t)\|_V^2 + \int_0^t \|\omega_\zeta^h(s)\|_V^2 ds + \|\theta_\zeta^h(t)\|^2_{L^2(\Omega)}\\ &+ \int_0^t \|\theta_\zeta^h(s)\|_Q^2 ds + \|\varphi_\zeta^h(t)\|_W^2 ds \le c, \quad \forall\, t \in (0,T),\end{aligned} \tag{60}$$

for a positive constant c which is independent of h.

Proof. To prove Lemma 4.2, we use Theorem 2.1 with $F := V \times W \times V \times Q$ and $G = L^2(\Omega)^d \times W \times V \times L^2(\Omega)$. We also define the following two operators defined by

$$\mathcal{B} : G \to G', \quad \mathcal{B}X = \mathcal{B}\begin{pmatrix}\omega\\ \varphi\\ u\\ \theta\end{pmatrix} = \begin{pmatrix}\omega\\ 0\\ \theta\\ R_e\,u\end{pmatrix}, \tag{61}$$

$$\mathcal{A}(t,\cdot) : F \to F', \quad \mathcal{A}(t,X) = \begin{pmatrix} A\,\omega + F\,u + E_1\,\varphi - M_1\theta + J^h\omega\\ B\varphi + J_2^h\varphi - E_2\,u - P\,\theta\\ K\theta + h_\zeta(\theta) - M\omega + N\varphi\\ -R_e\,\omega\end{pmatrix}. \tag{62}$$

We also choose the two elements $X_0 \in G$ and $L \in F$ given by

$$X_0 = \begin{pmatrix} v_0\\ \varphi_0\\ u_0\\ \theta_0\end{pmatrix} \quad \text{and} \quad L = \begin{pmatrix} f\\ q_e\\ \Theta\\ 0\end{pmatrix}. \tag{63}$$

By using (61) and (63), we get that Problem $(\mathcal{PV}_\zeta^{1h})$ is equivalent to the problem below.

$$\begin{aligned} &\text{Find } X_\zeta^h = (\omega_\zeta^h, \varphi_\zeta^h, \theta_\zeta^h, u_\zeta^h)^{'} \text{ such that} \\ &\qquad\qquad \mathcal{B}\dot{X}_\zeta^h(t) + \mathcal{A}X_\zeta^h(t) = L \ \text{ in } \ \mathbb{F}^{'}, \\ &\qquad\qquad \mathcal{B}X_\zeta^h(0) = BX_0 \ \text{ in } \ G^{'}. \end{aligned} \tag{64}$$

We will show that the operators $\mathcal{A}$ and $\mathcal{B}$ satisfy conditions of Theorem 2.1. Indeed, from the assumptions stated in Theorem 4.1, we can easily prove that the operator $\mathcal{B} : G \to G^{'}$ is linear, bounded, positive and symmetric and the operator $\mathcal{A}(t,\cdot)$ verifies the conditions (1) and (2). Thus, due to Theorem 2.1, we get that problem (64) has a unique solution $X_\zeta^h = (w_\zeta^h, \varphi_\zeta^h, u_\zeta^h, \theta_\zeta^h)$. Consequently, Problem $(\mathcal{PV}_\zeta^{1h})$ admits a unique solution $(w_\zeta^h, \varphi_\zeta^h, u_\zeta^h, \theta_\zeta^h) \in \mathbb{V} \times \mathbb{W} \times \mathbb{V} \times \mathbb{Q}$. Next, in order to verify the estimate (60), we multiply (55) by w_ζ^h to obtain

$$\langle \dot{w}_\zeta^h, w_\zeta^h \rangle + \langle Aw_\zeta^h + Fu_\zeta^h + J_\zeta^h w_\zeta^h, w_\zeta^h \rangle - \langle M_1 \theta_\zeta^h, w_\zeta^h \rangle = \langle f, w_\zeta^h \rangle. \tag{65}$$

Recalling (A_1), (A_2) and (65), by employing several times Cauchy's inequality

$$ab \leq \epsilon a^2 + \frac{1}{4\epsilon} b^2, \quad \forall a, b \in \mathbb{R}, \epsilon > 0, \tag{66}$$

we find

$$\begin{aligned} &\|w_\zeta^h(t)\|_{L^2(\Omega)^d}^2 + \|u_\zeta^h(t)\|_V^2 + \int_0^t \|w_\zeta^h(s)\|_V^2 ds \\ &\leq c \Big(\|u_0\|_V^2 + \|v_0\|^2 + \int_0^t (\|\zeta_1(s)\|_{L^2(\Gamma_C)}^2 + \|f(s)\|_{L^2(\Omega)}^2) \, ds \\ &\qquad + \int_0^t \|\theta_\zeta^h(s)\|_Q^2 ds + \int_0^t \|\varphi_\zeta^h(s)\|_W^2 ds \Big), \quad \forall t \in (0,T). \end{aligned} \tag{67}$$

Next, we let the potential equation (56) act on φ_ζ^h to get

$$\langle B\varphi_\zeta^h, w_\zeta^h \rangle - \langle E_2 u_\zeta^h, \varphi_\zeta^h \rangle - \langle M_2 w_\zeta^h, \varphi_\zeta^h \rangle + \langle J_2^h \varphi_\zeta^h, \varphi_\zeta^h \rangle = \langle \Theta, \varphi_\zeta^h \rangle.$$

Then, from assumptions (A_1), (A_2) and (53), we deduce after some manipulations that

$$\|\varphi_\zeta^h(t)\|_W^2 \leq c \left(\|u_\zeta^h(t)\|_V^2 + \|\theta_\zeta^h(t)\|_{L^2(\Omega)}^2 + \|q_e(t)\|_W^2 \right), \quad \forall \, t \in (0,T). \tag{68}$$

Next, let the energy equation (57) act on θ_ζ^h. Then we have

$$\langle \dot{\theta}_\zeta^h, \theta_\zeta^h \rangle + \langle K\theta_\zeta^h + N\varphi_\zeta^h - M_2 w_\zeta^h, \theta_\zeta^h \rangle + \langle h_c(\theta_\zeta^h), \theta_\zeta^h \rangle = \langle \Theta, \theta_\zeta^h \rangle.$$

It follows from hypotheses (A_1), (A_2), (A_4), (A_5) and the monotonicity of φ_L that

$$\begin{aligned} &\|\theta_\zeta^h(t)\|_{L^2(\Omega)}^2 + \int_0^t \|\theta_\zeta^h(s)\|_Q^2 ds \\ &\leq c \Big(\|\theta_0\|_Q^2 + \int_0^t \|\varphi_\zeta^h(s)\|_W^2 ds + \int_0^t \|w_\zeta^h(s)\|_V^2 ds \\ &\qquad + \int_0^t \|\Theta(s)\|_{Q'}^2 ds + \int_0^t \|\zeta_2(s)\|_V^2 ds \Big). \end{aligned} \tag{69}$$

Inserting the estimation (67) and (68) into (69), we find

$$\begin{aligned}
&\|\theta_\zeta^h(t)\|^2_{L^2(\Omega)} + \int_0^t \|\theta_\zeta^h(s)\|^2_Q ds \\
&\leq c\Big(\|\theta_0\|^2_{L^2(\Omega)} + \|u_0\|^2_V + \|v_0\|^2_{L^2(\Omega)^d} + \int_0^t \|\Theta(s)\|^2_{Q'} ds + \int_0^t \|q_e(s)\|^2_W ds \\
&\quad + \int_0^t \|f(s)\|^2_{L^2(\Omega)} ds + \int_0^t \|\zeta_1(s)\|^2_{L^2(\Gamma_C)} ds + \int_0^t \|\zeta_2(s)\|^2_V ds\Big).
\end{aligned}$$

Thus,

$$\|\theta_\zeta^h(t)\|^2_{L^2(\Omega)} + \int_0^t \|\theta_\zeta^h(s)\|^2_Q ds \leq c. \tag{70}$$

Integrate (68) over $(0,t)$, where $t \in [0,T]$, and combine the result with (67) to obtain

$$\begin{aligned}
&\|w_\zeta^h(t)\|^2_{L^2(\Omega)^2} + \|u_\zeta^h(t)\|^2_V + \int_0^t \|w_\zeta^h(s)\|^2_V ds + \int_0^t \|\varphi_\zeta^h(s)\|^2_W ds \\
&\leq c\Big(\|u_0\|^2_V + \|v_0\|^2_{L^2(\Omega)^d} + \int_0^t \|q_e(s)\|^2_W ds + \int_0^t \|\zeta_1(s)\|^2_{L^2(\Gamma_C)} ds \\
&\quad + \int_0^t \|f(s)\|^2_{L^2(\Omega)} ds + \int_0^t \|u_\zeta^h(s)\|^2_V ds\Big).
\end{aligned}$$

Then, Grönwall's inequality and the inequality (70) lead to

$$\|u_\zeta^h(t)\|_V \leq c. \tag{71}$$

Hence,

$$\|\varphi_\zeta^h(t)\|_W \leq c. \tag{72}$$

Moreover, the estimations (70), (71) and (72) complete the proof of Lemma 4.2. □

Now, we have the ingredient which allows us to prove the existence and uniqueness of the solution of Problem (PV_ζ). Indeed, due to Lemma 4.2, we have for a given set of initial conditions $\{w_0^h, u_0^h, \theta_0^h\}_{h>0}$ that the family of solutions $\{w_\zeta^h, \varphi_\zeta^h, u_\zeta^h, \theta_\zeta^h\}_{h>0}$ is bounded in $\mathbb{V} \times \mathbb{W} \times \mathbb{V} \times \mathbb{Q}$. Then, from the latter result and Problem (PV_ζ^h), we get that $\{\dot{w}_\zeta^h, R_e\dot{u}_\zeta^h, \dot{\theta}_\zeta^h\}$ is also bounded in $\mathbb{V}' \times \mathbb{V}' \times \mathbb{Q}'$. Then there exists a subsequence of parameters $\{h_k\}$ such that $h_k \to 0$ as $k \to \infty$ so that

$$u_\zeta^{h_k} \rightharpoonup u_\zeta^* \quad \text{weakly in } \mathbb{V}, \tag{73}$$

$$\omega_\zeta^{h_k} \rightharpoonup \omega_\zeta^* \quad \text{weakly in } \mathbb{V}, \tag{74}$$

$$\varphi_\zeta^{h_k} \rightharpoonup \varphi_\zeta^* \quad \text{weakly in } \mathbb{W}, \tag{75}$$

$$\theta_\zeta^{h_k} \rightharpoonup \theta_\zeta^* \quad \text{weakly in } \mathbb{Q}, \tag{76}$$

$$\dot{\theta}_\zeta^{h_k} \rightharpoonup \dot{\theta}_\zeta^* \quad \text{weakly in } \mathbb{Q}', \tag{77}$$

$$\dot{\omega}_\zeta^{h_k} \rightharpoonup \dot{\omega}_\zeta^* \quad \text{weakly in } \mathbb{V}', \tag{78}$$

$$R_e\dot{u}_\zeta^{h_k} \rightharpoonup R_e\dot{u}_\zeta^* \quad \text{weakly in } \mathbb{V}'. \tag{79}$$

We are going now to prove that the triplet $(w_\zeta^*, \varphi_\zeta^*, u_\zeta^*, \theta_\zeta^*)$ verifies (53)-(59). Indeed, by passing to the limit as $k \to \infty$ in the relations $J_\zeta^{h_k}$, $J_2^{h_k}$ and $h_c(\theta_\zeta^{h_k})$, we obtain

$$\begin{aligned}
\lim_{k\to\infty} \langle J_\zeta^{h_k}\omega_\zeta^{h_k}, v-\omega_\zeta^*\rangle &= \lim_{k\to\infty} \int_0^T \int_{\Gamma_C} \zeta_1(t)\nabla\psi^h(\omega_{\zeta\tau}^{h_k}).(v_\tau - \omega_{\zeta\tau}^*)\, da\, dt \\
&\le \lim_{k\to\infty} \int_0^T \int_{\Gamma_C} |\zeta_1(t)|(\psi^h(v_\tau - \omega_{\zeta\tau}^* + \omega_{\zeta\tau}^{h_k}) - \psi^h(\omega_{\zeta\tau}^*))\, da\, dt \\
&\le \lim_{k\to\infty} \int_0^T \int_{\Gamma_C} |\zeta_1(t)|(|v_\tau|) - |\omega_{\zeta\tau}^*|))\, da\, dt,
\end{aligned} \tag{80}$$

$$\begin{aligned}
\lim_{k\to\infty} \langle J_2^{h_k}\varphi_\zeta^{h_k}, \xi-\varphi_\zeta^*\rangle &= \lim_{k\to\infty} \int_{\Gamma_C} \frac{\varphi_\zeta^{h_k}\,(\xi-\varphi_\zeta^*)}{\sqrt{|\varphi_\zeta^{h_k}|^2+h}}\, da \\
&\le \lim_{k\to\infty} \int_{\Gamma_C} \frac{|\varphi_\zeta^{h_k}|\,|\xi|}{\sqrt{|\varphi_\zeta^{h_k}|^2+h}} - \frac{\varphi_\zeta^{h_k}\varphi_\zeta^*}{\sqrt{|\varphi_\zeta^{h_k}|^2+h}}\, da \le j_2(\xi) - j_2(\varphi_\zeta^*),
\end{aligned} \tag{81}$$

and

$$\lim_{k\to\infty} \langle h_c(\theta_\zeta^{h_k}), \eta\rangle = \langle h_c(u_\zeta^*, \theta_\zeta^*), \eta\rangle. \tag{82}$$

Next, due to assumptions (A_1)-(A_6), and conditions (73)-(79) and (80)-(82), the weak limit $(u_\zeta^*, \varphi_\zeta^*, \theta_\zeta^*)$ of the subsequence $(u_\zeta^{h_k}, \varphi_\zeta^{h_k}, \theta_\zeta^{h_k})$ is a solution to Problem $(\mathcal{PV}_\zeta^1)$. Furthermore, to prove the uniqueness of the solution of Problem (PV_ζ), let $(u_1, \varphi_1, \theta_1) \in \mathbb{V}\times\mathbb{W}\times\mathbb{Q}$ and $(u_2, \varphi_2, \theta_2) \in \mathbb{V}\times\mathbb{W}\times\mathbb{Q}$ be two solutions corresponding to the same data ζ. We substitute u_ζ in (46) by u_1 and u_2, respectively, we obtain

$$\begin{aligned}
f &\in \ddot{u}_1 + A\,\dot{u}_1 + Fu_1 + E_1\varphi_1 - M_1\theta_1 + \partial j_\zeta^1(\dot{u}_1) \ \text{ in } \ \mathbb{V}', \\
f &\in \ddot{u}_2 + A\,\dot{u}_2 + Fu_2 + E_1\varphi_2 - M_1\theta_2 + \partial j_\zeta^1(\dot{u}_2) \ \text{ in } \ \mathbb{V}'.
\end{aligned}$$

Let the resulting expressions act on $\dot{u}_2 - \dot{u}_1$ and $\dot{u}_1 - \dot{u}_2$, respectively, we find

$$\begin{aligned}
\langle f, \dot{u}_2 - \dot{u}_1\rangle = &\langle \ddot{u}_1, \dot{u}_2 - \dot{u}_1\rangle + \langle A\dot{u}_1, \dot{u}_2 - \dot{u}_1\rangle + \langle Fu_1, \dot{u}_2 - \dot{u}_1\rangle \\
&+ \langle E_1\varphi_1, \dot{u}_2 - \dot{u}_1\rangle - \langle M_1\theta_1, \dot{u}_2 - \dot{u}_1\rangle \\
&+ \langle \mathcal{Z}(\dot{u}_1), \dot{u}_2 - \dot{u}_1\rangle \ \text{ with } \ \mathcal{Z}(\dot{u}_1) \in \partial j_\zeta^1(\dot{u}_1) \ \text{ in } \ \mathbb{V}',
\end{aligned} \tag{83}$$

$$\begin{aligned}
\langle f, \dot{u}_1 - \dot{u}_2\rangle = &\langle \ddot{u}_2, \dot{u}_1 - \dot{u}_2\rangle + \langle A\dot{u}_2, \dot{u}_1 - \dot{u}_2\rangle + \langle Fu_2, \dot{u}_1 - \dot{u}_2\rangle \\
&+ \langle E_1\varphi_2, \dot{u}_1 - \dot{u}_2\rangle - \langle M_1\theta_2, \dot{u}_1 - \dot{u}_2\rangle \\
&+ \langle \mathcal{Z}(\dot{u}_2), \dot{u}_1 - \dot{u}_2\rangle \ \text{ with } \ \mathcal{Z}(\dot{u}_2) \in \partial j_\zeta^1(\dot{u}_2) \ \text{ in } \ \mathbb{V}'.
\end{aligned} \tag{84}$$

On the other hand, it comes from the convexity of the functional j_ζ^1 that

$$\langle \mathcal{Z}(\dot{u}_1), \dot{u}_2 - \dot{u}_1\rangle \le j_\zeta^1(\dot{u}_2) - j_\zeta^1(\dot{u}_1) \ \text{ and } \ \langle \mathcal{Z}(\dot{u}_2), \dot{u}_1 - \dot{u}_2\rangle \le j_\zeta^1(\dot{u}_1) - j_\zeta^1(\dot{u}_2).$$

Therefore, the sum of two previous relations leads to

$$\langle \mathcal{Z}(\dot{u}_2) - \mathcal{Z}(\dot{u}_1), \dot{u}_1 - \dot{u}_2\rangle \le 0. \tag{85}$$

Keeping in mind (85), by adding two inequalities (83) and (84), we find

$$\begin{aligned}&\langle \ddot{u}_2-\ddot{u}_1,\dot{u}_1-\dot{u}_2\rangle+\langle A\dot{u}_2-A\dot{u}_1,\dot{u}_1-\dot{u}_2\rangle\\&+\langle Fu_2-Fu_1,\dot{u}_1-\dot{u}_2\rangle+\langle E_1\varphi_2-E_1\varphi_1,\dot{u}_1-\dot{u}_2\rangle\\&-\langle M_1\theta_2-M_1\theta_1,\dot{u}_1-\dot{u}_2\rangle=-\langle \mathcal{Z}(\dot{u}_2)-\mathcal{Z}(\dot{u}_1),\dot{u}_1-\dot{u}_2\rangle\geq 0.\end{aligned}$$

Now, by integrating the previous inequality over $(0,t)$, we deduce

$$\begin{aligned}&\int_0^t\langle \ddot{u}_1-\ddot{u}_2,\dot{u}_1-\dot{u}_2\rangle ds+\int_0^t\langle A\dot{u}_1-A\dot{u}_2,\dot{u}_1-\dot{u}_2\rangle ds+\int_0^t\langle Fu_1-Fu_2,\dot{u}_1-\dot{u}_2\rangle ds\\&\leq\int_0^t\langle E_1\varphi_1-E_2\varphi_2,\dot{u}_1-\dot{u}_2\rangle ds+\int_0^t\langle M_1\theta_1-M_1\theta_2,\dot{u}_1-\dot{u}_2\rangle ds.\end{aligned}$$

Then, using the same assumptions as in Lemma 4.1, we can obtain

$$\begin{aligned}&\|\dot{u}_1(t)-\dot{u}_2(t)\|^2_{L^2(\Omega)^d}+\int_0^t\|\dot{u}_1(s)-\dot{u}_2(s)\|^2_V\,ds+\|u_1(t)-u_2(t)\|^2_V\\&\leq c\Big(\int_0^t\|\varphi_1(s)-\varphi_2(s)\|^2_W\,ds+\int_0^t\|\theta_1(s)-\theta_2(s)\|^2_{L^2(\Omega)}\,ds\Big).\end{aligned}\tag{86}$$

Following the same tricks as above, we can also find

$$\int_0^t\|\varphi_1(s)-\varphi_2(s)\|^2_W ds\leq c\Big(\int_0^t\|u_1(s)-u_2(s)\|^2_V ds+\int_0^t\|\theta_1(s)-\theta_2(s)\|^2_{L^2(\Omega)}ds\Big).\tag{87}$$

Next, we replace θ_1 and θ_2 in the relation (48), respectively, we get

$$\begin{aligned}&\dot{\theta}_1+K\theta_1+N\varphi_1-M_2\dot{u}_1+h_c(\theta_1)=\Theta\ \text{ in }\ \mathbb{Q}',\\&\dot{\theta}_2+K\theta_2+N\varphi_2-M_2\dot{u}_2+h_c(\theta_2)=\Theta\ \text{ in }\ \mathbb{Q}'.\end{aligned}$$

Then, by acting the obtained results on $\theta_1-\theta_2$ and by subtracting them, we find

$$\begin{aligned}&\langle\dot{\theta}_1-\dot{\theta}_2,\theta_1-\theta_2\rangle+\langle K(\theta_1-\theta_2),\theta_1-\theta_2\rangle\\&+\langle N(\varphi_1-\varphi_2),\theta_1-\theta_2\rangle-\langle M_2(\dot{u}_1-\dot{u}_2),\theta_1-\theta_2\rangle=h_c(\theta_2)-h_c(\theta_1).\end{aligned}$$

We next integrate over $(0,t)$, then the first integrals are estimated by

$$\begin{aligned}\int_0^t\langle\dot{\theta}_1(s)-\dot{\theta}_2(s),\theta_1(s)-\theta_2(s)\rangle\,ds&=\frac{1}{2}\int_0^t\frac{d\,\|\theta_1(s)-\theta_2(s)\|^2_{L^2(\Omega)}}{ds}ds\\&=\frac{1}{2}\|\theta_1(s)-\theta_2(s)\|^2_{L^2(\Omega)}-\frac{1}{2}\|\theta_1(0)-\theta_2(0)\|^2_{L^2(\Omega)}.\end{aligned}$$

For more details on the relation above, see [18, Theorem 1(2)]. The other integrals are estimated by using Cauchy's inequality, the properties of the operators K, N and M_2, and of the functional h_c. Combining all estimates of these integrals, we obtain

$$\begin{aligned}&\|\theta_1(t)-\theta_2(t)\|^2_{L^2(\Omega)}+\int_0^t\|\theta_1(s)-\theta_2(s)\|^2_Q\,ds\\&\leq c\Big(\int_0^t\|\varphi_1(s)-\varphi_2(s)\|^2_W\,ds+\int_0^t\|\dot{u}_1(s)-\dot{u}_2(s)\|^2_V\,ds\Big).\end{aligned}\tag{88}$$

Then, we deduce that

$$\begin{aligned}&\|\theta_1(t)-\theta_2(t)\|^2_{L^2(\Omega)}+\|u_1(t)-u_2(t)\|^2_V\\&\leq c\,\Big(\int_0^t\|\theta_1(s)-\theta_2(s)\|^2_{L^2(\Omega)}\,ds+\int_0^t\|u_1(s)-u_2(s)\|^2_V\,ds\Big).\end{aligned}\tag{89}$$

Now Gronwall's inequality implies that $\theta_1=\theta_2$ and $u_1=u_2$, and consequently, $\varphi_1=\varphi_2$, which completes the proof of Lemma 4.1. □

Now, we introduce $\mathcal{L}: L^2(0,T;L^2(\Gamma_C)\times V)\to L^2(0,T;L^2(\Gamma_C)\times V)$ defined by

$$\mathcal{L}(\zeta):=\left(\mu(\theta_\zeta)\,|R\sigma_\nu(u_\zeta,\varphi_\zeta,\theta_\zeta)|\,;\,k_c(u_{\zeta,\nu}-g)\right)\tag{90}$$

for all $\zeta=(\zeta_1,\zeta_2)\in L^2(0,T;L^2(\Gamma_C)\times V)$ and where $(u_\zeta,\varphi_\zeta,\theta_\zeta)$ is the unique solution of Problem (PV_ζ) corresponding to ζ. We also consider the space Y defined as follows:

$$Y=\big\{\zeta\in L^2([0,T],L^2(\Gamma_C)\times V):\ \|\zeta\|_{L^2([0,T],L^2(\Gamma_C)\times V)}\leq T\sqrt{meas(\Gamma_C)}(M_\mu M_R+M_{k_c})\big\}.$$

Then, we provide the following result that states that $\mathcal{L}$ has a fixed point on Y.

Lemma 4.3 *The operator $\mathcal{L}$ has a unique fixed point $\zeta^*\in Y$.*

Proof. Let $\zeta=(\zeta_1,\zeta_2)$, $\lambda=(\lambda_1,\lambda_2)\in L^2(0,T;L^2(\Gamma_C)\times V)$, and let us denote by $(u_\zeta,\varphi_\zeta,\theta_\zeta)$ and $(u_\lambda,\varphi_\lambda,\theta_\lambda)$ the solution of Problem $(\mathcal{PV}^1_\zeta)$ corresponding to ζ and λ, respectively. By using the definition (90) of the operator $\mathcal{L}$, we obtain

$$\begin{aligned}&\|\mathcal{L}(\zeta)(t)-\mathcal{L}(\lambda)(t)\|^2_{L^2(\Gamma_C)\times V}\\&=\|\mu(\theta_\zeta)\,|R\sigma_\nu(u_\zeta,\varphi_\zeta,\theta_\zeta)|-\mu(\theta_\lambda)\,|R\sigma_\nu(u_\lambda,\varphi_\lambda,\theta_\lambda)|\|^2_{L^2(\Gamma_C)}\\&\quad+\|k_c(u_{\zeta\nu}-g)-k_c(u_{\lambda\nu}-g)\|^2_V.\end{aligned}\tag{91}$$

First, it comes from hypothesis $(A_4)(b)$ that

$$\|k_c(u_{\zeta\nu}-g)-k_c(u_{\lambda\nu}-g)\|^2_V\leq L^2_{k_c}c_1^2\|u_\zeta-u_\lambda\|^2_V.\tag{92}$$

Also, by using the hypotheses (A_3) and (A_6), we deduce

$$\begin{aligned}&\big\|\mu(\theta_\zeta)\,|R\sigma_\nu(u_\zeta,\varphi_\zeta,\theta_\zeta)|-\mu(\theta_\lambda)\,|R\sigma_\nu(u_\lambda,\varphi_\lambda,\theta_\lambda)|\big\|^2_{L^2(\Gamma_3)}\\&\leq M^2_\mu L^2_R\|\sigma_\nu(u_\zeta,\varphi_\zeta,\theta_\zeta)-\sigma_\nu(u_\lambda,\varphi_\lambda,\theta_\lambda)\|^2_{H^{-\frac12}(\Gamma_C)}+M^2_RL^2_\mu\|\theta_\zeta-\theta_\lambda\|^2_{L^2(\Gamma_3)}.\end{aligned}$$

Moreover, we know that there exists a constant $c_F>0$ such that

$$\begin{aligned}&\big\|\sigma_\nu(u_\zeta,\varphi_\zeta,\theta_\zeta)-\sigma_\nu(u_\lambda,\varphi_\lambda,\theta_\lambda)\big\|_{H^{-\frac12}(\Gamma_C)}\\&=\sup_{v\in H^{1/2}(\Gamma_C)}\frac{\langle\sigma_\nu(u_\zeta,\varphi_\zeta,\theta_\zeta)-\sigma_\nu(u_\lambda,\varphi_\lambda,\theta_\lambda),v_\nu\rangle_{L^2(0,T;\mathcal{H})\times H^{-1/2}(\Gamma_C)}}{\|v_\nu\|_{H^{-1/2}(\Gamma_C)}}\\&\leq c_F\,\left(\|\dot u_\zeta-\dot u_\lambda\|_V+\|u_\zeta-u_\lambda\|_V+\|\varphi_\zeta-\varphi_\lambda\|_W+\|\theta_\zeta-\theta_\lambda\|_Q\right).\end{aligned}$$

Thus, by combining two previous inequalities, we get

$$\begin{aligned}&\big\|\mu(\theta_\zeta)\,|R\sigma_\nu(u_\zeta,\varphi_\zeta,\theta_\zeta)|-\mu(\theta_\lambda)\,|R\sigma_\nu(u_\lambda,\varphi_\lambda,\theta_\lambda)|\big\|^2_{L^2(\Gamma_3)}\\&\leq c^*\,(M^2_\mu L^2_R+M^2_RL^2_\mu)\,\left(\|\dot u_\zeta-\dot u_\lambda\|^2_V+\|\theta_\zeta-\theta_\lambda\|^2_Q\right)\\&\quad+c\left(\|\varphi_\zeta-\varphi_\lambda\|^2_W+\|\theta_\zeta-\theta_\lambda\|^2_{L^2(\Omega)}+\|u_\zeta-u_\lambda\|^2_V\right).\end{aligned}\tag{93}$$

Using relations (39), (51), and assumptions (A_1), (A_7), we get

$$\begin{aligned}
&\|\dot{u}_\zeta(t)-\dot{u}_\lambda(t)\|^2_{L^2(\Omega)^d}+\|u_\zeta(t)-u_\lambda(t)\|^2_V+\int_0^t\|\dot{u}_\zeta(s)-\dot{u}_\lambda(s)\|^2_V\,ds\\
&\leq c\Big(\int_0^t\|\zeta_1(s)-\lambda_1(s)\|^2_{L^2(\Gamma_C)}ds+\int_0^t\|u_\zeta(s)-u_\lambda(s)\|_V\,ds\\
&\quad+\int_0^t\|\varphi_\zeta(s)-\varphi_\lambda(s)\|^2_W\,ds\Big),\quad\forall\,t\in[0,T].
\end{aligned}\tag{94}$$

From relation (40) and assumptions (A_1)-(A_2), we find

$$\|\varphi_\zeta(t)-\varphi_\lambda(t)\|^2_W\leq c\left(\|u_\zeta-u_\lambda\|^2_V+\|\theta_\zeta(t)-\theta_\lambda(t)\|^2_Q\right),\quad\forall\,t\in[0,T].\tag{95}$$

Moreover, keeping in mind (41), assumptions (A_1), (A_2), (A_4) and (A_5), we obtain

$$\begin{aligned}
&\|\theta_\zeta(t)-\theta_\lambda(t)\|^2_Q+\int_0^t\|\theta_\zeta(s)-\theta_\lambda(s)\|^2_Q\,ds\\
&\leq c\Big(\int_0^t\|\varphi_\zeta(s)-\varphi_\lambda(s)\|^2_W\,ds+\int_0^t\|\zeta_2(s)-\lambda_2(s)\|^2_V\,ds\\
&\qquad+\int_0^t\|\dot{u}_\zeta(s)-\dot{u}_\lambda(s)\|^2_V\,ds\Big),\quad\forall\,t\in(0,T).
\end{aligned}\tag{96}$$

We combine now the inequalities (94)-(96) to get that for all $t\in[0,T]$, we have

$$\begin{aligned}
&\|\theta_\zeta(t)-\theta_\lambda(t)\|^2_Q+\|\dot{u}_\zeta(t)-\dot{u}_\lambda(t)\|^2_V+\|u_\zeta(t)-u_\lambda(t)\|^2_V+\|\varphi_\zeta(t)-\varphi_\lambda(t)\|^2_W\\
&+\int_0^t\|\dot{u}_\zeta(s)-\dot{u}_\lambda(s)\|^2_V\,ds+\int_0^t\|\theta_\zeta(s)-\lambda(s)\|^2_Q\,ds\\
&\leq c\Big(\int_0^t\|\zeta_2(s)-\lambda_2(s)\|^2_V\,ds+\int_0^t\|\zeta_1(s)-\lambda_1(s)\|^2_{L^2(\Gamma_C)}\,ds\\
&+\int_0^t\|\dot{u}_\zeta(s)-\dot{u}_\lambda(s)\|^2_V\,ds+\int_0^t\|\theta_\zeta(s)-\theta_\lambda(s)\|^2_Q\,ds+\int_0^t\|\varphi_\zeta(s)-\varphi_\lambda(s)\|^2_W\,ds\Big).
\end{aligned}$$

Moreover, by employing Gronwall's inequality, we deduce

$$\begin{aligned}
&\|\theta_\zeta(t)-\theta_\lambda(t)\|^2_Q+\|\dot{u}_\zeta(t)-\dot{u}_\lambda(t)\|^2_V+\|u_\zeta(t)-u_\lambda(t)\|^2_V+\|\varphi_\zeta(t)-\varphi_\lambda(t)\|^2_W\\
&+\int_0^t\|\dot{u}_\lambda(s)-\dot{u}_\lambda(s)\|^2_V+\int_0^t\|\theta_\zeta(s)-\theta_\lambda(s)\|^2_Q\,ds\\
&\leq c\Big(\int_0^t\|\zeta_2(s)-\lambda_2(s)\|^2_V\,ds+\int_0^t\|\zeta_1(s)-\lambda_1(s)\|^2_{L^2(\Gamma_C)}\,ds\Big),\ \forall\,t\in(0,T).
\end{aligned}\tag{97}$$

We integrate (91) over $[0,t]$ for a given $t\in(0,T)$, then use (92), (93) and (97) to get

$$\|\mathcal{L}(\zeta)(t)-\mathcal{L}(\lambda)(t)\|^2_{L^2([0,T],L^2(\Gamma_C)\times V)}\leq c\,\|\zeta(s)-\lambda(s)\|^2_{L^2([0,T],L^2(\Gamma_C)\times V)}.\tag{98}$$

Thus, the operator $\mathcal{L}$ is Lipschitz continuous on $L^2([0,T],L^2(\Gamma_C)\times V)$. In addition, we can easily show that the operator Λ is continuous from Y into itself. We have also Y is a nonempty, convex closed subset of the reflexive space $L^2([0,T],L^2(\Gamma_C)\times V)$, then

Y is weakly compact. Finally, it follows from Schauder's fixed point theorem that the operator $\mathcal{L}$ admits a unique fixed point $\zeta^* \in Y$, and finally, Lemma 4.3 holds. □

To finish the proof of Theorem 4.1, let $\zeta^* \in Y$ be a fixed point $\mathcal{L}$ defined by (90), it is straightforward to show that the solution $(u_{\zeta^*}, \varphi_{\zeta^*}, \theta_{\zeta^*})$ of Problem (PV_ζ) corresponding to ζ^*, is also a solution of Problem (PV) (called the weak solution of Problem (P)). Moreover, the uniqueness of the solution to Problem (PV) can be provided from the uniqueness of the solution to Problem (PV_ζ), which ends the proof of Theorem 4.1. □

5 Conclusion

The main contribution here is the proof of the unique solvability of a new dynamic thermo-electro-elastic contact model, i.e., Problem (P), which takes into account the effects of thermal softening and frictional heating at the contact surface. So, an existence and uniqueness result has been obtained when $M_\mu L_R + M_R L_\mu$ is sufficiently small. We note here that estimating the allowed size of coefficient $M_\mu L_R + M_R L_\mu$ remains an open and very interesting question.

References

[1] A. Amassad, K.L. Kuttler, M. Rochdi and M. Shillor. Quasi-static thermoviscoelastic contact problem with slip dependent friction coefficient. *Mathematical and computer modelling* **36** (7-8) (2002) 839–854.

[2] J.P. Aubin. *Approximation of Elliptic Boundary Value Problems.* John Wiley, New York, 1972.

[3] R.C. Batra and J.S. Yang. Saint-Venant's principle in linear piezoelectricity. *J. Elasticity* **38** (1995) 209–218.

[4] H. Benaissa, E-l. H. Essoufi and R. Fakhar. Analysis of a Signorini problem with nonlocal friction in thermo-piezoelectricity. *Glasnik matematički* **51** (2) (2016) 391–411.

[5] P. Bisegna, F. Lebon and F. Maceri. The unilateral frictional contact of a piezoelectric body with a rigid support. In: *Contact Mechanics.* Kluwer, Dordrecht, 2002, 347–354.

[6] M. Cocu, E. Pratt and M. Raous. Formulation and approximation of quasistatic frictional contact. *Int. Jou. Engng. Sc.* **34** (7) (1996) 783–798.

[7] Z. Denkowski, S. Migórski and A. Ochal. A class of optimal control problems for piezoelectric frictional contact models. *Nonlinear Anal. Real World Appl.* **12** (2011) 1883–1895.

[8] El H. Essoufi, El H. Benkhira and R. Fakhar. Analysis and numerical approximation of an electro-elastic frictional contact problem. *Adv. Appl. Math. Mech.* **2** (2010) 355–378.

[9] T. Ikeda. *Fundamentals of piezoelectricity*, Oxford University Press, Oxford, 1990.

[10] D. Motreanu and M. Sofonea. Evolutionary variational inequalities arising in quasistatic frictional contact problems for elastic materials. *Abstract and Applied Analysis.* **4** (4) (1999) 255–279.

[11] S. Migórski. Hemivariational inequality for a frictional contact problem in elasto-piezoelectricity. *Discrete Contin. Dyn. Syst. Ser. B.* **6** (2006) 1339–1356.

[12] S. Migórski. A class of hemivariational inequality for electroelastic contact problems with slip dependent friction. *Discrete Contin. Dyn. Syst. Ser. S.* **1** (2008) 117–126.

[13] S. Migórski, A. Ochal and M. Sofonea. Weak solvability of a piezoelectric contact problem. *European Jou. Appl. Math.* **20** (2009) 145–167.

[14] R.D. Mindlin. On the equations of motion of piezoelectric crystals, problems of continuum. In: *Muskelishvili, N.I. (Ed.), Mechanics, 70th Birthday Volume*. SIAM, Philadelphia, 1961, 282-–290.

[15] R.D. Mindlin. *Equation of High Frequency of Thermo-Piezoelectric. Crystals Plates, Interactions in Elastic Solids*. Springer, Wein, 1979.

[16] M. Sofonea and EL-H. Essoufi. A piezoelectric contact problem with slip dependent coefficient of friction. *Math. Model. Anal.* **9** (2004) 229–242.

[17] H.F. Tiersten. On the nonlinear equations of thermoelectroelasticity. *Internat. J. Engrg. Sci.* **9** (1971) 587–604.

[18] M. Rochdi and M. Shillor. Existence and uniqueness for a quasistatic frictional brlateral contact problem in thermoviscoelasticity. *Quart. Appl. Math.* **58** (3) (2000) 543–560.

Nonlinear Dynamics and Systems Theory, **24** (1) (2024) 99–110

Regional Weak and Strong Stabilization of Time Delay Infinite Dimensional Bilinear Systems

E. Zerrik [1*], A. Akoubi [1] and A. Ait Aadi [2]

[1] *MACS Team, Department of Mathematics, Faculty of Sciences.*
[2] *Department of Sciences, ENS, University of Moulay Ismail, Meknes, Morocco.*

Received: April 3, 2023; Revised: January 23, 2024

Abstract: The current study focuses on the regional stabilization of time delay infinite dimensional bilinear systems evolving in a spatial domain Ω. It consists in studying the asymptotic behavior of such a system in a subregion ω of Ω. Then we demonstrate regional weak stabilization under weak observability conditions, while regional strong stabilization can be achieved under the exact observability condition. Illustrative examples and simulations are included to affirm the accuracy of the theoretical results.

Keywords: *infinite dimensional systems; delay bilinear systems; regional stabilization; weak and strong observability.*

Mathematics Subject Classification (2010): 93D15.

1 Introduction

There has been a growing interest in the study of infinite dimensional bilinear systems, which are a type of nonlinear systems that exhibit nonlinearity as a result of the interaction between the state and control. These systems are widely used in various industrial and natural processes, including heat transfer through conduction-convection, neutron kinetics in nuclear reactors, and dynamic heat exchanger with a controlled flow [3], among others. Bilinear systems are also often used as simple approximations for nonlinear systems [6]. In some cases, time delay may also be present in the system variables, either due to intrinsic delays or due to delays in the reaction of the control. This makes it important to consider time delay when designing these systems to accurately reflect real processes. Bilinear systems with time delay can be found in the fields such as viscoelasticity, mechanics, nuclear reactions, heat flow, and neural networks, etc [9].

* Corresponding author: mailto:zerrik3@yahoo.fr

The stabilization of an infinite dimensional bilinear system with time delay has been a topic of discussion in numerous research studies: in [7], the researchers delved into the stabilization of a category of time-delayed bilinear systems within a Hilbert space. Their approach was rooted in the decreasing energy property of the system under examination. By employing a set of continuous controls, the researchers analyzed both weak and strong stabilization, and established a polynomial decay rate estimate for the stabilized state. They also tackled exponential stabilization through bounded feedback control and provided a clear decay rate estimate for the stabilized state.

The regional stabilization of an infinite dimensional bilinear system evolving over a spatial domain $\Omega \subset R^n$ $(n \geq 1)$ and ω being a subregion of Ω refers to the ability to stabilize the system only in the region ω or where the focus is solely on the state's behavior within ω. This concept is crucial because stabilizing the system in a subregion is more cost-effective than stabilizing it over the entire domain. Additionally, there are systems that cannot be stabilized over the entire domain of evolution, but stabilization can be achieved in specific subdomains within it (see [11]). This notion has been developed in many works: in [13], the researchers studied the regional stabilization of an infinite dimensional bilinear system that evolves in a spatial domain Ω with an unbounded control operator. Likewise, in [12], the researchers introduced controls that guarantee weak, strong, and exponential regional stabilization for a particular class of bilinear systems, as well as a control that regionally weakly stabilizes these systems with a minimal performance cost. In [14], the authors investigated the regional exponential stabilization of an infinite dimensional bilinear systems using bounded controls.
In [4], the authors presented preliminary results on the well-posedness of time-delayed bilinear systems in a real Hilbert space. They used a decomposition technique to demonstrate strong stabilization.

In this study, we delve into the subject of regional stabilization for infinite dimensional bilinear systems with time delay. Then we present sufficient conditions ensuring the regional weak and strong stabilization of such systems. The approach is a combination of energy decay, weak and exact observability conditions, and properties of semigroups. Furthermore, we provide application examples and simulations to support the obtained theoretical results.

More precisely, we consider a system defined by

$$\begin{cases} \dot{y}(t) = Ay(t) + u(t)By(t-r), \quad t \geq 0, \\ y_0 = \varphi \in \mathcal{C}, \end{cases} \tag{1}$$

where A is the infinitesimal generator of a linear $\mathcal{C}_0$-semigroup $S(t)$ on $L^2(\Omega)$, $B : L^2(\Omega) \longrightarrow L^2(\Omega)$ is a linear bounded control operator and $u \in L^2([0, +\infty[: R)$ is the scalar-valued control. The delay is indicated by the positive constant r, and $\mathcal{C}$ is a Banach space of continuous functions $\psi : [-r, 0] \to L^2(\Omega)$ with the norm $||\psi||_c = \sup_{-r \leq \theta \leq 0} ||\psi(\theta)||$.
The history function $y_t : [-r; \infty) \longrightarrow L^2(\Omega)$ is given by $y_t(\theta) = y(t+\theta)$ for all $\theta \in [-r, 0]$.
Let us consider a non-empty open subregion ω of Ω, with a positive Lebesgue measure. Define the restriction operator to ω by

$$\begin{aligned} \chi_\omega : \ L^2(\Omega) &\longrightarrow L^2(\omega) \\ y &\longmapsto y|_\omega, \end{aligned}$$

and $\chi_\omega^* : L^2(\omega) \longrightarrow L^2(\Omega)$ is the adjoint operator of χ_ω given by

$$\chi_\omega^* y(x) = \begin{cases} y(x) & \text{if} \quad x \in \omega, \\ 0 & \text{else} \ \ x \in \Omega \backslash \omega. \end{cases}$$

Let us recall that system (1) is said to be regionally weakly stabilizable if there exists a feedback control u such that for any initial condition $\varphi \in \mathcal{C}$, the corresponding solution $y(t)$ of system (1) is global and verifies $\forall \phi \in L^2(\omega), \ \langle \chi_\omega y(t), \phi \rangle_{L^2(\omega)} \longrightarrow 0 \ as \ t \longrightarrow \infty$, and regionally strongly stabilizable if there exists a feedback control u such that for any initial condition $\varphi \in \mathcal{C}$, the corresponding solution $y(t)$ of system (1) is global and verifies $||\chi_\omega y(t)||_{L^2(\omega)} \longrightarrow 0 \ as \ t \longrightarrow \infty$.

The paper is structured as follows. Section 2 focuses on the regional weak stabilization of (1). Section 3 is dedicated to the regional strong stabilization of (1). Multiple examples are given in Section 4 as applications. The final Sections 5 and 6 present illustrative simulations and conclusions.

2 Regional Weak Stabilization

This section gives sufficient conditions for the regional weak stabilization of (1).

Theorem 2.1 *Assume that A generates a semigroup $(S(t))_{t\geq 0}$ of contractions on $L^2(\Omega)$, and B is a compact operator. If the conditions*

1. $\langle \chi_\omega^* \chi_\omega A\phi, \phi \rangle \leq 0, \forall \phi \in \mathcal{D}(A)$,
2. $\langle \chi_\omega^* \chi_\omega By(t-r), y(t) \rangle \langle By(t-r), y(t) \rangle \geq 0, \ \forall y \in L^2(\Omega)$,
3. $\langle \chi_\omega^* \chi_\omega BS(t-r)y(t), S(t)y(t) \rangle = 0, \ \forall t \geq r \Longrightarrow \chi_\omega y(t) = 0$

hold, then the control

$$u(t) = -\langle \chi_\omega^* \chi_\omega By(t-r), y(t) \rangle \tag{2}$$

regionally weakly stabilizes the system (1).

Proof. Since $\varphi \in \mathcal{C}$, the function $t \longmapsto \| \chi_\omega y(t) \|_{L^2(\omega)}^2$ is continuously differentiable (see [10]). Then

$$\frac{1}{2}\frac{d}{dt}||\chi_\omega y(t)||_{L^2(\omega)}^2 = \langle \chi_\omega^* \chi_\omega Ay(t), y(t) \rangle + u(t) \langle \chi_\omega^* \chi_\omega By(t-r), y(t) \rangle.$$

Thanks to condition (1) of Theorem 2.1, it follows that

$$\frac{1}{2}\frac{d}{dt}||\chi_\omega y(t)||_{L^2(\omega)}^2 \leq u(t) \langle \chi_\omega^* \chi_\omega By(t-r), y(t) \rangle. \tag{3}$$

In order to make the function $\frac{1}{2}\frac{d}{dt}||\chi_\omega y(t)||_{L^2(\omega)}^2$ nonincreasing, we take the control

$$u(t) = -\langle \chi_\omega^* \chi_\omega By(t-r), y(t) \rangle. \tag{4}$$

The resulting closed-loop system becomes

$$\begin{cases} \dot{y}(t) = Ay(t) + f(y_t), \quad t \geq 0, \\ y_0 = \varphi \in \mathcal{C}, \end{cases} \tag{5}$$

where $f(\psi) = -\langle \chi_\omega^* \chi_\omega B\psi(-r), \psi(0)\rangle B\psi(-r), \ \ \forall \psi \in \mathcal{C}$. The function f is locally Lipschitz, indeed, for all $\psi_1, \psi_2 \in \mathcal{C}$, with $||\psi_1||_{\mathcal{C}} \leq R$ and $||\psi_2||_{\mathcal{C}} \leq R$, we have

$$||f(\psi_1) - f(\psi_2)|| \leq M||\psi_1 - \psi_2||_{\mathcal{C}},$$

where $M = ||\chi_\omega||^2_{L^2(\omega)}||B||^2(||\psi_1||^2_{\mathcal{C}} + ||\psi_1||_{\mathcal{C}}||\psi_2||_{\mathcal{C}} + ||\psi_2||^2_{\mathcal{C}})$. Then the system (5) possesses a unique mild solution $y \in \mathcal{C}([-r, t_{max}[; \mathcal{H})$ expressed as

$$\begin{cases} y(t) = S(t)\varphi(0) + \displaystyle\int_0^t S(t-s)f(y_s)ds, \quad t \in [0, t_{max}[, \\ y_0 = \varphi \in \mathcal{C}. \end{cases} \tag{6}$$

Since A generates a semigroup of contractions, we have

$$\frac{d}{dt}||y(t)||^2 \leq -2\langle \chi_\omega^* \chi_\omega By(t-r), y(t)\rangle \langle By(t-r), y(t)\rangle. \tag{7}$$

By integrating the inequality (7), for all $t \geq 0$, we get

$$||y(t)||^2 - ||y(0)||^2 \leq -2\int_0^t \langle \chi_\omega^* \chi_\omega By(s-r), y(s)\rangle \langle By(s-r), y(s)\rangle \, ds.$$

Using condition (2) of Theorem 2.1, we obtain

$$||y(t)|| \leq ||\varphi||_{\mathcal{C}}, \ t \geq -r. \tag{8}$$

Therefore, the system (1) possesses a unique global solution $y \in \mathcal{C}([-r, \infty); \mathcal{H})$ (see Theorem 2.6 in [10]).

By using (3) together with the control (2), we get

$$\frac{d}{dt}||\chi_\omega y(t)||^2_{L^2(\omega)} \leq -2|\langle \chi_\omega^* \chi_\omega By(t-r), y(t)\rangle|^2. \tag{9}$$

By integrating the inequality (9) over the interval $[0, t]$, we get

$$||\chi_\omega y(t)||^2_{L^2(\omega)} - ||\chi_\omega y(0)||^2_{L^2(\omega)} \leq -2\int_0^t |\langle \chi_\omega^* \chi_\omega By(s-r), y(s)\rangle|^2 \, ds. \tag{10}$$

From (6), we have

$$y(t) - S(t)\varphi(0) = -\int_0^t S(t-s)\langle \chi_\omega^* \chi_\omega By(s-r), y(s)\rangle By(s-r)ds. \tag{11}$$

For $T > r$ fixed, using (8), (11), Schwartz's inequality and the fact $||S(t)|| \leq 1, \ \forall t \geq 0$, we get

$$||y(t) - S(t)\varphi(0)|| \leq ||B||||\varphi||_{\mathcal{C}} \left((T-r)\int_r^T |\langle \chi_\omega^* \chi_\omega By(s-r), y(s)\rangle|^2 ds \right)^{\frac{1}{2}}, \ \ \forall t \in [r, T]. \tag{12}$$

For all $\varphi \in \mathcal{C}$ and $t \geq 0$, we have

$$\begin{aligned} |\langle \chi_\omega^* \chi_\omega BS(t-r)\varphi(0), S(t)\varphi(0)\rangle| \ \leq & |\langle \chi_\omega^* \chi_\omega BS(t-r)\varphi(0) - \chi_\omega^* \chi_\omega By(t-r), S(t)\varphi(0)\rangle| \\ & + |\langle \chi_\omega^* \chi_\omega By(t-r), y(t) - S(t)\varphi(0)\rangle| \\ & + |\langle \chi_\omega^* \chi_\omega By(t-r), y(t)\rangle|. \end{aligned} \tag{13}$$

By using (13), and taking into account that both B and χ_ω are bounded operators, we obtain

$$\begin{aligned}|\langle \chi_\omega^* \chi_\omega BS(t-r)\varphi(0), S(t)\varphi(0)\rangle| \quad &\leq ||\chi_\omega||^2_{L^2(\omega)}||B||\,||y(t-r)-S(t-r)\varphi(0)||\,||\varphi||_{\mathcal{C}} \\ &+||\chi_\omega||^2_{L^2(\omega)}||B||\,||y(t)-S(t)\varphi(0)||\,||\varphi||_{\mathcal{C}} \\ &+|\langle \chi_\omega^* \chi_\omega By(t-r), y(t)\rangle|.\end{aligned} \tag{14}$$

From (11), (12), and Schwartz's inequality, we have

$$\begin{aligned}&||y(t-r)-S(t-r)\varphi(0)|| \leq \\ &||B||||\varphi||_{\mathcal{C}}(T-r)^{\frac{1}{2}}\left(\int_r^T |\langle \chi_\omega^* \chi_\omega By(s-r), y(s)\rangle|^2 ds\right)^{\frac{1}{2}}, \quad \forall t \in [r,T].\end{aligned} \tag{15}$$

Replacing $\varphi(0)$ by $y(t)$ in (12) and (14), we get

$$\begin{aligned}|\langle \chi_\omega^* \chi_\omega BS(t-r)y(t), S(t)y(t)\rangle| \quad &\leq N(T-r)^{\frac{1}{2}}\left(\int_r^T |\langle \chi_\omega^* \chi_\omega By(s-r), y(s)\rangle|^2\, ds\right)^{\frac{1}{2}} \\ &+|\langle \chi_\omega^* \chi_\omega By(t-r), y(t)\rangle|,\end{aligned} \tag{16}$$

where $N = 2||\chi_\omega||^2_{L^2(\omega)}||B||^2||\varphi||^2_{\mathcal{C}}$.

By integrating this relation over the interval $[r,T]$ and applying Schwartz's inequality, we get

$$\begin{aligned}&\int_r^T |\langle \chi_\omega^* \chi_\omega BS(s-r)y(s), S(s)y(s)\rangle| ds \leq \\ &(N+1)(T-r)^{\frac{1}{2}}\left(\int_{t+r}^{t+T} |\langle \chi_\omega^* \chi_\omega By(s-r), y(s)\rangle|^2 ds\right)^{\frac{1}{2}}.\end{aligned} \tag{17}$$

Thus, as $t \longrightarrow +\infty$,

$$\left(\int_r^T |\langle \chi_\omega^* \chi_\omega BS(s-r)y(s), S(s)y(s)\rangle| ds\right)^2 = O\left(\int_{t+r}^{t+T} |\langle \chi_\omega^* \chi_\omega By(s-r), y(s)\rangle|^2 ds\right). \tag{18}$$

Let us consider the nonlinear semi-group $\Gamma(t)\varphi(0) := y(t)$ and let $(t_n)_{n\geq 0}$ be a sequence of real numbers such that $t_n \longrightarrow +\infty \; as \; n \longrightarrow +\infty$.

From (8), $\Gamma(t)\varphi(0)$ is bounded in $L^2(\Omega)$, and since $L^2(\Omega)$ is reflexive, there exists a subsequence $(t_{\phi(n)})$ of (t_n) such that $\Gamma(t_{\phi(n)})\varphi(0) \rightharpoonup \psi \; as \; n \longrightarrow +\infty$.

Since B is compact and χ_ω continuous, we have

$$\lim_{n \longmapsto +\infty} \langle \chi_\omega^* \chi_\omega BS(t-r)\Gamma(t_{\phi(n)})\varphi(0), \mathrm{S(t)}\Gamma(t_{\phi(n)})\varphi(0)\rangle = \langle \chi_\omega^* \chi_\omega BS(t-r)\psi, S(t)\psi\rangle.$$

For all $n \geq 0$, we set

$$\Lambda_n(t_{\phi(n)}) := \int_{t_{\phi(n)}+r}^{t_{\phi(n)}+T} |\langle \chi_\omega^* \chi_\omega B\Gamma(s-r)\varphi(0), \Gamma(s)\varphi(0)\rangle|^2 ds.$$

Using (10), we obtain

$$\int_0^t |\langle \chi_\omega^* \chi_\omega By(s-r), y(s)\rangle|^2\, ds \leq \frac{1}{2}||\chi_\omega y(0)||^2_{\gamma},$$

which gives $\int_0^t |\langle \chi_\omega^* \chi_\omega B y(s-r), y(s)\rangle|^2 \, ds < +\infty$. Then $\forall t \geq 0$, $\Lambda_n(t) \longrightarrow 0$ as $n \longrightarrow +\infty$.

By replacing $y(t)$ by $\Gamma(t)\varphi(0)$ and $y(t-r)$ by $\Gamma(t-r)\varphi(0)$ in (17), we have

$$\int_r^T |\langle \chi_\omega^* \chi_\omega BS(s-r)\Gamma(s)\varphi(0), S(s)\Gamma(s)\varphi(0)\rangle| ds \leq (N+1)(T-r)^{\frac{1}{2}} \sqrt{\Lambda_n(t)}.$$

Since $\Lambda_n(t_{\phi(n)}) \longrightarrow 0$ as $n \longrightarrow +\infty$, we get

$$\lim_{n \longmapsto +\infty} \int_r^T |\langle \chi_\omega^* \chi_\omega BS(s-r)\Gamma(t_{\phi(n)})\varphi(0), S(s)\Gamma(t_{\phi(n)})\varphi(0)\rangle| ds = 0.$$

Then, using the dominated convergence theorem, we have

$$\int_r^T |\langle \chi_\omega^* \chi_\omega BS(s-r)\psi, \mathrm{S(s)}\psi\rangle| ds = 0.$$

It follows that

$$\langle \chi_\omega^* \chi_\omega BS(s-r)\psi, S(s)\psi\rangle = 0, \ \forall s \in [0,t].$$

Using condition (3) of Theorem 2.1, we deduce that

$$\chi_\omega \Gamma(t_{\phi(n)})\varphi(0) \rightharpoonup 0 \ as \ n \longrightarrow +\infty. \tag{19}$$

On the other hand, it is clear that (19) holds for each subsequence $(t_{\phi(n)})$ of (t_n), and $\chi_\omega \Gamma(t_{\phi(n)})\varphi(0)$ weakly converges in $L^2(\Omega)$. This implies that $\forall \psi \in L^2(\Omega)$, we have $\langle \chi_\omega \Gamma(t_n)\varphi(0), \psi\rangle \longrightarrow 0 \ as \ n \longrightarrow +\infty$ and hence $\chi_\omega \Gamma(t)\varphi(0) \rightharpoonup 0 \ as \ t \longrightarrow +\infty$.

3 Regional Strong Stabilization

The following results provide conditions for the regional strong stabilization of the system (1).

Theorem 3.1 *Assume that A generates a semiproup $(S(t))_{t\geq 0}$ of contractions on $L^2(\Omega)$ and B is a bounded linear operator. If the conditions (1) and (2) of Theorem 2.1 hold, and there exist T, $\delta > 0$ such that the inequality*

$$\int_r^T |\langle \chi_\omega^* \chi_\omega BS(s-r)\psi, S(s)\psi\rangle| ds \geq \delta(r) ||\chi_\omega \psi||^2_{L^2(\omega)}, \quad \forall \psi \in L^2(\Omega), \tag{20}$$

holds, then the control defined in (2) regionally strongly stabilizes the system (1).

Proof. Let $T \geq r$ be such that (20) is satisfied. Using (10) allows

$$||\chi_\omega y(kT)||^2_{L^2(\omega)} - ||\chi_\omega y((k+1)T)||^2_{L^2(\omega)} \geq 2 \int_{kT}^{T(k+1)} |\langle \chi_\omega^* \chi_\omega B y(s-r), y(s)\rangle|^2 ds, \ \ k \geq 0.$$

From (18) and (20), we have

$$||\chi_\omega y(kT)||^2_{L^2(\omega)} - ||\chi_\omega y((k+1)T)||^2_{L^2(\omega)} \geq \alpha ||\chi_\omega y(kT)||^4_{L^2(\omega)}, \tag{21}$$

where $\alpha = \dfrac{2\delta(r)^2}{(N+1)^2(T-r)}$. Taking $p_k = ||\chi_\omega y(kT)||^2_{L^2(\omega)}$, the inequality (21) can be expressed as follows:

$$\beta p_k^2 + p_{k+1} \leq p_k, \ \ \forall k \geq 0.$$

As $p_{k+1} \leq p_k$, we get $\beta p_{k+1}^2 + p_{k+1} \leq p_k, \ \ \forall k \geq 0$.

Using Lemma 5.2 from [1], we have $p_k \leq \dfrac{M}{k+1} \quad for\ all\ k \geq 0$. As $||\chi_\omega y(t)||_{L^2(\omega)}$ decreases, we conclude the estimate

$$||\chi_\omega y(t)||_{L^2(\omega)} = O\left(\frac{1}{\sqrt{t}}\right)\ as\ t \longrightarrow +\infty,$$

which proves the regional strong stabilization of the system (1).

4 Applications

This section presents illustrative examples with respect to regional stabilization.

Example 4.1 Let us consider the system defined on $\Omega =]0, +\infty)$ by

$$\begin{cases} \dfrac{\partial y(t,x)}{\partial t} = -\dfrac{\partial y(t,x)}{\partial x} + u(t)By(t-1,x), & x \in \Omega,\ t \geq 0, \\ y(t,x) = t\sin(\pi x), & x \in \Omega,\ t \in [-1,0], \end{cases} \tag{22}$$

where $u \in L^2([0,+\infty[:\mathbb{R})$, $By(.) = \displaystyle\int_\omega y(x)dx\mathbb{1}_\omega(.)$ for $\omega \subset \Omega$.

Let $Ay = -\dfrac{\partial y}{\partial x}$, with the domain $\mathcal{D}(A) = \{y \in H^1(\Omega)|\ y(0) = 0,\ y(x) \longrightarrow 0\ as\ x \longrightarrow +\infty\}$, the operator A generates a semigroup of contractions

$$S(t)y = \begin{cases} y(x-t) & if\ x \geq t \\ 0 & if\ x < t. \end{cases}$$

Let $\omega =]0,1[$ be a subregion of Ω. For all $y \in \mathcal{D}(A)$, we have

$$\left\langle \chi_\omega^* \chi_\omega Ay, y \right\rangle = -\int_0^1 y^{'}(x)y(x)dx = -\frac{y^2(1)}{2} \leq 0.$$

Then condition (1) of Theorem 2.1 is verified. The condition (2) of Theorem 2.1 is satisfied since

$$\begin{aligned} \left\langle \chi_\omega^* \chi_\omega By(t-1), y(t) \right\rangle \left\langle By(t-1), y(t) \right\rangle &= \int_0^1 By(t-1)y(t)dx \int_\Omega By(t-1)y(t)dx \\ &= \int_0^1 \big(By(t-1)y(t)\big)^2 dx \geq 0. \end{aligned}$$

The operator B is compact and verifies

$$\left\langle \chi_\omega^* \chi_\omega BS(t-1)y, S(t)y \right\rangle = \left(\int_0^{1-t} y(x)dx\right)^2.$$

Therefore

$$\left\langle \chi_\omega^* \chi_\omega BS(t-1)y, S(t)y \right\rangle = 0,\ \forall t \geq 0 \Longrightarrow \chi_\omega y = 0.$$

Then the condition (3) of Theorem 2.1 holds.

We deduce that the control

$$u(t) = -\int_0^1 y(t-1,x)y(t,x)dx$$

regionally weakly stabilizes the system (22).

Example 4.2 On $\Omega =]0,1[$, let us consider the following system:

$$\begin{cases} \dfrac{\partial y(t,x)}{\partial t} = -i\Delta y(t,x) + u(t)y(t-2,x), & x \in \Omega,\ t \geq 0, \\ y(t,0) = y(t,1) = 0, & x \in \partial\Omega,\ t \geq 0, \\ y(t,x) = tx(1-x), & x \in \Omega,\ t \in [-2;0]\,, \end{cases} \tag{23}$$

where $u \in L^2([0,+\infty[:\mathbb{R})$ and $B = I$.

Let ω be a subregion of Ω that verifies the geometric control condition (GCC) (see [2]). The operator $A = -i\Delta$ $(i \in \mathbb{C})$ with the domain $\mathcal{D}(A) = H^2(\Omega) \cap H_0^1(\Omega)$ generates a semigroup of isometry on $L^2(\Omega)$.

We have $Re(\langle \chi_\omega^* \chi_\omega Ay, y \rangle) = 0,\ \forall y \in \mathcal{D}((A))$. Then the condition (1) of Theorem 2.1 is satisfied. Since the operator B is the identity, the condition (2) of Theorem 2.1 is satisfied. Indeed,

$$\begin{aligned} \left\langle \chi_\omega^* \chi_\omega By(t-2), y(t) \right\rangle \left\langle By(t-2), y(t) \right\rangle &= \int_\omega y(t-2)y(t)dx \int_\Omega y(t-2)y(t)dx \\ &= \int_\omega \int_\Omega \big(y(t-2)y(t)\big)^2 dx \geq 0. \end{aligned}$$

For all $\psi \in L^2(\Omega)$, we obtain $\left\langle \chi_\omega^* \chi_\omega BS(t-2)\psi, S(t)\psi \right\rangle = \left\langle S(t-2)\psi, S(t)\psi \right\rangle_{L^2(\omega)}$.

Integrating this inequality, we get

$$\int_2^T \left\langle \chi_\omega^* \chi_\omega BS(t-2)\psi, S(t)\psi \right\rangle dt \geq \int_2^T \left\langle S(t-2)\psi, S(t)\psi \right\rangle_{L^2(\omega)} dt.$$

Since the subregion ω verifies GCC, there exist $\alpha, T > 0$ such that the inequality

$$\int_r^T \left\langle \chi_\omega^* \chi_\omega BS(t-2)\psi, S(t)\psi \right\rangle dt \geq \alpha ||\psi||^2 \geq \alpha ||\chi_\omega \psi||^2_{L^2(\omega)}$$

holds (see [2]). We deduce that the control

$$u(t) = -\int_\omega y(t-2,x)y(t,x)dx$$

regionally strongly stabilizes the system (23).

5 Algorithm and Simulations

The algorithm for the computation of the stabilizing control is as follows.

Algorithm 5.1 Step 1: Initial data.
The information required includes the evolution domain Ω, a time discretization (t_i), initial state y_0, delay r, initial control u_0, and desired precision ε.
Step 2 : Calculating the Control.
Using formula (2), calculate the control to get $u(t_i)$.
Step 3 : Finding the State.
Solve system (24) using the explicit finite difference method to obtain the state $y(t_{i+1})$.
Step 4 : Checking the Accuracy.
Proceed to Step 2 again by incrementing i if $\| y(t_i) \| > \varepsilon$.

For simulation purposes, we examine the transport equation, which is defined on $\Omega =]0, +\infty)$ by

$$\begin{cases} \dfrac{\partial y(x,t)}{\partial t} = -0.01\dfrac{\partial y(x,t)}{\partial x} + u(t)By(x,t-r), & x \in \Omega,\ t \geq 0, \\ y(x,t) = t\sin(\pi x), & x \in \Omega,\ t \in [-r, 0], \end{cases} \tag{24}$$

where $u \in L^2([0, +\infty[: \mathbb{R})$, $By(.) = \displaystyle\int_\omega y(x)dx\mathbb{1}_\omega(.)$ for $\omega \subset \Omega$.
Consider the subregion $\omega =]0, 4[$. The control

$$u(t) = -\int_\omega y(x, t-r)y(x,t)dx \tag{25}$$

regionally weakly stabilizes (24) on ω.

We take the delay $r = 1$, and applying the above algorithm with $\varepsilon = 10^{-4}$, we have the following figures.

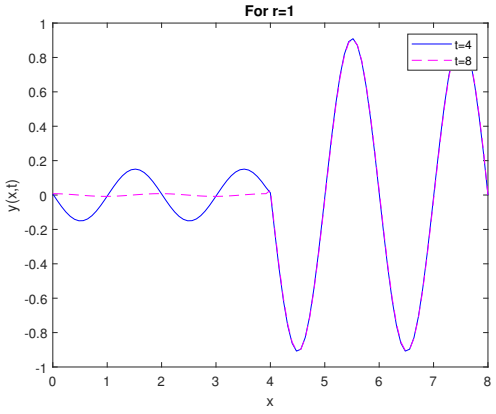

Figure 1: Stabilization on ω.

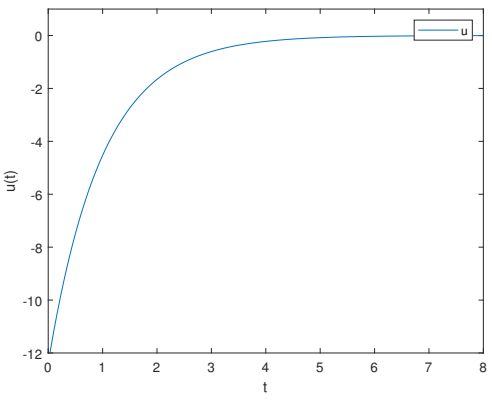

Figure 2: The control function.

Figure 1 shows the stabilization of the state on ω with the error equal to $0.1725 * 10^{-4}$. Figure 2 shows the decay of the system energy.

For $r = 2$, we get Figure 4 which shows that system (24) is still stabilized on the subregion ω.

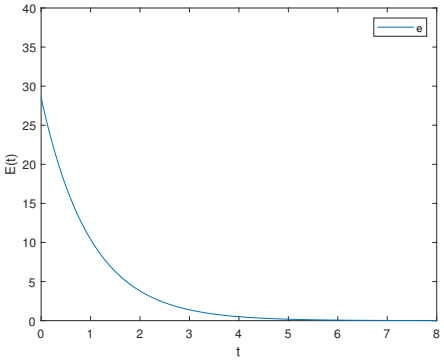

Figure 3: The energy decay.

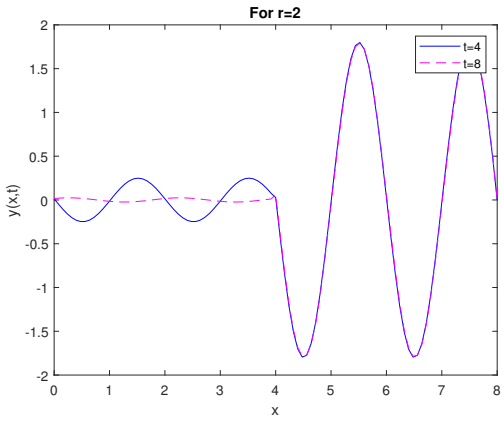

Figure 4: Stabilization on ω.

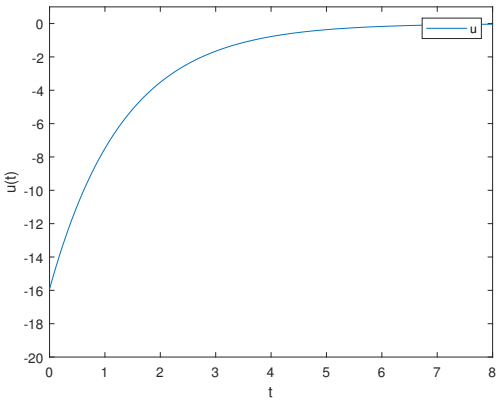

Figure 5: The control function.

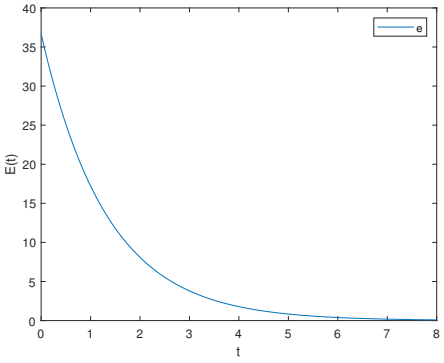

Figure 6: The energy decay.

Remark 5.1 The control (25) only stabilizes the state within the subregion ω. Yet,

if condition (2) outlined in Theorem 2.1 is satisfied, the state remains bounded even in the residual region $\Omega\backslash\omega$.

Now we consider system (24) with $r = 10$. Applying the previous algorithm with control (25), we obtain Figures 7, 9 which show the instability of system (24) over the

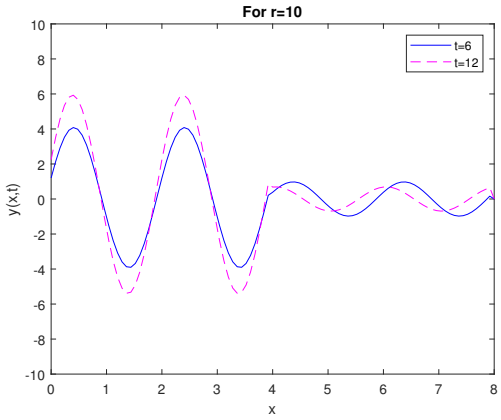

Figure 7: Instability on ω.

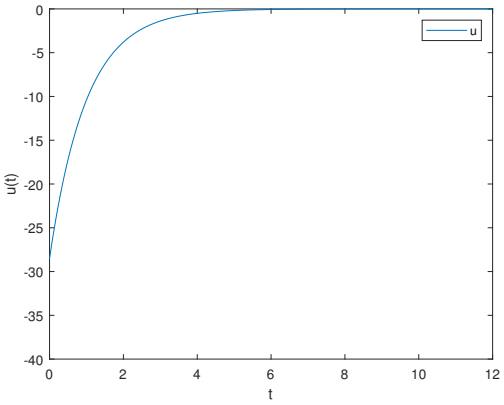

Figure 8: The control function.

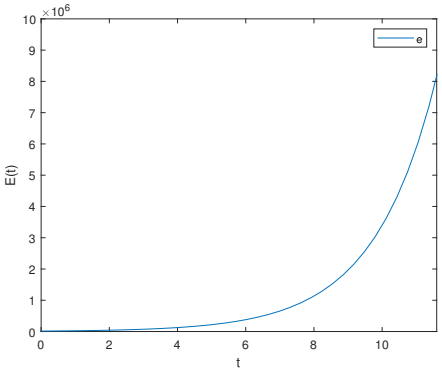

Figure 9: The energy growth.

subregion ω.

Remark 5.2 The stabilization on ω is obtained for low delay, and when the delay increases, the system (24) becomes unstable on ω.

6 Conclusion

This study examines the regional stabilization of an infinite dimensional delayed bilinear system. It offers sufficient conditions for weak and strong stabilization. The approach is a combination of energy decay, weak and exact observability conditions, and properties of semigroups. Furthermore, we provide examples and illustrations to support the obtained

theoretical results. At the same time, there are still some unanswered questions such as the application of these results to delayed semilinear systems, these issues are currently under investigation and will be dealt with in a future paper.

Acknowledgement

The work has been carried out with a grant from Hassan II Academy of Sciences and Technology.

References

[1] K. Ammari and M. Tucsnak. Stabilization of Bernoulli-Euler beams by means of a pointwise feedback force. *SIAM J. Control Optim.* **39** (4) (2000) 1160–1181.

[2] C. Bardos, G. Lebeau and J. Rauch. Sharp sufficient conditions for the observation, control and stabilization of waves from the boundary. *SIAM J. Control and Optimization* **30** (1992) 1024–1065.

[3] T. Gao and J. Gong. Modeling the airside dynamic behavior of a heat exchanger under frosting conditions. *Journal of Mechanical Science and Technology* **25** (10) (2011) 2719–2728.

[4] Z. Hamidi, M. Ouzahra and A. Elazzouzi. Strong Stabilization of Distributed Bilinear Systems with Time Delay. *Journal of Dynamical and Control Systems* **26** (4) (2019) 243–254.

[5] I. Lasiecka and D. Tataru. Uniform boundary stabilisation of semilinear wave equation with nonlinear boundary damping. *Journal of Differential and Integral Equations* **6** (3) (1993) 507–533.

[6] R. R. Mohler. Bilinear control processes: with application to engineering, Ecology, and Medicine. *Mathematics in science and engineering.* Elsevier **106** (3) (1973) 223.

[7] A. Tsouli, A. El Houch, Y. Benslimane and A. Attioui. Feedback stabilisation and polynomial decay estimate for time delay bilinear systems. *International Journal of Control* (2019) https://doi.org/10.1080/00207179.2019.1693061.

[8] A. Pazy. *Semigroups o Linear Operators and Applications to Partial Differential Equations.* Springer Verlag, New York, 1983.

[9] J. P. Richard. Time-delay systems: an overview of some recent advances and open problems. *Automatica* **39** (10) (2003) 1667–1694.

[10] J. Wu. *Theory and Applications of Partial Functional Differential Equations.* Springer-Verlag, New York, 1996.

[11] E. Zerrik and M. Ouzahra. Regional stabilization for infinite dimensional systems. *International Journal of Control* **76** (1) (2003) 73–81.

[12] E. Zerrik, A. Ait Aadi and R. Larhrissi. Regional stabilization for a class of bilinear systems. *IFAC-PapersOnLine* **50** (1) 4540–4545.

[13] E. Zerrik, A. Ait Aadi and R. Larhrissi. On the stabilization for a class of infinite dimensional bilinear systems with unbounded control operator. *Nonlinear Dynamics and Systems Theory* **18** (4) (2018) 418–425.

[14] E. Zerrik and A. Ait Aadi. On the stabilization for a class of distributed bilinear systems using bounded controls. *Proceedings of International Mathematical Sciences* **1** (1) (2019) 28–40.